Spring 2016

Nonlinear Flight Control Design Using Backstepping Methodology

Thanh Trung Tran
Old Dominion University, ttran022@odu.edu

NONLINEAR FLIGHT CONTROL DESIGN USING BACKSTEPPING METHODOLOGY

by

Thanh Trung Tran
B.S. July 2002, Vietnam National University, Vietnam
M.S. May 2007, Vietnam National University, Vietnam
Ph.D. June 2012, Jeju National University, South Korea

A Dissertation Submitted to the Faculty of
Old Dominion University in Partial Fulfillment of the
Requirements for the Degree of

DOCTOR OF PHILOSOPHY

AEROSPACE ENGINEERING

OLD DOMINION UNIVERSITY
May 2016

Approved by:

Brett A. Newman (Director)

Thomas E. Alberts (Member)

Jen-Kuang Huang (Member)

Duc T. Nguyen (Member)

ABSTRACT

NONLINEAR FLIGHT CONTROL DESIGN USING BACKSTEPPING METHODOLOGY

Thanh Trung Tran
Old Dominion University
Director: Dr. Brett A. Newman

The subject of nonlinear flight control design using backstepping control methodology is investigated in the dissertation research presented here. Control design methods based on nonlinear models of the dynamic system provide higher utility and versatility because the design model more closely matches the physical system behavior. Obtaining requisite model fidelity is only half of the overall design process, however. Design of the nonlinear control loops can lessen the effects of nonlinearity, or even exploit nonlinearity, to achieve higher levels of closed-loop stability, performance, and robustness. The goal of the research is to improve control quality for a general class of strict-feedback dynamic systems and provide flight control architectures to augment the aircraft motion. The research is divided into two parts: theoretical control development for the strict-feedback form of nonlinear dynamic systems and application of the proposed theory for nonlinear flight dynamics. In the first part, the research is built on two components: transforming the nonlinear dynamic model to a canonical strict-feedback form and then applying backstepping control theory to the canonical model. The research considers a process to determine when this transformation is possible, and when it is possible, a systematic process to transfer the model is also considered when practical. When this is not

the case, certain modeling assumptions are explored to facilitate the transformation. After achieving the canonical form, a systematic design procedure for formulating a backstepping control law is explored in the research. Starting with the simplest subsystem and ending with a full system, pseudo control concepts based on Lyapunov control functions are used to control each successive subsystem. Typically, each pseudo control must be solved from a nonlinear algebraic equation. At the end of this process, the physical control input must be re-expressed in terms of the physical states by eliminating the pseudo control transformations. In the second part, the research focuses on nonlinear control design for flight dynamics of aircraft motion. Some assumptions on aerodynamics of aircraft are addressed to transform full nonlinear flight dynamics into the canonical strict-feedback form. The assumptions are also analyzed, validated, and compared to show the advantages and disadvantages of the design models. With the achieved models, investigation focuses on formulating the backstepping control laws and provides an advanced control algorithm for nonlinear flight dynamics of the aircraft. Experimental and simulation studies are successfully implemented to validate the proposed control method. Advancement of nonlinear backstepping control theory and its application to nonlinear flight control are achieved in the dissertation research.

ACKNOWLEDGMENTS

This dissertation is the apex of five years of study and research at the Department of Mechanical and Aerospace Engineering of Old Dominion University. Many people have helped me over the past five years and this is a good opportunity to express my gratitude to them all. The first person I would like to thank is my supervisor Dr. Brett A. Newman. I have pursued my Ph.D. with him since 2010. During this time, he has taught me every corner of life: From the way of speaking to the approach of exploring a scientific topic and how to deal with encountered problems. Dr. Newman has helped me from a student with poor knowledge of dynamics and control topics to one who knows how to state and deal with a scientific problem. His support and encouragement has helped me in all the time of research. His deep physical insight and wide knowledge in the field of dynamics and control was always of great assistance. Besides, Dr. Newman is not only a excellent professor but also a good friend to me. Words cannot express my thankfulness. I wish I had the words to express my appreciation for his gift and kindness.

The second person I would like to thank is Dr. Thomas E. Alberts who is a expert in applied dynamics and control. Courseworks and advice from him have helped me to know how to balance between theoretical and applied research. I would also like to thank the other members of my Ph.D. committee who monitored my work and took effort in reading and providing me with valuable comments on earlier versions of this dissertation: Dr. Jen-Kuang Huang and Dr. Duc T. Nguyen. I wish to offer my humble gratitude to Dr. Han Bao, Dr. Robert L. Ash, Dr. Colin P.

Britcher, Dr. Drew Landman, and Dr. Ramamurthy Prabhakaran for their inspiring and encouraging way to lead me to a deeper understanding of knowledge, and their invaluable comments during the coursework.

Staying away from home is always challenging and tough. However, I am glad to have friends at Old Dominion University who always made me believe they are there when it matters and have been part of my happiness and hardships. I thank them all for giving me so many memories to cherish during my stay in Norfolk. I also thank all the members of the Vietnam Student Association who have been very cooperative and supportive. I am also grateful for the Department of Mechanical and Aerospace Engineering at Old Dominion University for providing me with a teaching assistant position and an excellent work environment during my study and I also thank all the staff for their cheerful assistance in the office work. Many thanks to the Vietnam Education Foundation funded by the United States government for supporting me during my stay in the United States, and also the Graduate School of Old Dominion University has been gracious to waive the tuition fee for my doctoral studies. I wish to recognize the financial support for experimental study of this research from the NASA Langley Research Center under Cooperative Agreements NCC-1-02043 and NNL09AA00A (NIA Activity 2951).

Finally, I will never find words enough to express the gratitude that I owe to my wife, Vi Hong Nguyen, my daughters, Vy Linh Nguyen Tran and Vy Anh Nguyen Tran, my brothers, my sisters, and my parents. Their tender love and affection has always been the cementing force for building the blocks of my academic career.

The all-round support rendered by them provided the much needed stimulant to sail through the phases of stress and strain. I would also like to thank all those whom I have not mentioned above but helped me in numerous ways to my success.

TABLE OF CONTENTS

LIST OF TABLES

LIST OF FIGURES

CHAPTER 1

INTRODUCTION

1.1 MOTIVATION

Aircraft flight control has been a challenge to conventional control design methods due to the large variations in aircraft aerodynamics over different operating conditions. The standard approach for flight control design for nonlinear aircraft systems is gain-scheduling. In this approach, linear approximation of dynamic equations at several important operating points within the flight envelope is achieved. Depending on these points, linear controllers are designed and then combined continuously as the vehicle flies from one operating point to another. Due to linearization, the actual system performance and stability can be significantly different from the design results due to the approximated nonlinearities. With the rapid development of high-performance computational computers, sensor technology, and integrated electronic devices, nonlinear flight control design methods are expected to provide a control system with high precision and reliability. Thus, the investigation and development of advanced control methods for nonlinear aircraft flight dynamics has been addressed considerably by the aerospace control community, but is by no means complete.

A popular classical method known as feedback linearization is used to enforce a nonlinear dynamic system to behave linearly from a synthetic input to a desired output. Then linear control design methods for a linear system of aircraft dynamics

are used as an outer control loop over the entire flight envelope. However, investigations have revealed the method sometimes provides poor performance and reduced robustness across the entire flight envelope of aircraft flight systems. A more recent method, known as backstepping control design, has been introduced and used in exploring new directions in control design for nonlinear dynamic systems. With the advantages and flexibility of backstepping control design such as stability guarantee, avoidance of dynamic nonlinearity cancellation, and wide applicabilities, the backstepping control design approach for nonlinear flight dynamics has also been considered by many researchers. However, proposed approaches either used poor assumptions or has not yet been presented systematically for a class of nonlinear dynamic systems. In this dissertation, backstepping control design methodology is presented systematically for the strict-feedback form of nonlinear dynamic systems and then applied for aircraft flight dynamic systems to provide an architecture to augment performance and stability of the aircraft motion.

1.2 BACKGROUND

A dynamic system is a set of interconnected time-dependent functional components organized for certain specific tasks in the physical world. A control system is a set of processes applied to the signals of a dynamic system and some externally acting signals for the purpose of altering the behavior of the dynamic system in a benefical way. There are two types of control systems: open-loop and closed-loop (feedback). A closed-loop control system that is capable of adapting to system changes and uncertainties to achieve high performance plays an important role in the development

of science and technology.

Classical control theory, control applications, and the history of feedback control can be found in References [1], [2], [3], [4]. Many design methods based on different control objectives and system conditions have been developed and verified in theory and practice such as proportion-integrator-derivative (PID) control in References [2], [5], pole placement control in References [6], [7], and robust control in References [8], [9]. These control design methods are typically applied to linear systems but realistic models of engineering systems are nonlinear in which the dynamic behavior of a system to be controlled changes with the operating region. Thus, a typical approach to this situation has been to apply the notion of gain-scheduling, where a set of linear control systems are combined through an interpolation process dependent on the operating condition or state condition. A systematic concept for the gain-scheduling technique and applications of gain-scheduling for engineering systems can be found in References [10], [11]. Some advanced design methods directly addressing nonlinear dynamics, such as feedback linearization in References [8], [12], [13], [14], [15], [16], [17], [18], [19], adaptive control in References [4], [20], [21], backstepping control in References [8], [21], [22], have been addressed and applied for engineering systems by many researchers. These methods have been applied to nonlinear aircraft systems, nonlinear magnetic systems, and nonlinear robotic systems, for example.

The standard approach for designing controllers for nonlinear aircraft systems is gain-scheduling. In this strategy, linear approximation of dynamic equations at several important operating points within the flight envelope is achieved. Depending on

these points, linear controllers are designed and then combined continuously as vehicle flies from one operating point to another. Due to linearization, the actual system performance and stability can be significantly different from the design results due to the approximated nonlinearities. In recent years, the investigation and development of flight control methods for nonlinear aircraft dynamics has been achieved by the aerospace control community in References [23], [24], [25], [26], [27], [28], [29], [30], [31], [32], [33], [34], [35], [36], [37].

Instead of gain-fitting and interpolating between several operation points, the application of a variable-gain optimal output feedback control design methodology is proposed in References [25], [32] where the feedback gains are continuously calculated and scheduled as a function of the state variables. In the approach in Reference [32], the feedback gains are calculated and scheduled by minimizing a cost function that is dependent on attack angle and surface deflections. The approach is not fully effective and robust for short period mode control due to the computational cost and convergence of the associated constrained optimization problem.

Nonlinear dynamic inversion (NDI) in References [23], [30], [33], [34], [36], [37] for flight control system design has been proposed to eliminate the drawbacks of gain-scheduling based design. Reference [30] uses assumptions in which aerodynamic force coefficients and moment coefficients are nonlinear functions of the angle of attack, sideslip angle, and thrust coefficient but linear functions of the elevator, aileron, and rudder. The motion equations can be re-written as a triangular system of general form and then a nonlinear dynamic inverse controller is generated and proven valid

over the entire flight envelope. The limitation of the proposed strategy is that aerodynamic moments must be linearly represented in terms of control variables through the control derivatives. The main assumptions in Reference [30] is that the governing equations are known precisely and the aircraft states are measured or estimated accurately. If either of these requirements are not met, the cancellation of the nonlinear dynamics will not be exact. Thus, a methodology has been proposed in Reference [33], [34] to improve aircraft performance by using a combination of dynamic inversion and structured singular value μ synthesis.

A better approach of NDI design for full nonlinear flight control is presented in References [36], [37] which uses the fact that control surface deflections do not directly affect slow dynamics. Therefore, control systems are designed separately for slow-state variable dynamics and fast-state variable dynamics. With the designed fast-state controller, a separate and approximate inversion procedure is carried out to design the slow-state controller for slow-state variable dynamics. The achieved slow-state control system outputs are used as commands for the controller augmenting the fast-state variable dynamics. A justification of reliability of the proposed algorithm is confirmed analytically using the longitudinal dynamics. A general disadvantage of the NDI approach that prevents the popular adoption of the method for nonlinear flight systems is the poor robustness of NDI-based control design, i.e., system parameters of the aircraft dynamics are included and essentially inverted in the control law. Therefore, the aircraft model used for control design needs to be accurate in order to achieve good performance and stability of the system.

In recent years, many researchers have addressed backstepping control (BSC) design from References [21], [22], [38], [39], [40]. The concept of backstepping design was introduced for the first time in References [21], [22] and has been a motivated basis for exploring new directions in control design for nonlinear dynamic systems. Backstepping control design is seen as a recursive design process which breaks a design problem on the full system down to a sequence of sub-problems on lower order systems. Considering each lower order system with a control Lyapunov function (CLF) and paying attention to the interaction between the various subsystems makes the design of a stabilizing controller modular and easier. The advantages of backstepping control are a stability guarantee, avoidance of dynamic nonlinearity cancellation, wide applicability for a class of nonlinear dynamic systems, and elimination of the requirement for the designed system to appear linear, as noted in References [21], [41]. Applications of the backstepping design approach for nonlinear flight control have been considered by many researchers in References [24], [26], [27], [28], [31], [35].

An online approximation-based backstepping control approach for advanced flight vehicles is presented in Reference [24] in which the control law is designed using three feedback loops with online approximation of the aerodynamic force and moment coefficient functions. The approach maintains stability (in the sense of Lyapunov) of the online function approximation process in the presence of magnitude, rate, and bandwidth limitations on the intermediate states and the surfaces. Reference [28] shows how the equations of motion for aircraft are restructured in linear strict-feedback

form, and then backstepping control design and adaptive gain scheduling are employed to achieve full envelope flight control. The research in Reference [35] assumes aerodynamic forces and moments as a linear function of attack angle, pitch angle and elevator. Then backstepping control design is applied to the aircraft model in strict-feedback form. The new contribution is that aerodynamic parameters of the aircraft are approximated by nominal values and error models and then a parameter adaptive scheme using a multilayer neural network is employed to improve the performance and stability of the aircraft. Limitations of these approaches in References [28], [35] are the assumptions of linear like behavior for the design model used for generating the control law. These disadvantages have been eliminated in References [26], [27]. However, in these approaches, it is assumed that flight path angle is not significantly affected by the gravitational term which is fixed at the reference value. Also, the product of angle of attack and the time derivative of flight path angle is assumed to be positive with nonzero attack angles. The model of the nonlinear longitudinal dynamics of the aircraft is re-written in nonlinear strict-feedback form and then the backstepping-based control algorithm is used.

These above works have not yet addressed in a significant way the robustness and adaptive issues in flight control of nonlinear dynamic systems. Nonlinear adaptive flight control in the presence of unmodeled parameters and external disturbances is presented in References [29], [42], [43], [44]. Neural network (NN) based methods for adaptive control are presented in References [29], [42] in which the NN uses table lookup approaches to reduce the amount of memory and computation time required.

Also, the NN can provide interpolation between training points with no additional computational effort to adapt controllers in achieving desired performance. Reference [43] suggests an adaptive backstepping strategy to improve the process of parameter estimation by using the modified tracking error. Use of assumptions of constant velocity and no lift and drag effects of the control surfaces, the standard affine system is achieved for applying the adaptive backstepping-based design. The authors use a combination of fuzzy logic and a modified Lyapunov function to achieve an effective way for adapting the time-variant parameters. Works in References [45], [46], [47], [48], [49] strive to improve the dynamic performance of aircraft under the presence of parameter variation and disturbances. In these studies, the combination of stochastic robustness procedures and dynamic inversion is proposed to minimize the probability of instability and probability of design requirement violations by using the genetic algorithm to search the design parameter space. The soundness of using a robustless method to consider the robust design is of concern for these methods. All of the above control design methodologies for nonlinear flight dynamics of aircraft need to be improved and modified extensively for the goal of safe and reliable application to flight vehicles.

The dissertation author has been involved in the research of References [38], [39], [40], [50], [51], [52], [53] in which the backstepping control methodology is applied successfully to a roll-to-roll (R2R) web system for printed electronics technology. References [39], [51] assume no web slippage occurs, the web has no permanent

deformation due to applied tension, and the load cell and dancer dynamics are neglected. Therefore, the nonlinear dynamics of a single-span R2R web system can be written in single-input single-output (SISO) strict-feedback form. After applying the backstepping-based design method with the achieved system, the resulting controller is proven to achieve the performance specifications and is globally asymptotically stabilized with the optimal gains in Reference [52]. Also, a modified genetic algorithm for optimally determining the gains of nonlinear controllers is proposed in Reference [52] by using a state space model approach and a scheme for designing the control system with automatic gain tuning due to the presence of disturbances and changing parameters. The experimental and simulation results validated the proposed strategy. The backstepping control methodology was also extended to a multi-span R2R web system in References [38], [40] in which nonlinear dynamics of the multi-span R2R web system are written in multi-input multi-output (MIMO) strict-feedback form. A technique using backstepping control design was applied to achieve the control laws that meet the demand of performance and global stability. Simulation and experimental results were implemented to validate the proposed design method. In some sense, the dissertation research is an extension of these previous works by the author.

1.3 RESEARCH OBJECTIVES

This dissertation investigates backstepping-based nonlinear control design methodology for nonlinear flight dynamics of aircraft. From the author's experience with nonlinear flight dynamic systems and backstepping controllers for web

manufacturing systems, the potential use of the backstepping control methodology for nonlinear flight dynamical systems appears feasible. The research provides a basis for understanding a general class of strict-feedback dynamic systems which plays an important role in improving control quality for nonlinear flight dynamic systems. The results provide backstepping and integrator-backstepping control design methodologies for strict-feedback models of nonlinear dynamic systems. Application of the proposed theories will be implemented for nonlinear flight dynamic systems in order to provide robust flight control architecture to augment the aircraft motion. The dissertation work consists of two primary components. First, the research focuses on specifying conditions under which a flight dynamic system is able to be transformed into a strict-feedback system. Second, an application of the proposed backstepping and integrator-backstepping control strategy for nonlinear dynamic systems with strict-feedback form are investigated in order to provide architecture to augment the aircraft motion.

The first specific aim of the research is to study necessary conditions under which a nonlinear dynamic model is able to be transformed into a strict-feedback system form. The research considers a process to determine when this transformation is possible, and when it is possible, a systematic process to transfer the model is also considered. If not possible, some assumptions are made and then the nonlinear flight dynamic system is able to be transformed approximately to strict-feedback form. In the second specific aim, the research concentrates on providing a backstepping control design methodology for the strict-feedback model of a nonlinear dynamic system.

Starting with the simplest subsystem and ending with the full system, pseudo control concepts based on Lyapunov control functions are used to control each successive subsystem. At the end of this process, the physical control input must be re-expressed in terms of the physical states by eliminating the pseudo control transformations. In the third specific aim, the research investigates an equivalence of the feedback linearization-based design method and the backstepping-based design approach for a triangular affine system. The research addresses a fundamental question here: "Are these two design methods unique or does there exist some type of equivalence between the two methods for a specific type of nonlinear dynamic system?" In the fourth specific aim, an integrator-backstepping (IBSC) control methodology is addressed for the strict-feedback form in the presence of disturbances.

In the fifth and final specific aim, the research applies the proposed theories for flight path angle control and roll angle control corresponding to the longitudinal and lateral dynamics of an aircraft in order to improve the performance and stability capability. Some assumptions on lift will be addressed and the nonlinear longitudinal dynamic model of an aircraft will be restructured in the strict-feedback form for direct applicability of the proposed control approach. The backstepping control design framework is then applied and validated for the flight dynamic systems. To address wind disturbance and model error effects on nonlinear flight dynamics, a strict-feedback model of the longitudinal dynamics with uncertain parameters and wind disturbances is formulated and the IBSC-based control strategy is applied to improve the performances and stability of aircraft motion in the presence of parameter

errors and environment disturbances. Finally, the research applies the BSC/IBSC-based control strategy for roll angle control of aircraft under the presence of varying pitching and yawing angles. The proposed control methods are validated in computational studies using an F-16 aircraft simulation model, and in experimental studies using a model of the L-59 aircraft dynamics.

1.4 DISSERTATION OUTLINE

In this dissertation, six technical chapters beyond the Introduction (Chapter 1) are considered. In Chapter 2, a mathematical background is provided on the general theory of stability and stability in the sense of Lyapunov. Then Lyapunov-based control design, which plays an important role in control design of nonlinear dynamic systems, is presented and applied for a specific type of nonlinear affine system. The concept of robust backstepping control design is also introduced for supporting the research. Then a formulation of the equations of motion (EOM) of a six degrees of freedom (DOF) aircraft are provided for later applications.

In Chapter 3, the research investigates how a nonlinear dynamic model can be transformed into a strict-feedback model form. With the achieved model, the research then provides a methodology of backstepping-based control design for the model. Then an integrator-backstepping control methodology is addressed for the strict-feedback form in the presence of system parameter errors or external environment disturbances by introducing an integral term in the control law. Advantages and disadvantages of the proposed theory are discussed here.

In Chapter 4, the model conversion to strict-feedback form and control design using the backstepping framework for a model of aircraft longitudinal dynamics is addressed. The specific aircraft model used here is a full envelope nonlinear simulation characterization of the F-16 airframe. Flight path angle control design for aircraft is studied for investigating and validating the proposed control design methodology in Chapter 3. Numerical simulations and discussion of the results are made here.

In Chapter 5, an equivalence between the feedback linearization-based design method and the backstepping-based design approach is investigated for a triangular affine form of nonlinear dynamic systems. A theorem and proof are provided for supporting the theoretical equivalence. Both analytical and numerical results for aircraft flight path angle control are used to validate the equivalence results. Some discussions and conclusions are also presented here.

In Chapter 6, a strict-feedback form for longitudinal dynamics of the F-16 aircraft model in the presence of disturbance is provided for investigation. Then, a systematic procedure is presented for formulating an integrator-backstepping control law for longitudinal dynamics of the F-16 aircraft model. With the achieved control law, a block diagram is provided for deeper understanding of the flight path angle control system architecture. Discussions of simulation results and conclusions are made here.

In Chapter 7, an introduction of the L-59 aircraft model is provided and then backstepping-based control design for aircraft roll angle control is presented. Both the BSC and IBSC formulations are applied to the pure roll motion of the aircraft.

A gain scheduling strategy is explored to achieve gain selection as a function of performance specifications and measurements. By doing so, the gains are able to adapt to varying environments based on the measurements in order to minimize control power usage and achieve the desired conditions. Finally, simulation and indoor experimental studies for a scaled model of the L-59 aircraft dynamics are presented here, followed by discussion of the results.

In Chapter 8, conclusions are made by summarizing and analyzing the proposed approaches, the specific research results, and the overall achievement of the dissertation work. Discussions regarding applicability and limitations in actual implementation settings are offered, and then future research directions are addressed to improve the applicability and precision of the investigated nonlinear control methodology.

CHAPTER 2

RESEARCH FOUNDATION

This chapter is divided into two parts. In the first part, a mathematical basis is provided for dynamic system models, stability concepts, and control logic providing stable behavior. This basis helps to support the investigated dissertation research. In the second part, a brief review of aircraft flight dynamics with a focus on the governing differential equations for symmetric longitudinal motion is then presented. This review also supports the investigated dissertation research.

2.1 STABILITY AND CONTROL PRINCIPLES

In this section, some definitions, theorems, and examples in References [54], [55] are introduced to facilitate investigating the stability of a nonlinear system. Then basic concepts of Lyapunov-based control design from References [8], [21] are presented to show how a stabilizing control law is systematically formulated for a nonlinear affine system. Also, some basic concepts of backstepping control design from References [8], [21], [22] are presented and discussed to lay a foundation for the investigated dissertation research. Some discussions about advantages and disadvantages of these methods are made here.

2.1.1 CONCEPTS AND DEFINITIONS

Consider a general state equation for a nonlinear system with state vector x as

$$\dot{x} = f(x, t) \tag{2.1}$$

where $f \in R^n$, t is scalar forward time or $t \in R_+$, and $x \in R^n$ with initial condition $x(t_0) = x_0$.

Definition 2.1. *(Equilibrium State)*

A state x_e is called an equilibrium state of the system (2.1) *if* $f(x_e, t) = 0,\ \forall\ t > t_0$.

Definition 2.2. *(Stable Equilibrium State)*

An equilibrium state x_e of the system (2.1) *is said to be stable if, for each $\varepsilon(t_0) > 0$ and $t_0 \in R_+$, there exists a $\delta(\varepsilon, t_0) > 0$ such that $\|x_0 - x_e\| \leq \delta(\varepsilon, t_0)$, $\forall t_0 \implies \|x(t; x_0, t_0) - x_e\| \leq \varepsilon(t_0),\ \forall\ t \geq t_0$.*

Figure 2.1 shows the basic concept of the stable equilibrium state definition. If the equilibrium state x_e is stable, then the time propagated state trajectory arising from any initial state x_0 that lies within a closed neighborhood with δ radius around x_e remains within a closed neighborhood with ε radius around x_e.

Definition 2.3. *(Asymptotically Stable Equilibrium State)*

An equilibrium state x_e of the system (2.1) *is said to be asymptotically stable if it is stable in the sense of Lyapunov and $x(t; x_0, t_0) \longrightarrow x_e$ as t increases infinitely.*

The definition of the stability in the sense of Lyapunov is discussed in the next section.

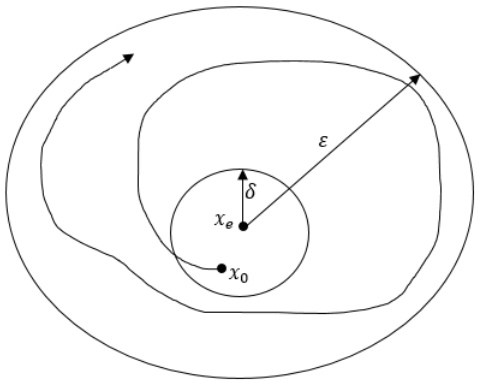

Figure 2.1: Stable Equilibrium State

Definition 2.4. *(Lie Derivative)*

Let function $V(x) : R^n \longmapsto R$ *be continuously differentiable with respect to its arguments, then the Lie derivative of* $V(x)$ *with respect to a function* $f(x)$ *is denoted as* $L_f V(x)$ *and is defined by*

$$L_f V(x) = \frac{\partial V(x)}{\partial x} f(x) \tag{2.2}$$

Definition 2.5. *(Class K)*

A function $\phi(\|x\|) : R_+ \longmapsto R_+$ *is of class K if*

i) $\phi(0) = 0$,

ii) $\phi(\|x\|) > 0, \ \forall \ \|x\| > 0$, *and*

iii) $\phi(\|x\|)$ *is strictly monotonically increasing and continuous with* $\|x\|$.

Definition 2.6. *(Positive Definite Function)*

Function $V(x,t) : R^n \times R_+ \longmapsto R$ *is said to be a positive definite (PD) function if there exists a class K function* $\phi(\|x\|)$ *such that*

$$V(x,t) \geq \phi(\|x\|), \ \forall \ x \in R^n \tag{2.3}$$

Example 2.1. Consider a function $V(x)$ with $x = [x_1\ x_2]^T \in R^2$ indicated below.

$$V(x_1, x_2) = x_1^2 + x_2^2$$

The function $V(x_1, x_2)$ satisfies the conditions of a class K function in terms of Definition 2.5. Thus, $V(x_1, x_2)$ is a class K function. Also, there exists a function $\phi(\|x\|)$ of class K, specifically $\phi(\|x\|) = \frac{1}{2}(x_1^2+x_2^2)$, such that $V(x,t) \geq \phi(\|x\|),\ \forall\ x \in R^2$. So, $V(x_1, x_2)$ is a PD function in terms of Definition 2.6.

Definition 2.7. *(Decrescent Function)*

Function $V(x,t) : R^n \times R_+ \longmapsto R$ is called a decrescent function if there exists a class K function $\phi(\|x\|)$ such that

$$V(x,t) \leq \phi(\|x\|),\ \forall\ x \in R^n \tag{2.4}$$

Example 2.2. Consider a function $V(x)$ with $x = [x_1\ x_2]^T \in R^2$ from Example 2.1 indicated below.

$$V(x_1, x_2) = x_1^2 + x_2^2$$

There exists a function $\phi(\|x\|)$ of class K, specifically $\phi(\|x\|) = 2(x_1^2 + x_2^2)$ such that $V(x,t) \leq \phi(\|x\|),\ \forall\ x \in R^2$. So, $V(x_1, x_2)$ is a decrescent function in terms of Definition 2.7.

2.1.2 STABILITY IN THE SENSE OF LYAPUNOV

For linear dynamic systems, the Nyquist stability criterion, Routh's stability criterion, and the first method of Lyapunov (indirect method of Lyapunov) are used for analyzing the stability of the system. For nonlinear dynamic systems, the second

method of Lyapunov (direct method of Lyapunov) is used for analyzing stability of the system without requiring a solution to the differential equations. To be more precise, this method analyzes the stability of the equilibrium solution of the nonlinear system. The idea behind the method is from the fact that a vibratory system is stable if the total energy (a positive definite function) is continuously decreasing (which means that the time derivative of the total energy must be negatively definite) until an equilibrium state is reached. In this section, some definitions, theorems, and examples are provided to introduce stability in the sense of Lyapunov. The theoretical basis presented in this section is used to assist in Lyapunov-based control design of nonlinear dynamic systems.

Definition 2.8. *(Lyapunov Function)*

Function $V(x,t) : R^n \times R_+ \longmapsto R$ *is said to be a Lyapunov function with respect to the system* (2.1) *if the Lie derivative of* $V(x,t)$ *with respect to* $f(x,t)$ *satisfies the condition*

$$\dot{V}(x,t) \leq 0, \ \forall \ x \in R^n, \ \forall \ t \geq t_0 \tag{2.5}$$

Definition 2.9. *(Stability in the Sense of Lyapunov)*

Let $S_\delta = \{x_0 : \|x_0 - x_e\| \leq \delta(\varepsilon, t_0), \ \forall t_0\}, \Phi(t; x_0, t_0)$ *be a solution of the equation* (2.1)*, and* $S_\varepsilon = \{\Phi(t; x_0, t_0) : \|\Phi(t; x_0, t_0) - x_e\| \leq \varepsilon(t_0), \ \forall \ t \geq t_0\}$*. An equilibrium state* x_e *of the system* (2.1) *is said to be stable in the sense of Lyapunov if, for each* S_ε *, there exists a* S_δ *such that trajectories starting in* S_δ *do not leave* S_ε *as* t *increases infinitely.*

Definition 2.10. *(Lyapunov Asymptotic Stability)*

An equilibrium state x_e of the system (2.1) *is said to be asymptotically stable in the sense of Lyapunov if it is stable in the sense of Lyapunov and if every solution starting within S_δ converges, without leaving S_δ, to x_e as t increases infinitely.*

Theorem 2.1. *(Stability in the Sense of Lyapunov)*

An equilibrium state x_e of the system (2.1) *is stable in the sense of Lyapunov if there exists a function $V(x,t) : R^n \times R_+ \longmapsto R$ such that $V(x,t)$ is a positive definite, decrescent, and Lyapunov function.*

Theorem 2.2. *(Lyapunov Asymptotic Stability)*

An equilibrium state x_e of the system (2.1) *is asymptotically stable in the sense of Lyapunov if there exists a function $V(x,t) : R^n \times R_+ \longmapsto R$ such that*

i) $V(x,t)$ is a positive definite, decrescent, and Lyapunov function, and

ii) The Lie derivative of $V(x,t)$ is negatively definite.

Example 2.3. Consider a nonlinear system indicated below

$$\dot{x} = -g(x),\ x\ \in [0, +\infty) \tag{2.6}$$

and assume that $g(0) = 0$ and $g(x) > 0,\ \forall\ x\ \in (0, +\infty)$. Choose a $V(x)$ function as

$$V(x) = \int_0^x g(y)dy \tag{2.7}$$

It is easy to determine that the chosen function is a positive definite, decrescent, and Lyapunov function. Taking the time derivative of both sides of function (2.7) and

using the system (2.6), note that

$$\dot{V}(x) = \frac{\partial V(x)}{\partial x}(-g(x)) = -g^2(x) < 0 \ \forall \ x \ \in (0, +\infty) \tag{2.8}$$

The Lie derivative of the Lyapunov function in equation (2.8) results in a negatively definite function with every nonzero x. Thus, the origin equilibrium of the system (2.6) is asymptotically stable based on Theorem 2.2.

The second method of Lyapunov plays an important role in analyzing and designing for stability of nonlinear dynamic systems without solving the solution of differential equations. Based on the theory, several methods of analysis and design for nonlinear control systems have been developed such as backstepping control, adaptive control, robust control, and sliding mode control. Those methods have provided many important contributions in analysis and design of nonlinear engineering systems.

In general, the selection of the Lyapunov function in which its derivative along with the dynamic equations is negatively definite is not always successful, especially for complex dynamic systems. However, several methods such as the Lyapunov equation synthesis method, variable gradient algorithm, and Kravoskiis generalized method are able to find the Lyapunov function for linear systems, and a specific class of nonlinear systems. On the other hand, some approaches for nonlinear control design are proposed in which a Lyapunov function for the system is chosen arbitrarily and a control law is derived such that the time derivative of the Lyapunov function is negatively definite. The achieved control law then provides asymptotic stability. In the next section, the use of Lyapunov stability for developing the methods of control

analysis and design for an affine form of nonlinear dynamic systems is considered.

2.1.3 LYAPUNOV-BASED CONTROL DESIGN

This section provides a fundamental tool for the control design of nonlinear dynamic systems with an affine form. Control design within the context of integrator-backstepping in References [8], [41] is used to present the process for achieving a stabilizing control law by using the Lyapunov stability theorem in Section 2.1.2.

Consider a special nonlinear system from References [8], [56] indicated below

$$\begin{aligned} \dot{z} &= f(z) + g(z)\xi \\ \dot{\xi} &= u \end{aligned} \tag{2.9}$$

where $[z^T, \xi]^T$ is the state vector and $u \in R$ is the input. The functions $f(z)$ and $g(z)$ are smooth and known. Assumes that $f(0) = 0$. This system can be viewed as a cascade connection of two components where the first component is an integrator and the second component is an affine nonlinear system, as shown in Figure 2.2. The goal of the control design is to formulate a state feedback control law to stabilize the system (2.9) at the origin ($z = 0, \xi = 0$). The following discussion provides two steps for formulating the state feedback controller.

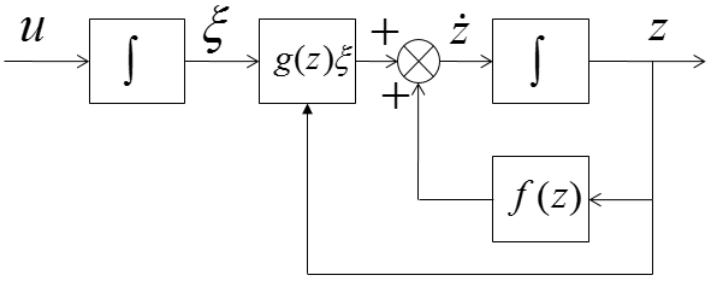

Figure 2.2: System without Control

Step 1.

Suppose that the first equation of system (2.9) can be asymptotically stabilized at the origin with a virtual control law $\xi = \phi(z)$ with $\phi(0) = 0$. This condition corresponds to the existence of a Lyapunov function $V_1(z)$ as in Theorem 2.2 such that

$$\dot{V}_1(z) = \frac{\partial V_1(z)}{\partial z}[f(z) + g(z)\phi(z)] \leq -W(z) < 0 \tag{2.10}$$

where $W(z)$ is a positive definite function. If the Lyapunov function $V_1(z)$ and the $W(z)$ function are specified, then a virtual control law $\phi(z)$ can be determined by satisfying the inequality in equation (2.11) indicated below.

$$\frac{\partial V_1(z)}{\partial z}[f(z) + g(z)\phi(z)] \leq -W(z) \tag{2.11}$$

Step 2.

A change of state is introduced as

$$y = \xi - \phi(z) \tag{2.12}$$

which transforms system (2.9) to the (z, y) coordinate system as

$$\begin{aligned} \dot{z} &= f(z) + g(z)\phi(z) + g(z)y \\ \dot{y} &= u - \dot{\phi}(z, y) \end{aligned} \tag{2.13}$$

where $\dot{\phi}(z, y) = \frac{\partial \phi}{\partial z}[f(z) + g(z)(y + \phi(z))]$ and Figure 2.3 shows the system (2.13) in the (z, y) coordinate system. This changing of variable is often called backstepping since it backsteps the control $-\phi(z)$ through the integrator. Since $f(z), g(z)$ and

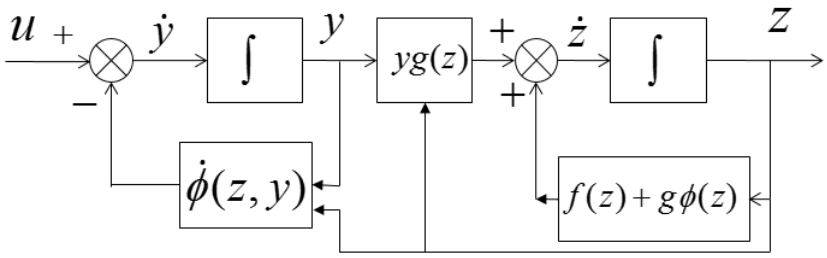

Figure 2.3: Backstepping Control through Integrator

$\phi(z)$ are known, the derivative of the virtual controller $\phi(z)$ can be written as

$$v = u - \dot{\phi}(z, y) \tag{2.14}$$

The new system (2.13) is re-written as

$$\begin{aligned} \dot{z} &= f(z) + g(z)\phi(z) + g(z)y \\ \dot{y} &= v \end{aligned} \tag{2.15}$$

which has the same form as the system (2.9) with the exception that the first system is asymptotically stable at the origin. This modular property of backstepping will be exploited to stabilize the overall system.

For the system (2.15), there exists a Lyapunov function $V_2(z, y)$ such that when the control law v is applied, its time derivative becomes negatively definite. The function is chosen as

$$V_2(z, y) = V_1(z) + \frac{1}{2}y^2 \tag{2.16}$$

Differentiating equation (2.16) on both sides in time and combining with the system (2.15) result in

$$\dot{V}_2(z, y) = \frac{\partial V_1(z)}{\partial z}(f(z) + g(z)\phi(z)) + \frac{\partial V_1(z)}{\partial z}g(z)y + yv \tag{2.17}$$

Substituting the inequality in equation (2.11) into equation (2.17) results in

$$\dot{V}_2(z,y) \leq -W(z) + y(\frac{\partial V_1(z)}{\partial z}g(z) + v) \tag{2.18}$$

To meet the asymptotically stable condition in the sense of Lyapunov in Theorem 2.2 for equation (2.18), a control law v can be chosen such that

$$\begin{aligned} -ky &= \frac{\partial V_1(z)}{\partial z}g(z) + v \\ \Rightarrow v &= -\frac{\partial V_1(z)}{\partial z}g(z) - ky \end{aligned} \tag{2.19}$$

where k is a positive gain. By doing so, the required sign condition on $\dot{V}_2(z,y)$ is achieved or

$$\dot{V}_2(z,y) \leq -W(z) - ky^2 < 0 \;\forall\; z, y \neq 0 \tag{2.20}$$

which implies the origin $(z,y) = (0,0)$ is asymptotically stable. Since $\phi(0) = 0$, this implies that the origin $z = 0$ and $\xi = 0$ is also asymptotically stable. Substituting equation (2.19) and $\dot{\phi}(z,y)$ into equation (2.14) results in

$$u = -\frac{\partial V_1(z)}{\partial z}g(z) - ky + \frac{\partial \phi}{\partial z}[f(z) + g(z)(y + \phi(z))] \tag{2.21}$$

Returning equation (2.21) to the original states (z,ξ) by substituting equation (2.12) into equation (2.21) result in

$$u = \frac{\partial \phi}{\partial z}[f(z) + g(z)\xi] - \frac{\partial V_1(z)}{\partial z}g(z) - k[\xi - \phi(z)] \tag{2.22}$$

where k is a positive gain.

2.1.4 DISCUSSION

The Lyapunov-based design provides an important tool for analysis and design of nonlinear control systems. The Lyapunov design provides a basis for which many control design methods for nonlinear dynamic systems have been developed in recent years. From the flexibility of using the Lyapunov function and selection of virtual control laws, Lyapunov-based design is able to be used to estimate uncertain parameters or improve performance by adding new parameters as shown in Chapter 6. Also, robust stability properties can be guaranteed with proper selection of the gains. However, the backstepping procedure as has been discussed so far has a number of drawbacks. The first is a tedious analytic calculation of the virtual control derivatives and, therefore, the achieved control law is usually very complex, especially for large systems. Further, in many cases, the control signal must be computed by solving a nonlinear algebraic equation at each compute cycle. The second is that the procedure can only handle systems that can be expressed in certain specific forms of nonlinear systems such as strict-feedback form, or affine systems. The third drawback of the backstepping-based design is that parameters of the dynamic system model must be known precisely to get good performance.

2.2 AIRCRAFT MOTION EQUATIONS

In this section, some concepts regarding aircraft and related background are introduced to assist in formulating the scalar equations of motion of aircraft as described in References [57], [58], [59], [60]. After this introduction, the scalar motion equations

of aircraft are achieved by using Newton's second law. In the final section, a mathematical model of aircraft longitudinal dynamics will be provided for investigating flight path control design of aircraft in Chapter 4, Chapter 5, and Chapter 6.

2.2.1 SOME CONCEPTS

Several concepts are provided for the derivation of the equations of motion (EOM) of six degree of freedom (DOF) aircraft in Reference [57].

Body Axis System

The body axis system (x_B, y_B, z_B) in Figure 2.4 is fixed to the aircraft with its origin at the aircraft's center of mass (cm). The x_B axis is positive out the nose of the aircraft in the plane of symmetry of the aircraft, the z_B axis is perpendicular to the x_B axis, in the plane of symmetry of the aircraft, positive below the aircraft, and the y_B axis is perpendicular to the $x_B z_B$-plane, positive determined by the right-hand rule (generally, positive out the right wing).

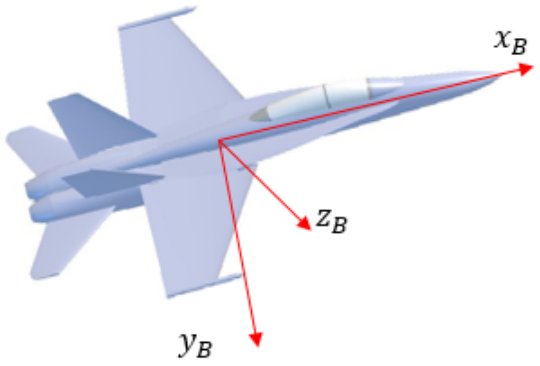

Figure 2.4: Body Axis System

Earth Axis System

Figure 2.5 shows the Earth axis system (x_E, y_E, z_E) or inertial axis system. This system is assumed to be an inertial axis system fixed to the Earth with the the x_E axis being positive in the direction of north, the y_E axis being positive in the direction of east, and the z_E axis being positive towards the center of the Earth.

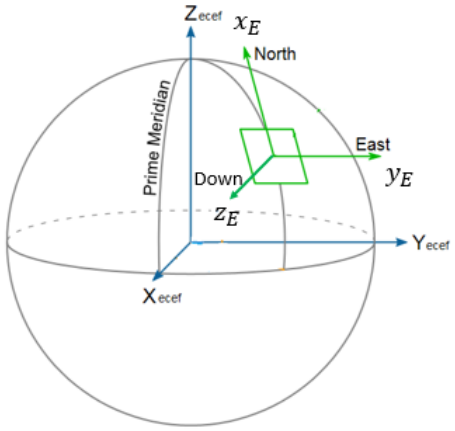

Figure 2.5: Earth Axis System

Wind Axis System

Figure 2.6 represents the wind axis system (x_W, y_W, z_W) that is defined with respect to the relative wind. The x_W axis is positive in the direction of the velocity vector of the aircraft relative to the air. The z_W axis is perpendicular to the x_W axis in the plane of symmetry of the aircraft, positive below the aircraft, and the y_W axis is perpendicular to the $x_W z_W$-plane and positive determined by the right-hand rule (generally, positive to the right). When sideslip angle β is zero, then the wind axis system becomes the stability axis system.

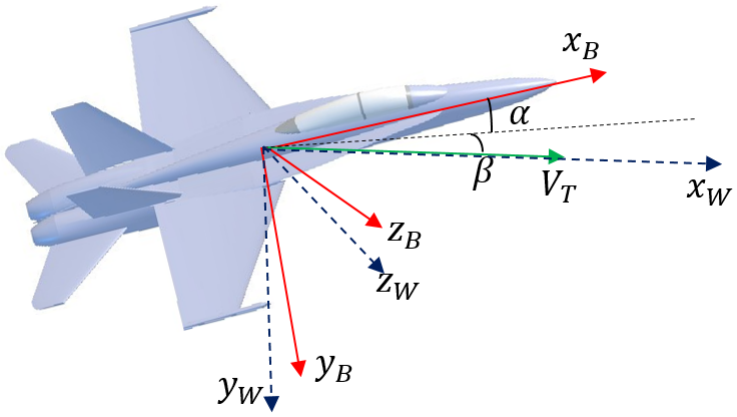

Figure 2.6: Wind Axis System

2.2.2 SCALAR EQUATIONS OF MOTION

Figure 2.7 represents velocity components with respect to a body axis system. The components U, V, W are inertial velocities of the aircraft mass center along the body x_B, y_B, z_B axes respectively. Variables P, Q, R are inertial angular velocity components along the body x_B, y_B, z_B axes respectively. Figure 2.8 represents components of propulsive forces and moments, gravitational forces, and aerodynamic forces and moments with respect to the body axis system. The g_x, g_y, g_z components are gravitational acceleration along the body x_B, y_B, z_B axes respectively, the $F_{A_x}, F_{A_y}, F_{A_z}$ components are aerodynamic forces along the body x_B, y_B, z_B axes respectively, the $F_{P_x}, F_{P_y}, F_{P_z}$ components are propulsive forces along the body x_B, y_B, z_B axes respectively, the L_A, M_A, N_A components are aerodynamic moments about the body x_B, y_B, z_B axes respectively, and the L_T, M_T, N_T components are propulsive moments about the body x_B, y_B, z_B axis, respectively.

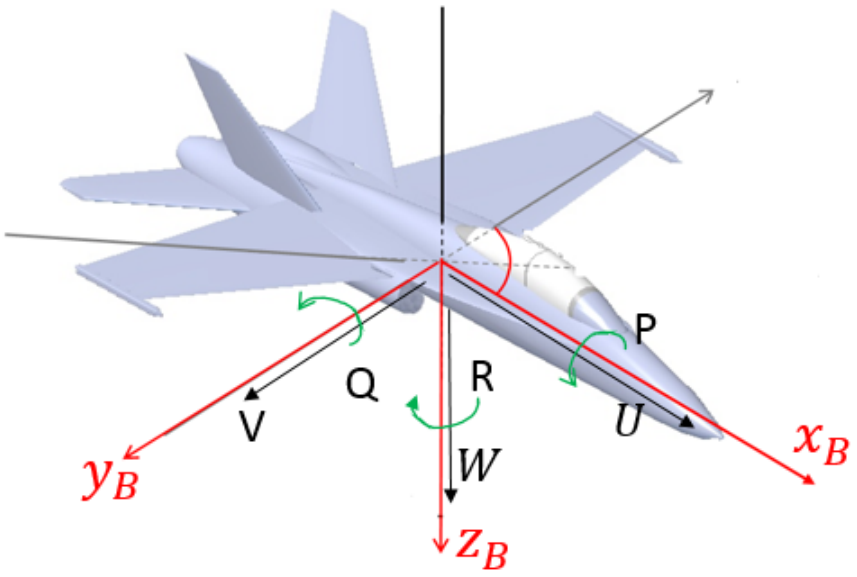

Figure 2.7: Velocity Components of Aircraft

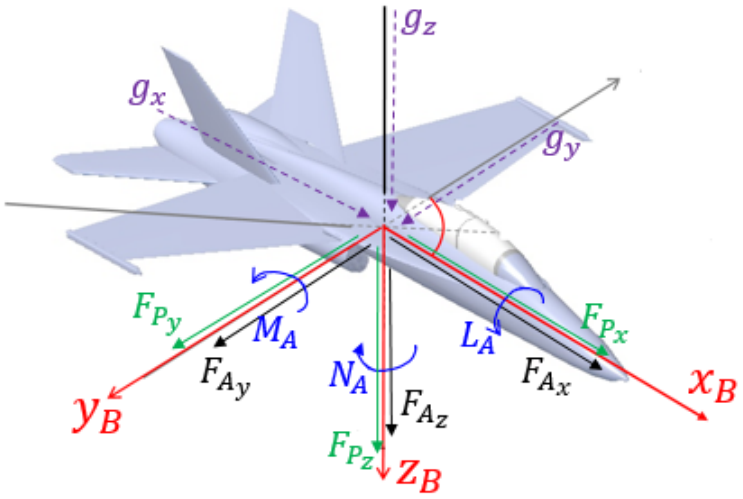

Figure 2.8: Force and Moment Components on Aircraft

For derivation of motion equations of six DOF aircraft, assume that the aircraft is a rigid body, with a constant mass, and with inertia symmetry. By using Newton's second law with respect to the inertial axis system and coordinate transformations between axis systems, the equations of motion of six DOF aircraft in References [57], [58] can be represented in the body axis system as

Force Equations

$$\begin{aligned} mg_x + F_{A_x} + F_{P_x} &= m(\dot{U} + QW - RV) \\ mg_y + F_{A_y} + F_{P_y} &= m(\dot{V} + RU - PW) \\ mg_z + F_{A_z} + F_{P_z} &= m(\dot{W} + PV - QU) \end{aligned} \tag{2.23}$$

Moment Equations

$$\begin{aligned} L_A + L_T &= I_{xx}\dot{P} - I_{zx}\dot{R} + (I_{zz} - I_{yy})QR - I_{zx}PQ \\ M_A + M_T &= I_{yy}\dot{Q} + (I_{xx} - I_{zz})RP + I_{zx}(P^2 - R^2) \\ N_A + N_T &= I_{zz}\dot{R} - I_{zx}\dot{P} + (I_{yy} - I_{xx})PQ + I_{zx}QR \end{aligned} \tag{2.24}$$

where m is total mass of aircraft, I_{xx}, I_{yy}, I_{zz} are moments of inertia about the cm for body x_B, y_B, z_B axes respectively, and I_{zx} is the product of inertia about the mass center for body x_B and z_B axes.

By combining these relations with the six kinematic equations, the EOMs of a six DOF aircraft consists of twelve nonlinear, coupled ordinary differential equations. For purposes of the study of flight dynamics, the three force equations in equation (2.23) and three moment equations in equation (2.24) are usually used for analysis and design.

2.2.3 LONGITUDINAL DYNAMICS

For the convenience of study of aircraft dynamics, the six aircraft equations in equations (2.23)-(2.24) can be decoupled into two sets of three equations. There are three longitudinal EOMs and three lateral-directional EOMs. One way of thinking of the longitudinal EOMs is to picture an aircraft with its xz plane coincident with an xz plane fixed in space and thus longitudinal motions would only occur within the xz plane.

Assuming that an aircraft is in wings-level flight with no sideslip or no lateral-direction motion, the pitching motion can be analyzed using only the longitudinal EOMs for an aircraft. With these assumptions, the nonlinear longitudinal dynamics of the aircraft can be written in the body frame in Reference [58] as

$$\begin{aligned} m(\dot{U} + QW) &= mg_x + F_{A_x} + F_{P_x} \\ I_{yy}\dot{Q} &= M_A + M_T \\ m(\dot{W} - QU) &= mg_z + F_{A_z} + F_{P_z} \end{aligned} \tag{2.25}$$

For convenience of control analysis and design, the components in the body axes are re-represented in the wind frame by an axis system transformation. By doing so, the mathematical model of the nonlinear longitudinal dynamics can be written in the stability axis system (wind axis system under longitudinal motion), as shown in Reference [61].

$$\begin{aligned}
\dot{V}_T &= \frac{1}{m}(-D + F_T cos\alpha - mgsin\gamma) \\
\dot{\alpha} &= q - \frac{1}{mV_T}(L + F_T sin\alpha - mgcos\gamma) \\
\dot{\theta} &= q \\
\dot{q} &= \frac{1}{I_y}(M + F_T z_{TF})
\end{aligned} \tag{2.26}$$

Variables and parameters appearing in equation (2.26) include V_T: aircraft total velocity, m: total mass of aircraft, $L(\alpha, V_T, q)$: lift force, $D(\alpha, V_T, q)$: drag force, $M(\alpha, q, \delta_E, V_T)$: pitch moment, $F_T(\delta_{th})$: thrust force, γ: flight path angle, α: angle of attack, θ: pitch angle, $q = Q$: pitch rate, δ_E: elevator, δ_{th}: throttle, $I_y = I_{yy}$: inertial moment about the aircraft y axis, z_{TF}: thrust point offset, g: gravity.

The model of nonlinear longitudinal dynamics in equation (2.26) is used for control analysis and design later in this dissertation. A numerical data set consistent with these dynamics for an F-16 aircraft model in which data are derived from low-speed static and dynamic wind-tunnel tests at the NASA Langley Research Center in Reference [62] is available for the control analysis and design research.

CHAPTER 3

BACKSTEPPING CONTROL FOR STRICT-FEEDBACK SYSTEMS

The first objective of this chapter is to study the necessary conditions in which SISO nonlinear dynamic models are able to be transformed into SISO strict-feedback systems. The research considers a process to determine when this transformation is possible, and when it is possible, a systematic process to transfer the model is also considered. Secondly, the research concentrates on providing a backstepping control design for the SISO strict-feedback system. Starting with the simplest subsystem and ending with the full system, pseudo control concepts based on Lyapunov control functions are used to control each successive subsystem. At the end of this process, the system control input must be re-expressed in terms of the physical states by eliminating the pseudo control transformations. Finally, an integrator-backstepping control methodology is addressed for the SISO strict-feedback form in the presence of disturbances and discussions on the methods are made here.

3.1 STRICT-FEEDBACK SYSTEMS

Strict-feedback form is an attractive mathematical model structure useful for analysis and design of nonlinear dynamic systems. Although not completely applicable, many engineering systems may be expressed in the strict-feedback form.

Nonlinear dynamic systems may be written in strict-feedback form using two approaches. In the first, a nonlinear dynamic system may be written indirectly as a strict-feedback system by using assumptions for simplifying the system. However, the analysis and design of the simplified model sometimes leads to inaccurate results compared to the true model. Thus, the second direct approach thereby allowing a nonlinear dynamic system to be written as a strict-feedback system is achieved by using transformations and feedbacks. In this approach, the design model matches more closely to the physical system behavior, although the new coordinates may be more difficult to interpret. The question arises for which condition a nonlinear dynamic model is able or not able to be transformed into a strict-feedback system. In this section, the research will investigate and provide a mathematical basis on how a SISO nonlinear dynamic model can be transformed into a strict-feedback model. If an original nonlinear dynamic system cannot be transformed into a strict-feedback form by either approach, the conditions on the combined use of a simplified model with stronger assumptions and transformations are suggested. Firstly, the research provides conditions in which a SISO nonlinear dynamic system can be transformed into a SISO affine system. Secondly, the research is extended to the conditions in which an affine system can be transformed into normal form equations, which allows an affine system to be transformed into a strict-feedback form.

Consider a general SISO nonlinear dynamic system as

$$\begin{aligned} \dot{x} &= f(x,u) \\ y &= h(x) \end{aligned} \tag{3.1}$$

where $x \in R^n$ is the vector of state variables, $f(x)$ denotes an n-dimensional vector-valued function, $h(x)$ is a single-valued function, $u \in R$ is the control input, and $y \in R$ is the output. The desired objective is to find out in which condition the system (3.1) can be transformed into a system with a structure given by

$$\begin{aligned}
\dot{x}_1 &= f_1(x_1, x_2) \\
\dot{x}_2 &= f_2(x_1, x_2, x_3) \\
&\vdots \\
\dot{x}_{n-1} &= f_{n-1}(x_1, x_2, x_3, ..., x_{n-1}, x_n) \\
\dot{x}_n &= f_n(x_1, x_2, x_3, ..., x_{n-1}, x_n, u) \\
y &= h(x_1, x_2, ..., x_n)
\end{aligned} \tag{3.2}$$

where x_i $(i = 1, 2, ..., n) \in R$ are state variables, $f_i(x)$ $(i = 1, 2, 3, ..., n)$ are single-valued functions, $u \in R$ is the control input, and $y \in R$ is the output. Assume that the functions f_i $(i = 1, 2, ..., n)$ are continuous and differentiable with respect to the argument variables, and the variables $x_2, x_3, ..., x_n, u$ in equation (3.2) are solvable explicitly in terms of the other variables in $f_1, f_2, f_3, ..., f_{n-1}, f_n$, respectively. If system (3.1) satisfies the above requirements, then system (3.2) is called a strict-feedback form of the nonlinear dynamic system.

Through investigation, it is found out that the system (3.1) can be transformed into a system with strict-feedback structure by two steps: 1) state transformations of the system (3.1) into an affine system, and 2) coordinate transformation and feedback selection of the achieved affine system to obtain the strict-feedback form. The first step can always be implemented as in Reference [15] if the function $f(x, u)$ has a

linear term of the control input but, if not, an alternative implementation using the new state vector $\xi = [x\ u]^T$ with new state equation $\dot{u} = v$ where v is the new input and u is considered as a state variable can be achieved. By doing so, system (3.1) can be re-written as an affine form in the new state coordinates and with the new input from References [8], [15], [63]. Thus, the research is centered on how an affine system can be transformed into a strict-feedback form by providing a theorem and proof for clarity.

Consider a n^{th} order SISO affine form of the nonlinear dynamic system as

$$\begin{aligned} \dot{x} &= f(x) + g(x)u \\ y &= h(x) \end{aligned} \tag{3.3}$$

where $x \in R^n$, $f(x)$ and $g(x)$ are n-dimensional vector-valued functions, $u \in R$ is the control input, and $y \in R$ is the output.

Definition 3.1. *(Relative Degree)*

A SISO affine nonlinear system (f, g, h) *in equation* (3.3) *is said to have relative degree* r *at* x^0 *if* $L_g L_f^k h(x) = 0\ \forall\ x \in U^0, k = 0, 1, 2, \cdots, r-2$ *and* $L_g L_f^{(r-1)} h(x^0) \neq 0$*, where* U^0 *denotes a set of neighborhood points of* x^0*.*

The following development provides a theorem and proof regarding the situation in which a SISO affine system (3.3) can be transformed into a controllable linear strict-feedback form via coordinate transformations and state feedback. The proof of the theorem emphasizes a third order SISO affine system but a general order system (3.3) can be extended similarly.

Theorem 3.1. *(Controllable Linear Strict-Feedback Form)*

If the SISO affine nonlinear system (f, g, h) *in equation* (3.3) *has a full relative degree* $r = n$ *at equilibrium* x^0*, then local coordinate transformations*

$$z_i = (-1)^{i-1} L_f^{i-2} h(x) + L_f^{i-1} h(x) \ (i = 1, 2, ..., n)$$

$$\text{where} \tag{3.4}$$

$$L_f^{-1} h(x) = 0, L_f^0 h(x) = h(x)$$

and state feedback with a new input v

$$u = \frac{v - L_f^n h(x)}{L_g L_f^{n-1} h(x)} \tag{3.5}$$

transform the system (3.3) *into a controllable linear strict-feedback form as*

$$\begin{aligned} \dot{z} &= \begin{pmatrix} nz & 1 & 0 & 0 & ... & 0 & 0 \\ nz & nz & 1 & 0 & ... & 0 & 0 \\ \vdots & \vdots & \vdots & \vdots & \ddots & \vdots & \vdots \\ nz & nz & nz & nz & ... & nz & 1 \\ nz & nz & nz & nz & ... & nz & nz \end{pmatrix} z + \begin{pmatrix} 0 \\ 0 \\ \vdots \\ 0 \\ 1 \end{pmatrix} v \\ y &= \begin{pmatrix} 1 & 0 & \dots & 0 & 0 \end{pmatrix} z \end{aligned} \tag{3.6}$$

where $z \in R^n$*, and* nz *denotes a nonzero value.*

Proof. (Proof for a Third Order SISO Affine System)

Local coordinate transformations in equation (3.4) for a third order SISO affine system are written as

$$\begin{aligned} z_1 &= h(x) \\ z_2 &= -h(x) + L_f h(x) \\ z_3 &= L_f h(x) + L_f^2 h(x) \end{aligned} \tag{3.7}$$

Also, state feedback with the new input v in equation (3.5) for a third order SISO affine system is

$$u = \frac{v - L_f^3 h(x)}{L_g L_f^2 h(x)} \tag{3.8}$$

The following development provides proof that the coordinate transformations (3.7) and state feedback with new input v in equation (3.8) can transform a third order SISO affine system into a controllable linear strict-feedback form in equation (3.6) with $n = 3$.

Taking the Lie derivative in time of the first coordinate z_1 of equation (3.7) results in

$$\dot{z}_1 = L_f h(x) + L_g h(x) u \tag{3.9}$$

Using the assumption of a relative degree $r = 3$ or $L_g L_f^k h(x) = 0, \ \forall \ k < 2$ in terms of Definition 3.1 achieves as

$$\dot{z}_1 = L_f h(x) = z_2 + z_1 \equiv \hat{f}(z_1, z_2) \tag{3.10}$$

Taking the Lie derivative in time of the second coordinate z_2 of equation (3.7) results in

$$\dot{z}_2 = -L_f h(x) - L_g h(x) u + L_f^2 h(x) + L_g L_f h(x) u \tag{3.11}$$

Replacing the terms $L_g L_f h(x) = 0$ and $L_g h(x) = 0$ into equation (3.11) results in

$$\dot{z}_2 = -L_f h(x) + L_f^2 h(x) = z_3 - 2(z_2 + z_1) \equiv \hat{f}_2(z_1, z_2, z_3) \tag{3.12}$$

Taking the Lie derivative in time of the third coordinate z_3 of equation (3.7) results

in

$$\dot{z}_3 = L_f^2 h(x) + L_g L_f h(x) u + L_f^3 h(x) + L_g L_f^2 h(x) u \tag{3.13}$$

Replacing the terms $L_g L_f h(x) = 0$ and the state feedback with new input in equation (3.8) into equation (3.13) results in

$$\dot{z}_3 = L_f^2 h(x) + v = z_3 - (z_2 + z_1) + v \equiv \hat{f}_3(z_1, z_2, z_3, v) \tag{3.14}$$

Collecting results from equations (3.10), (3.12), and (3.14), the new model in z_1, z_2, z_3 coordinates is re-written as

$$\begin{aligned} \dot{z} &= \begin{pmatrix} nz & 1 & 0 \\ nz & nz & 1 \\ nz & nz & nz \end{pmatrix} z + \begin{pmatrix} 0 \\ 0 \\ 1 \end{pmatrix} v \\ y &= \begin{pmatrix} 1 & 0 & 0 \end{pmatrix} z \end{aligned} \tag{3.15}$$

or

$$\begin{aligned} \dot{z}_1 &= \hat{f}(z_1, z_2) \\ \dot{z}_2 &= \hat{f}_2(z_1, z_2, z_3) \\ \dot{z}_3 &= \hat{f}_3(z_1, z_2, z_3, v) \end{aligned} \tag{3.16}$$

By state transformations in equation (3.7) and a feedback selection in equation (3.8), the third order SISO affine nonlinear system (f, g, h) represented in equation (3.3) can be transformed to achieve a controllable linear strict-feedback form (3.15) or (3.16), a specific form of strict-feedback systems, as shown in equation (3.2) with $n = 3$, $h(x) = x_1$. Looking at the system (3.15) or (3.16), the controllability matrix of the achieved linear dynamic system is with full rank. Thus, the system in new

coordinates can be written in the controllable linear strict-feedback form (3.6) by coordinate transformations and state feedback with new input.

3.2 BACKSTEPPING CONTROL FORMULATION

This section presents a portion of Reference [64] developed by the author in which a systematic procedure is presented for formulating the backstepping control (BSC) law for the strict-feedback form of nonlinear dynamic systems and then a backstepping control algorithm is proposed. Analysis and design is implemented to show that the performance specifications and stability of the system are achieved with high reliability. The research starts with the concept where backstepping design is seen as a recursive design process which breaks a design problem on the full system down to a sequence of sub-problems on lower order systems. Considering each lower order system with a Lyapunov function and paying attention to the interaction between two subsystems makes the process modular and easy to design the stabilizing controller. A third order SISO strict-feedback system is addressed for formulating the stabilizing control law but a general form of n^{th} order can be extended similarly.

Consider a third order SISO strict-feedback form of a nonlinear dynamic system as

$$\begin{aligned} \dot{x_1} &= f_1(x_1, x_2) \\ \dot{x_2} &= f_2(x_1, x_2, x_3) \\ \dot{x_3} &= f_3(x_1, x_2, x_3, u) \end{aligned} \tag{3.17}$$

where $x \in R^3$ is the vector of state variables, $f(x)$ is a three-dimensional vector of

scalar-valued functions, and $u \in R$ is the scalar control input.

Assume that the function f_i $(i = 1, 2, 3)$ is continuous and differentiable with respect to the variables and the variables x_2, x_3, u in equation (3.17) are solvable explicitly in terms of the other variables in the first, second, and third equations, respectively. The objective is to design a control law for the strict-feedback form of the nonlinear dynamic system (3.17) such that the output $y = h(x) = x_1 \longrightarrow x_{ref}$ asymptotically where x_{ref} is a constant, and global asymptotic stability is achieved with zero or acceptably small overshoot in the system response.

The backstepping control law for the strict-feedback structure is formulated by dividing the whole system into n subsystems such that the i^{th} subsystem consists of the $(i-1)^{th}$ subsystem plus an extra state and the n^{th} subsystem is the original n^{th} order system via coordinate transformations and state feedbacks. By consecutively applying the coordinate transformation and choosing a feedback law via the control Lyapunov function for each subsystem from the lowest to highest order and re-writing the feedback law in the original coordinates, the resulting controllers make the original deficient system a well-tracking and asymptotically globally stable system. The following steps are used for formulating the BSC law for the system (3.17).

Step 1.

The x_2 variable is regarded as a control input of the first relation in equation (3.17) which is considered as the first subsystem. Thus, x_2 is chosen to make the first subsystem globally asymptotically stable. The chosen function is called a virtual

control law. By introducing ξ_1 (an error signal) as

$$\xi_1 = x_1 - x_{ref} \tag{3.18}$$

and by differentiating both sides of equation (3.18) in time and combining with the first subsystem of equation (3.17),

$$\dot{\xi}_1 = \dot{x_1} = f_1(\xi_1 + x_{ref}, x_2) \tag{3.19}$$

For the system (3.19), a CLF can be chosen such that when the virtual control law is applied, its time derivative becomes negatively definite. The function is chosen as

$$V_1(\xi_1) = \frac{1}{2}{\xi_1}^2 \tag{3.20}$$

By taking the derivative in time of equation (3.20) and combining with equation (3.19), one finds the result

$$\dot{V_1}(\xi_1) = \xi_1\dot{\xi_1} = \xi_1 f_1(\xi_1 + x_{ref}, x_2) \tag{3.21}$$

By satisfying the asymptotically stable condition in the sense of Lyapunov in Theorem 2.2 for equation (3.21), a virtual control law denoted as α_1 for x_2 can be chosen as

$$\begin{aligned} -c_1\xi_1 &= f_1(\xi_1 + x_{ref}, x_2) \\ \Rightarrow x_2 &\equiv \alpha_1(c_1, x_1, x_{ref}) \end{aligned} \tag{3.22}$$

where c_1 is a positive gain. By doing so, the CLF derivative is negatively definite, or

$$\dot{V_1}(\xi_1) = \xi_1\dot{\xi_1} = -c_1\xi_1^2 < 0 \;\forall\; \xi_1 \neq 0 \tag{3.23}$$

Step 2.

By choosing the state feedback in equation (3.22) and a change of coordinate indicated below

$$\xi_2 = x_2 - \alpha_1(c_1, x_1, x_{ref}) \tag{3.24}$$

the second subsystem can be re-written as follows

$$\begin{aligned} \dot{\xi}_1 &= -c_1\xi_1 \\ \dot{\xi}_2 &= f_2(\xi_1 + x_{ref}, \xi_2 + \alpha_1, x_3) - \dot{\alpha}_1 \end{aligned} \tag{3.25}$$

A CLF $V_2(\xi_1, \xi_2)$ can be chosen such that it makes the subsystem in equation (3.25) asymptotically stable with the virtual control law, i.e.

$$V_2(\xi_1, \xi_2) = V_1(\xi_1) + \frac{1}{2}\xi_2^2 \tag{3.26}$$

By taking the derivative in time of equation (3.26) and combining with equation (3.25), one finds the result

$$\dot{V}_2(\xi_1, \xi_2) = -c_1\xi_1^2 + \xi_2\{f_2(\xi_1 + x_{ref}, \xi_2 + \alpha_1, x_3) - \dot{\alpha}_1\} \tag{3.27}$$

To meet the asymptotically stable condition in the sense of Lyapunov in Theorem 2.2 for equation (3.27), a virtual control law denoted as α_2 for x_3 can be chosen such that

$$\begin{aligned} -c_2\xi_2 &= f_2(\xi_1 + x_{ref}, \xi_2 + \alpha_1, x_3) - \dot{\alpha}_1 \\ \Rightarrow x_3 &\equiv \alpha_2(c_1, c_2, x_1, x_2, x_{ref}) \end{aligned} \tag{3.28}$$

where c_2 is a positive gain. By doing so, the CLF derivative is again negatively definite, or

$$\dot{V}_2(\xi_1, \xi_2) = -c_1\xi_1^2 - c_2\xi_2^2 < 0 \ \forall \ \xi_1, \xi_2 \neq 0 \tag{3.29}$$

Step 3.

By choosing the state feedbacks in equation (3.22) and equation (3.28), a change of coordinate as in equation (3.18) and equation (3.24), and the transformation below

$$\xi_3 = x_3 - \alpha_2(c_1, c_2, x_1, x_2, x_{ref}) \tag{3.30}$$

the third subsystem can be re-written as follows

$$\begin{aligned} \dot{\xi}_1 &= -c_1\xi_1 \\ \dot{\xi}_2 &= -c_2\xi_2 \\ \dot{\xi}_3 &= f_3(\xi_1 + x_{ref}, \xi_2 + \alpha_1, \xi_3 + \alpha_2, u) - \dot{\alpha}_2 \end{aligned} \tag{3.31}$$

A CLF $V_3(\xi_1, \xi_2, \xi_3)$ can be chosen such that it makes the system in equation (3.31) asymptotically stable with the associated control law. The CLF function is

$$V_3(\xi_1, \xi_2, \xi_3) = V_2(\xi_1, \xi_2) + \frac{1}{2}\xi_3^2 \tag{3.32}$$

Taking the time derivative of equation (3.32) and combining with equation (3.31) results in

$$\dot{V}_3(\xi_1, \xi_2, \xi_3) = -c_1\xi_1^2 - c_2\xi_2^2 + \xi_3\{f_3(\xi_1 + x_{ref}, \xi_2 + \alpha_1, \xi_3 + \alpha_2, u) - \dot{\alpha}_2\} \tag{3.33}$$

To meet the asymptotically stable condition in the sense of Lyapunov in Theorem 2.2 for equation (3.33), a control law u called the backstepping controller can be chosen

such that

$$\begin{aligned} -c_3\xi_3 &= f_3(\xi_1 + x_{ref}, \xi_2 + \alpha_1, \xi_3 + \alpha_2, u) - \dot{\alpha}_2 \\ \Rightarrow u &\equiv \alpha_3(c_1, c_2, c_3, x_1, x_2, x_3, x_{ref}) \end{aligned} \tag{3.34}$$

where c_3 is a positive gain. By doing so, the required sign condition on $\dot{V}_3(\xi_1, \xi_2, \xi_3)$ is achieved.

$$\dot{V}_3(\xi_1, \xi_2, \xi_3) = -c_1\xi_1^2 - c_2\xi_2^2 - c_3\xi_3^2 < 0 \; \forall \; \xi_1, \xi_2, \xi_3 \neq 0 \tag{3.35}$$

Thus, there exists a CLF in equation (3.32), state feedback laws in equations (3.22), (3.28) and (3.34), and a change of state transformations in equations (3.18), (3.24) and (3.30), such that the system (3.17) is transformed into the following form.

$$\begin{aligned} \dot{\xi}_1 &= -c_1\xi_1 \\ \dot{\xi}_2 &= -c_2\xi_2 \\ \dot{\xi}_3 &= -c_3\xi_3 \end{aligned} \tag{3.36}$$

By looking at the system in equation (3.36), it is clear that the input-output decoupling problem for the nonlinear system (3.17) can be obtained by coordinate transformations and a feedback control law and it is also easy to figure out that the system (3.36) is asymptotically globally stable and converges to zero with positive gains and the response of the system has no overshoot. The desired settling time and rise time of the system are obtained by gain selection. Thus, the stability and performance specifications on the system (3.17) are achieved with the proposed BSC law. Figure 3.1 shows the block diagram of the proposed backstepping control logic for the third order strict-feedback structure of nonlinear dynamic systems.

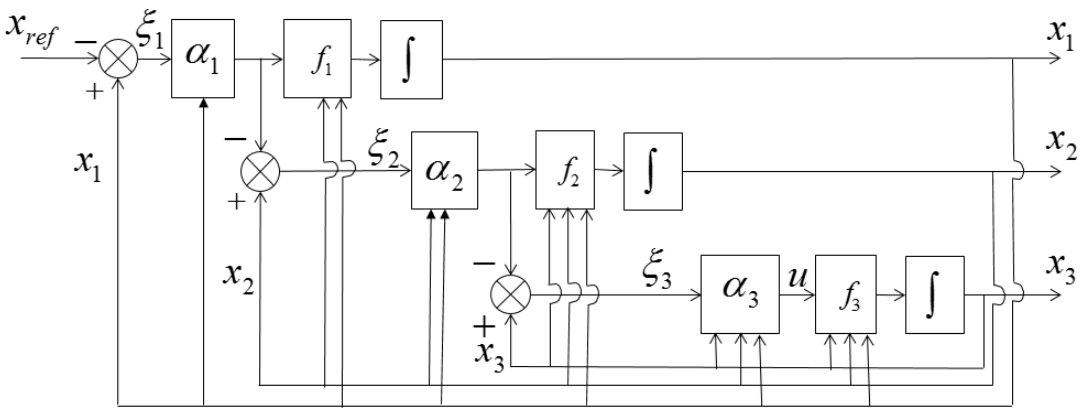

Figure 3.1: BSC Law for Third Order Generalized Strict-Feedback System

In order to implement the block diagram of the proposed control law, assume that the variable states x_1, x_2, x_3 used for state feedbacks can be obtained from the sensor systems. From the input command, a virtual control law α_1 is applied to achieve the performance specifications of the first subsystem. The output of control law α_1 is considered as a command for the second subsystem and a second virtual control law α_2 is created to achieve desired command α_1. The output of control law α_2 is considered as a command for the complete system (third subsystem) and a real control input u, obtained from the control law α_3, is applied to achieve desired command α_2. By doing so, the real control input u makes the output x_1 track the command x_{ref} asymptotically.

3.3 INTEGRATOR-BACKSTEPPING CONTROL FORMULATION

This section investigates an integrator-backstepping control (IBSC) methodology for a strict-feedback form of nonlinear dynamic systems in the presence of model parameter errors. A systematic procedure is addressed firstly for formulating the

IBSC law for the strict-feedback model. Formulation starts with a definition of modified tracking error by adding an integral term to the normal tracking error, and then a recursive sequence of coordinate transformations and Lyapunov function based feedback selections results in an IBSC law to make the system well-behaved in tracking and asymptotically stable. A control design algorithm is provided by the author to improve the stability, command tracking, and robustness of a high-performance aircraft in the presence of unmodeled dynamics in Reference [65].

Consider a third order SISO strict-feedback model as follows

$$\begin{aligned} \dot{x_1} &= f_1(\hat{\delta}, x_1, x_2) \\ \dot{x_2} &= f_2(\hat{\delta}, x_1, x_2, x_3) \\ \dot{x_3} &= f_3(\hat{\delta}, x_1, x_2, x_3, u) \end{aligned} \tag{3.37}$$

where $x \in R^3, f_i(x)$ $(i = 1, 2, 3)$ are scalar-valued functions of the nonlinear dynamics, $u \in R$ is a control input, and $\hat{\delta}$ is a vector of known parameters of the model. The unknown parameters δ in the system are approximated by known constant parameters $\hat{\delta}$. Assume that system (3.37) has a relative degree $r = 3$ and the x_2, x_3, u variables are solvable explicitly in terms of other variables in the backstepping subsystems, respectively.

The objective is to design a control law for the parameterized strict-feedback system (3.37) such that the output $x_1 \to x_{ref}$ asymptotically where x_{ref} is a constant, and global asymptotic stability is achieved with zero or acceptably small overshoot in the system in the presence of the model parameter errors. The following steps are used for formulating the IBSC law for system (3.37).

Step 1.

The state variable x_2 is regarded as a control input of the first relation in equation (3.37) which is considered as the first subsystem. Thus, x_2 is chosen to make the first subsystem globally asymptotically stable. The chosen α_1 function for x_2 is called a virtual control law. Introduce a modified tracking error ξ_1 as

$$\xi_1 = (x_1 - x_{ref}) + \sigma \tag{3.38}$$

where $\sigma = c_0 \int_0^t e(\tau)d\tau, e(t) = x_1 - x_{ref}$, and $e(t)$ is defined as the normal tracking error and c_0 is a positive gain. Differentiating both sides of equation (3.38) in time and combining with the first subsystem of equation (3.37),

$$\dot{\xi}_1 = \dot{x}_1 + \dot{\sigma} = f_1(\hat{\delta}, \xi_1 + x_{ref} - \sigma, x_2) + \dot{\sigma} \tag{3.39}$$

For the system (3.39), a CLF $V_1(\xi_1)$ in terms of Definition 2.8 can be chosen such that when the virtual control law is applied, its time derivative becomes negatively definite. The positive definite function is chosen as

$$V_1(\xi_1) = \frac{1}{2}{\xi_1}^2 \tag{3.40}$$

Taking the derivative in time of equation (3.40) and combining with equation (3.39), one achieves

$$\dot{V}_1(\xi_1) = \xi_1\dot{\xi}_1 = \xi_1[f_1(\hat{\delta}, \xi_1 + x_{ref} - \sigma, x_2) + \dot{\sigma}] \tag{3.41}$$

By satisfying the asymptotically stable condition in the sense of Lyapunov in Theorem 2.2 for equation (3.41), a virtual control law denoted as α_1 for x_2 can be chosen

as

$$\begin{aligned} -c_1\xi_1 &= f_1(\hat{\delta}, \xi_1 + x_{ref} - \sigma, x_2) + \dot{\sigma} \\ \Rightarrow x_2 &\equiv \alpha_1(\hat{\delta}, c_0, c_1, x_1, x_{ref}, \sigma) \end{aligned} \tag{3.42}$$

where c_1 is the positive gain. By doing so, the CLF derivative is negatively definite.

$$\dot{V}_1(\xi_1) = \xi_1\dot{\xi}_1 = -c_1\xi_1^2 < 0 \; \forall \; \xi_1 \neq 0 \tag{3.43}$$

Step 2.

By choosing the state feedback in equation (3.42) and a change of coordinate indicated below

$$\xi_2 = x_2 - \alpha_1(\hat{\delta}, c_0, c_1, x_1, x_{ref}, \sigma) \tag{3.44}$$

the second subsystem can be re-written as follows

$$\begin{aligned} \dot{\xi}_1 &= -c_1\xi_1 \\ \dot{\xi}_2 &= f_2(\hat{\delta}, \xi_1 + x_{ref} - \sigma, \xi_2 + \alpha_1, x_3) - \dot{\alpha}_1 \end{aligned} \tag{3.45}$$

where $\dot{\alpha}_1$ is determined as functions of the c_0, c_1 gains, the x_1 state, and x_{ref} command, and known parameters $\hat{\delta}$. The state variable x_3 is regarded as a control input in equation (3.45) and a CLF $V_2(\xi_1, \xi_2)$ can be chosen such that it makes the subsystem in equation (3.45) asymptotically stable with the virtual control law, i.e.,

$$V_2(\xi_1, \xi_2) = V_1(\xi_1) + \frac{1}{2}\xi_2^2 \tag{3.46}$$

By taking the derivative in time of equation (3.46) and combining with equation (3.45), one finds the result

$$\dot{V}_2(\xi_1, \xi_2) = -c_1\xi_1^2 + \xi_2\{f_2(\hat{\delta}, \xi_1 + x_{ref} - \sigma, \xi_2 + \alpha_1, x_3) - \dot{\alpha}_1\} \tag{3.47}$$

To meet the asymptotically stable condition in the sense of Lyapunov in Theorem 2.2 for equation (3.47), a virtual control law denoted as α_2 for x_3 can be chosen such that

$$\begin{aligned} -c_2\xi_2 &= f_2(\hat{\delta}, \xi_1 + x_{ref} - \sigma, \xi_2 + \alpha_1, x_3) - \dot{\alpha}_1 \\ \Rightarrow x_3 &\equiv \alpha_2(\hat{\delta}, c_0, c_1, c_2, x_1, x_2, x_{ref}, \sigma) \end{aligned} \tag{3.48}$$

where c_2 is a positive gain. By doing so, the CLF derivative is negatively definite.

$$\dot{V}_2(\xi_1, \xi_2) = -c_1\xi_1^2 - c_2\xi_2^2 < 0 \ \forall \ \xi_1, \xi_2 \neq 0 \tag{3.49}$$

Step 3.

By choosing the state feedback in equation (3.42) and equation (3.48), and a change of coordinate as in equation (3.38) and equation (3.44), and the transformation below

$$\xi_3 = x_3 - \alpha_2(\hat{\delta}, c_0, c_1, c_2, x_1, x_2, x_{ref}, \sigma) \tag{3.50}$$

the final subsystem (complete system) can be re-written as follows

$$\begin{aligned} \dot{\xi}_1 &= -c_1\xi_1 \\ \dot{\xi}_2 &= -c_2\xi_2 \\ \dot{\xi}_3 &= f_3(\hat{\delta}, \xi_1 + x_{ref} - \sigma, \xi_2 + \alpha_1, \xi_3 + \alpha_2, u) - \dot{\alpha}_2 \end{aligned} \tag{3.51}$$

where $\dot{\alpha}_2$ is determined as functions of the c_0, c_1, c_2 gains, the x_1, x_2 states, x_{ref} command, and known parameters $\hat{\delta}$. A CLF $V_3(\xi_1, \xi_2, \xi_3)$ in terms of Definition 2.8 can be chosen such that it makes the system in equation (3.51) asymptotically stable with the associated control law. The CLF function in terms of Definition 2.8 is

$$V_3(\xi_1, \xi_2, \xi_3) = V_2(\xi_1, \xi_2) + \frac{1}{2}\xi_3^2 \tag{3.52}$$

Taking the derivative of equation (3.52) in time and combining with equation (3.51) results in

$$\dot{V}_3(\xi_1, \xi_2, \xi_3) = -c_1\xi_1^2 - c_2\xi_2^2 + \xi_3\{f_3(\hat{\delta}, \xi_1 + x_{ref} - \sigma, \xi_2 + \alpha_1, \xi_3 + \alpha_2, u) - \dot{\alpha}_2\} \tag{3.53}$$

To meet the asymptotically stable condition in the sense of Lyapunov in Theorem 2.2 for equation (3.53), a control law u called the integrator-backstepping controller can be chosen such that

$$\begin{aligned} -c_3\xi_3 &= f_3(\hat{\delta}, \xi_1 + x_{ref} - \sigma, \xi_2 + \alpha_1, \xi_3 + \alpha_2, u) - \dot{\alpha}_2 \\ \Rightarrow u &\equiv \alpha_3(\hat{\delta}, c_0, c_1, c_2, c_3, x_1, x_2, x_3, x_{ref}, \sigma) \end{aligned} \tag{3.54}$$

where c_3 is a positive gain. By doing so, the required sign condition on $\dot{V}_3(\xi_1, \xi_2, \xi_3)$ is achieved.

$$\dot{V}_3(\xi_1, \xi_2, \xi_3) = -c_1\xi_1^2 - c_2\xi_2^2 - c_3\xi_3^2 < 0 \ \forall \ \xi_1, \xi_2, \xi_3 \neq 0 \tag{3.55}$$

Thus, there exists a CLF in terms of Definition 2.8 in equation (3.52), state feedback laws in equations (3.42), (3.48) and (3.54), and changes of state transformations in equations (3.38), (3.44) and (3.50), such that the system is transformed into a state decoupled linear system as

$$\begin{aligned} \dot{\xi}_1 &= -c_1\xi_1 \\ \dot{\xi}_2 &= -c_2\xi_2 \\ \dot{\xi}_3 &= -c_3\xi_3 \end{aligned} \tag{3.56}$$

By examining the system in equation (3.56), the state decoupling problem for the nonlinear system (3.37) can be obtained by coordinate transformations and feedback

control laws, and it is also easy to conclude that the state variable responses in the new coordinates are global asymptotically stable with positive gains. Therefore, the output response in the original coordinate of the system (3.37) is global asymptotically stable; however, the conclusion that this output converges to the command signal requires further analysis. Combining the modified tracking error in (3.38) and the stabilized condition $\xi_1 = 0$ results in

$$(x_1 - x_{ref}) + \sigma = 0 \tag{3.57}$$

Equation (3.57) can be re-written as

$$e(t) + c_0 \int_0^t e(\tau) d\tau = 0 \tag{3.58}$$

Thus, taking the derivative in time on both sides of the equation (3.58) yields

$$\dot{e}(t) = -c_0 e(t) \tag{3.59}$$

By examining the system in equation (3.59), the normal error converges to zero with every positive gain c_0, implying the output in the original coordinate converges to the command signal. The desired settling time and rise time of the system are obtained by an optimization algorithm in Reference [52]. Thus, the stability and performance specifications on the system in (3.37) are achieved with the proposed IBSC law. The integrator-backstepping control strategy is illustrated in Figure 3.2. In this approach, a virtual control law α_1 for the first subsystem is designed to enforce the output x_1 to asymptotically track the command x_{ref}. For the second subsystem, the virtual control law α_1 is considered a command and the second virtual control law α_2 for the second subsystem is designed to enforce the state x_2 to asymptotically track

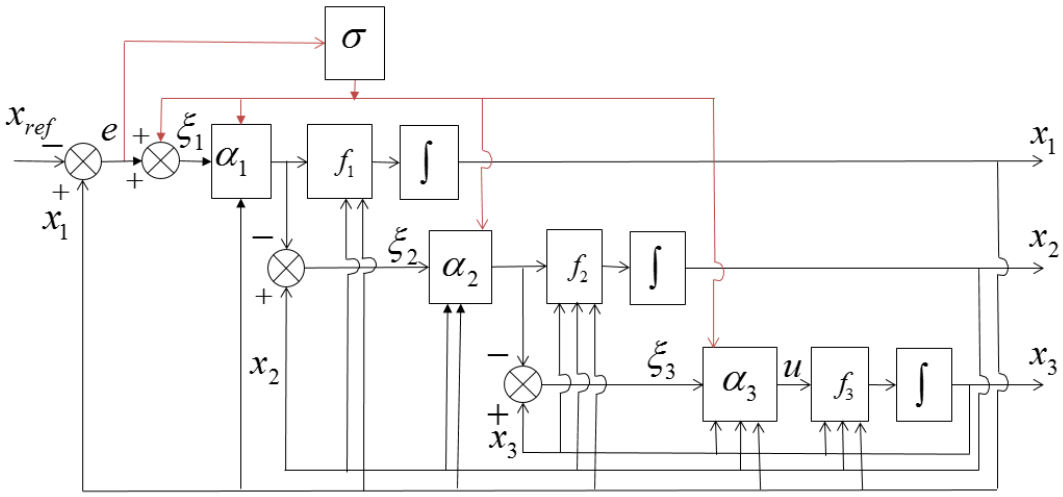

Figure 3.2: IBSC Law for Third Order Generalized Strict-Feedback System

the virtual command α_2. For the complete system, the virtual control law α_2 is considered a command, and the real control law u for the complete system, obtained from control law α_3, is designed to enforce the state x_3 to asymptotically track the virtual command α_2. By doing so, the output is logically augmented by the real control input via virtual control laws.

3.4 EXAMPLE

Consider a second order dynamic system from Reference [47] as

$$\begin{aligned} \dot{x}_1 &= x_2 \\ \dot{x}_2 &= ax_1^2 + bx_2 + cx_2^3 + u \\ y &= h(x) = x_1 \end{aligned} \tag{3.60}$$

where the variables $x_1, x_2 \in R$ are state variables, $y \in R$ is the output, and u is a control input. The constants a, b, c are assumed to be unknown, but bounded with

known bounds.

The objective is to design a control law for the system (3.60) with unknown constants a, b, c approximated by known $\hat{a}, \hat{b}, \hat{c}$ respectively such that the output $y = x_1 \to x_{ref}$ asymptotically where x_{ref} is a constant, and global asymptotic stability is achieved with zero or acceptably small overshoot in the system in the presence of the model parameter errors. By using the previously proposed backstepping control methodology in Section 3.2, the backstepping control law for the system (3.60) is achieved as

$$u = -c_1 c_2 e - (c_1 + c_2)x_2 - \hat{a}x_1^2 - \hat{b}x_2 - \hat{c}x_2^3 \tag{3.61}$$

By using the proposed integrator-backstepping control methodology in Section 3.3, the integrator-backstepping control law for the system (3.60) is achieved as

$$u = -k_0\sigma - k_1 e - k_2 x_2 - \hat{a}x_1^2 - \hat{b}x_2 - \hat{c}x_2^3 \tag{3.62}$$

where $e = x_1 - x_{ref}, \sigma = c_0 \int_0^t e(\tau)d\tau, k_0 = c_0c_1c_2, k_1 = c_0c_1 + c_0c_2 + c_1c_2, k_2 = c_0 + c_1 + c_2, k_3 = c_0c_1 + c_0c_2$, and c_0, c_1, c_2 are positive gains.

The achieved control laws in equations (3.61) and (3.62) are substituted in equation (3.60) and a closed-loop system is achieved for validating and demonstrating the proposed control methodology. The closed-loop simulations are implemented for three cases described below.

Case 1: Without System Parameter Errors

Figure 3.3 shows the system time response for a step command in which the expressions $a = \hat{a}, b = \hat{b}, c = \hat{c}$ hold, or no system parameter errors occurs. The results show that the performance specifications can be achieved with the BSC-based control design. Results were generated with the following numeric values: $a = 0.6, b = 2.5, c = 0.1$, and $c_1 = 1.3, c_2 = 1.4, x_{ref} = 1$, and initial states $x_1(0) = x_2(0) = 0$.

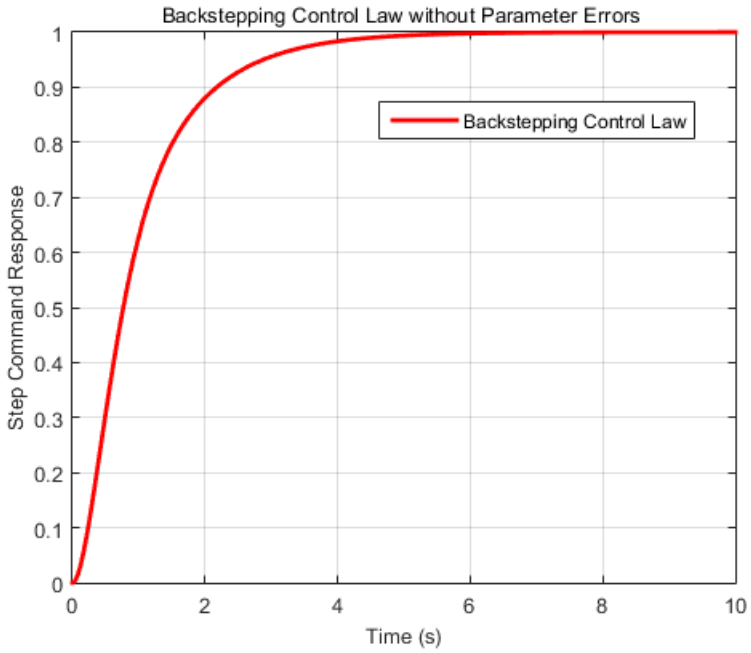

Figure 3.3: BSC without Parameter Errors

Case 2: With System Parameter Errors

In this case, numerical values used in the simulation are $a = 0.6, b = 2.5, c = 0.1, \hat{a} = 1, \hat{b} = 2, \hat{c} = 0, x_1(0) = x_2(0) = \sigma(0) = 0, x_{ref} = 1$. The simulations are implemented for both types of control laws for comparison. The simulation results

are shown in Figure 3.4. Figure 3.4 shows the closed-loop time response due to a step command in which the red or solid line presents the backstepping controller result and the blue or dash line presents the integrator-backstepping result. Results show that the response yields steady state error in the presence of parameter errors when the BSC-based control law is applied. Further, this error offset can be eliminated when IBSC-based control is applied.

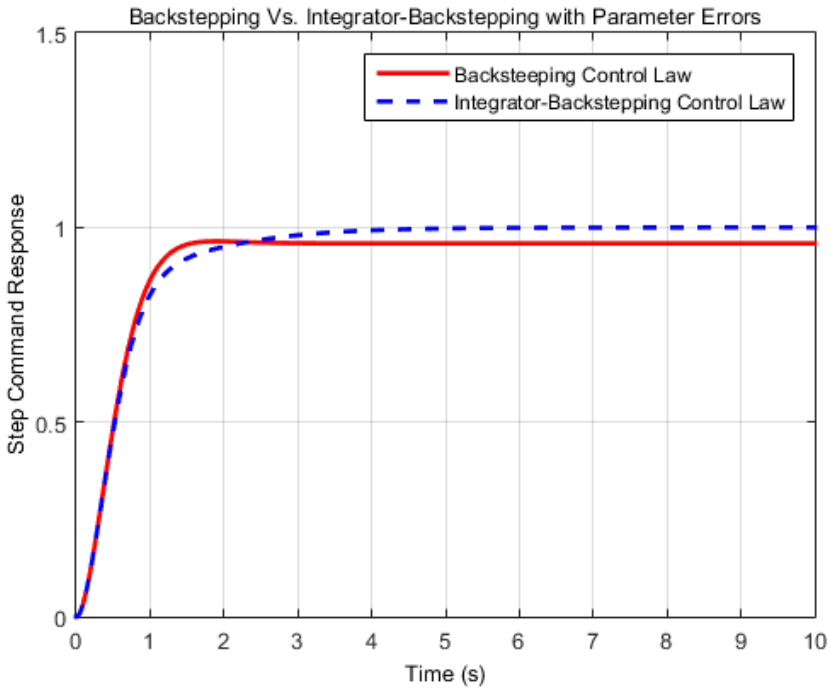

Figure 3.4: BSC vs. IBSC with Parameter Errors

Case 3: With Disturbance (No Parameter Errors)

In this case, a constant disturbance $d = 0.5$ is applied to the $\dot{x}_1$ governing equation after $t = 5\ s$. Numeric values for all other parameters, gains, initial conditions, and command are unchanged from Case 1. The simulation results in Figure 3.5 show that the integrator-backstepping control is able to recover and maintain the performance

and stability of the system in the presence of an external disturbance. The red line (or solid line) in Figure 3.5 shows the degraded time response when using the BSC-based logic when a disturbance with constant magnitude is present. The blue line (dash line) in Figure 3.5 shows the effectiveness of IBSC-based logic in rejecting the disturbance. The result shows that the tracking requirement is recovered after three seconds.

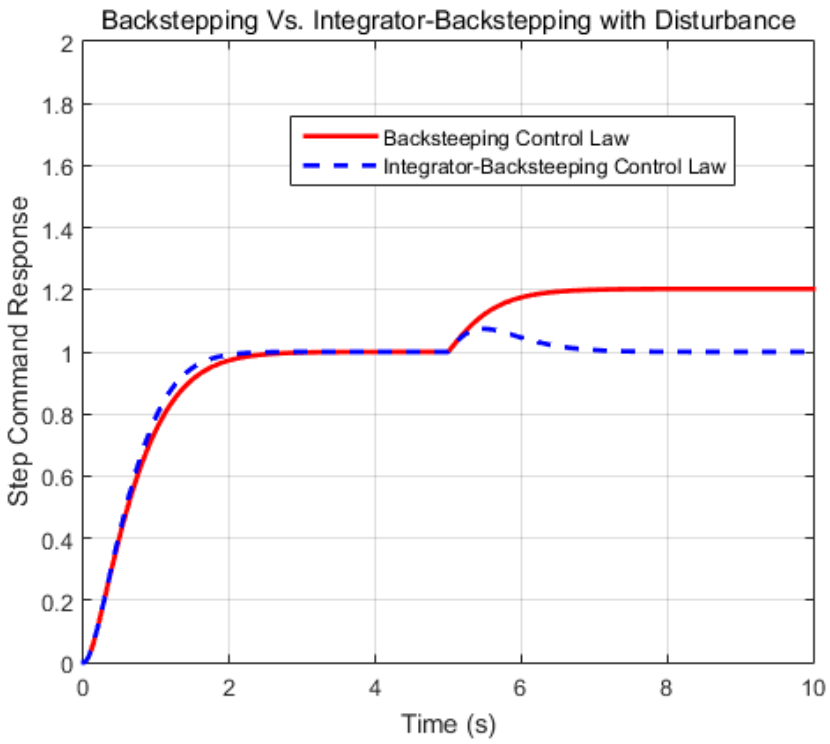

Figure 3.5: BSC vs. IBSC with Disturbance

3.5 SUMMARY AND DISCUSSION

In this chapter, the concepts and usefulness of the strict-feedback form of engineering systems is provided and analyzed. The research shows that a nonlinear dynamic system can be transformed into a strict-feedback form if it is able to be

transformed into an affine system and have a full relative degree. Then a systematic procedure is presented in order to show how a backstepping control law can be synthesized for the strict-feedback form of nonlinear dynamic systems. For the derived BSC law, numerical simulation testing was conducted and analyzed. In order to eliminate the deficiencies of the BSC-based design, the concept of modified error is then introduced. With similar steps as before, a systematic approach is presented for synthesizing the integrator-backstepping control law for the strict-feedback form of nonlinear dynamic systems in the presence of parameter errors. Also, the block diagram of both the BSC-based and IBSC-based control designs are provided for analysis and applications. Testing demonstrated the advancements and improvements with the modified logic.

The research shows that there are drawbacks of the backstepping-based control design. Firstly, the design model must be in strict-feedback form, which is not always obtainable with engineering systems. Usually, some assumptions on system parameters have to be considered to achieve this approximated model structure for the control design process. Secondly, approximated model parameters appear in the feedback control law. Thus, model parameter errors, or disturbances, may lead to degraded performance or even instability. This drawback can be eliminated by an integrator-backstepping-based control design. The feasibility of the proposed approaches is validated and analyzed for nonlinear flight dynamic systems in Chapter 4, Chapter 5, Chapter 6, and Chapter 7.

CHAPTER 4

BACKSTEPPING CONTROL FOR FLIGHT DYNAMICS

This chapter addresses a backstepping-based control algorithm for flight path angle control corresponding to the longitudinal dynamics of a high-performance aircraft simulation model. In the first section, some assumptions on aerodynamic forces of the aircraft are made to transform the aircraft dynamic model into a necessary canonical backstepping form for direct applicability to the developed control theoretic framework provided in Section 3.2 in Chapter 3. In the second section, a systematic procedure is provided for formulating the backstepping control law of nonlinear longitudinal aircraft dynamics. With the achieved BSC law, a block diagram and control strategy are provided for nonlinear closed-loop simulation. In the third section, the research is validated via a numerical study of flight path angle control of an F-16 aircraft model. Finally, some conclusions are made and discussed to point out the advantages and disadvantages of the control strategy research.

4.1 LONGITUDINAL DYNAMICS MODEL

Figure 4.1 shows the components of longitudinal aircraft dynamics. Using Section 2.2 in Chapter 2 for the governing EOMs of aircraft longitudinal dynamics in equation

(2.26), a mathematical model of nonlinear longitudinal dynamics can be written as

$$\begin{aligned}
\dot{V}_T &= \frac{1}{m}(-D + F_T cos\alpha - mgsin\gamma) \\
\dot{\gamma} &= \frac{1}{mV_T}(L + F_T sin\alpha - mgcos\gamma) \\
\dot{\theta} &= q \\
\dot{q} &= \frac{1}{I_y}(M + F_T z_{TF})
\end{aligned} \tag{4.1}$$

where

$$L = \frac{1}{2}\rho V_T^2 S C_L, D = \frac{1}{2}\rho V_T^2 S C_D, F_T = \frac{1}{2}\rho V_T^2 S C_T$$

Variables and parameters appearing in equation (4.1) include V_T: aircraft velocity, m: total mass of aircraft, $L(\alpha, V_T, q)$: lift force, $D(\alpha, V_T, q)$: drag force, $M(\alpha, q, \delta_E, V_T)$: pitch moment, $F_T(\delta_{th})$: thrust force, α: angle of attack, γ: flight path angle, θ: pitch angle, q: pitch rate, δ_{th}: throttle, δ_E: pitch control (elevator or horizontal vane), I_y: inertial moment about y axis of aircraft, z_{TF}: thrust point offset, g: gravity, ρ: density of air, S: reference area, C_L: lift coefficient, C_D: drag coefficient, C_T: thrust coefficient.

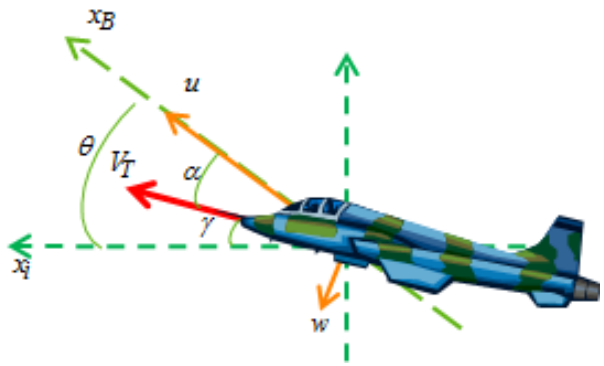

Figure 4.1: Aircraft Model of Longitudinal Motion

Some assumptions are considered to assist in transforming the aircraft model in equation (4.1) to the structure in equation (3.17): airspeed of aircraft is constant, i.e., $\dot{V}_T = 0$; lift force is a sinusoidal function of the angle of attack or $L = \tilde{L}\sin\alpha$, where $\tilde{L}$ is constant for a designated flight condition; thrust force is constant for the controller design purpose; and neglection of wind velocities is also considered for simplicity.

With these assumptions, the mathematical model of longitudinal motion of the aircraft is re-written as

$$\begin{aligned} \dot{\gamma} &= \frac{1}{mV_T}([\tilde{L} + F_T]sin\alpha - mgcos\gamma) \\ \dot{\theta} &= q \\ \dot{q} &= u \end{aligned} \tag{4.2}$$

where

$$u = \frac{1}{I_y}(M + F_T z_{TF})$$

For the aircraft longitudinal motion, the relationship between the flight path angle, pitch angle, and attack angle is represented as

$$\alpha = \theta - \gamma \tag{4.3}$$

By combining equations (4.3) and (4.1), the mathematical model of the aircraft longitudinal dynamics can be further changed to

$$\begin{aligned} \dot{\gamma} &= \frac{1}{mV_T}([\tilde{L} + F_T]sin(\theta - \gamma) - mgcos\gamma) \\ \dot{\theta} &= q \\ \dot{q} &= u \end{aligned} \tag{4.4}$$

Note that the system in equation (4.4) possesses the strict-feedback form (or lower triangular form) similar to the system (3.17) with the above assumptions. The next step is to design the backstepping controller using the aforementioned theory described in Section 3.2 in Chapter 3.

4.2 CONTROL LAW FORMULATION

The given problem is to design a control law that is required to keep flight path angle (γ) of the aircraft at a prescribed reference value (γ_{ref}) or to follow a command value, satisfy the performance specifications with zero or small overshoot and short settling time, and obtain high precision and stability. By using the method from Section 3.2 in Chapter 3, the complete system in equation (4.4) is divided into three subsystems. The first consists of the first relation of equation (4.4), the second consists of the first two relations of equation (4.4), and the last consists of the whole system in equation (4.4). After applying the backstepping method with each subsystem, as previously noted above, the resulting BSC is proven to possess globally asymptotic stability using the CLF and Theorem 2.2. The following development is the procedure to get the BSC law with a desired flight path angle of γ_{ref}.

Step 1.

Consider the first subsystem and introduce the flight path error signal

$$\tilde{\gamma} = \gamma - \gamma_{ref} \tag{4.5}$$

Taking the time derivative of both sides of equation (4.5) and combining with equation (4.4) results in

$$\dot{\tilde{\gamma}} = \dot{\gamma} = \frac{1}{mV_T}([\tilde{L} + F_T]sin(\theta - \tilde{\gamma} - \gamma_{ref}) - mgcos(\tilde{\gamma} + \gamma_{ref})) \tag{4.6}$$

For equation (4.6), a CLF $V_1(\tilde{\gamma})$ can be chosen such that when the virtual control law α_1 for θ is applied, its time derivative becomes negatively definite. The chosen function mathematically is

$$V_1(\tilde{\gamma}) = \frac{1}{2}\tilde{\gamma}^2 \tag{4.7}$$

By taking the time derivative of equation (4.7) and combining with equation (4.6), one finds

$$\dot{V}_1(\tilde{\gamma}) = \tilde{\gamma}\dot{\tilde{\gamma}} = \tilde{\gamma}(\frac{1}{mV_T}([\tilde{L} + F_T]sin(\theta - \tilde{\gamma} - \gamma_{ref}) - mgcos(\tilde{\gamma} + \gamma_{ref}))) \tag{4.8}$$

By satisfying the asymptotically stable condition in the sense of Lyapunov in Theorem 2.2 for equation (4.8), the virtual control can be chosen with the following logic where c_1 is a positive gain.

$$\begin{aligned} -c_1\tilde{\gamma} &= \frac{1}{mV_T}([\tilde{L} + F_T]sin(\theta - \tilde{\gamma} - \gamma_{ref}) - mgcos(\tilde{\gamma} + \gamma_{ref})) \\ \Rightarrow \theta_{ref} \equiv \alpha_1(c_1, \gamma, \gamma_{ref}) &= \gamma + arcsin\frac{1}{\tilde{L} + F_T}[-mV_Tc_1(\gamma - \gamma_{ref}) + mgcos\gamma] \end{aligned} \tag{4.9}$$

By doing so, the correct definiteness condition is satisfied.

$$\dot{V}_1(\tilde{\gamma}) = \tilde{\gamma}\dot{\tilde{\gamma}} = -c_1\tilde{\gamma}^2 < 0, \ \forall \ \tilde{\gamma} \neq 0 \tag{4.10}$$

Step 2.

By choosing the state feedback to be from equation (4.9) and using the change of state transformation in equation (4.5), and the transformation below

$$\tilde{\theta} = \theta - \alpha_1(c_1, \gamma, \gamma_{ref}) \tag{4.11}$$

the second subsystem can be re-written as

$$\begin{aligned} \dot{\tilde{\gamma}} &= -c_1\tilde{\gamma} \\ \dot{\tilde{\theta}} &= q - \dot{\alpha}_1 \end{aligned} \tag{4.12}$$

For the system (4.12), the q state variable is regarded as a control input. So, q can be chosen logically to make the subsystem (4.12) globally asymptotically stable. A CLF $V_2(\tilde{\gamma}, \tilde{\theta})$ can be chosen such that it makes the subsystem (4.12) asymptotically stable with the virtual control law, i.e.,

$$V_2(\tilde{\gamma}, \tilde{\theta}) = V_1(\tilde{\gamma}) + \frac{1}{2}\tilde{\theta}^2 \tag{4.13}$$

Taking the time derivative of equation (4.13) and combining with equation (4.12) results in

$$\dot{V}_2(\tilde{\gamma}, \tilde{\theta}) = -c_1\tilde{\gamma}^2 + \tilde{\theta}\dot{\tilde{\theta}} = -c_1\tilde{\gamma}^2 + \tilde{\theta}(q - \dot{\alpha}_1) \tag{4.14}$$

By satisfying the asymptotically stable condition in the sense of Lyapunov in Theorem 2.2 for equation (4.14), a virtual control law α_2 can be chosen. This control law is

$$\begin{aligned} -c_2\tilde{\theta} &= q - \dot{\alpha}_1 \\ \Rightarrow q_{ref} \equiv \alpha_2(c_1, c_2, \gamma, \theta, \gamma_{ref}) &= -c_2(\theta - \alpha_1) + \dot{\alpha}_1 \end{aligned} \tag{4.15}$$

where c_2 is a positive gain and $\dot{\alpha}_1$ is determined by equations (4.16), (4.17), (4.18).

$$\dot{\alpha}_1 = (1 - \frac{mgsin\gamma + mV_T c_1}{(\tilde{L} + F_T)\sqrt{1 - X^2}})F_\gamma \tag{4.16}$$

$$X = \frac{1}{\tilde{L} + F_T}[-mV_T c_1(\gamma - \gamma_{ref}) - mgcos\gamma] \tag{4.17}$$

$$F_\gamma = \frac{1}{mV_T}([\tilde{L} + F_T]sin(\theta - \gamma) - mgcos\gamma) \tag{4.18}$$

The time derivative of $V_2(\tilde{\gamma}, \tilde{\theta})$ then shows the necessary definiteness condition.

$$\dot{V}_2(\tilde{\gamma}, \tilde{\theta}) = -c_1\tilde{\gamma}^2 - c_2\tilde{\theta}^2 < 0, \ \forall \ \tilde{\gamma}, \tilde{\theta} \neq 0 \tag{4.19}$$

Step 3.

By choosing the state feedbacks in equations (4.9) and (4.15), changes of state transformation in equations (4.5) and (4.11), and introducing the final change of coordinates as

$$\tilde{q} = q - \alpha_2(c_1, c_2, \gamma, \theta, \gamma_{ref}) \tag{4.20}$$

the complete system can be re-written as

$$\begin{aligned} \dot{\tilde{\gamma}} &= -c_1\tilde{\gamma} \\ \dot{\tilde{\theta}} &= -c_2\tilde{\theta} \\ \dot{\tilde{q}} &= u - \dot{\alpha}_2 \end{aligned} \tag{4.21}$$

where $\dot{\alpha}_2(c_1, c_2, \gamma, \theta, \gamma_{ref})$ is determined by equations (4.22), (4.23), (4.24), (4.25), and (4.26).

$$\dot{\alpha}_2(c_1, c_2, \gamma, \theta, \gamma_{ref}) = -c_2(q - \dot{\alpha}_1) + \ddot{\alpha}_1 \tag{4.22}$$

$$\ddot{\alpha}_1(c_1, \gamma, \gamma_{ref}) = (1 - \frac{mgsin\gamma + mV_T c_1}{(\tilde{L} + F_T)\sqrt{1 - X^2}})\dot{F}_\gamma + \Psi F_\gamma \tag{4.23}$$

$$\dot{F}_\gamma = \frac{1}{mV_T}([\tilde{L} + F_T][q - F_\gamma]cos(\theta - \gamma) + mgsin\gamma F_\gamma) \tag{4.24}$$

$$\Psi = -\frac{mg(F_\gamma(1 - X^2)cos\gamma + X\dot{X}sin\gamma) + mV_T c_1 X\dot{X}}{(\tilde{L} + F_T)(1 - X^2)^{1.5}} \tag{4.25}$$

$$\dot{X} = \frac{1}{\tilde{L} + F_T}(-mV_T c_1 + mgsin\gamma)F_\gamma \tag{4.26}$$

For the system (4.21), a CLF $V_3(\tilde{\gamma}, \tilde{\theta}, \tilde{q})$ can be chosen as

$$V_3(\tilde{\gamma}, \tilde{\theta}, \tilde{q}) = V_2(\tilde{\gamma}, \tilde{\theta}) + \frac{1}{2}\tilde{q}^2 \tag{4.27}$$

Taking the time derivative of equation (4.27) and combining with equation (4.21) results in

$$\dot{V}_3(\tilde{\gamma}, \tilde{\theta}, \tilde{q}) = -c_1\tilde{\gamma}^2 - c_2\tilde{\theta}^2 + \tilde{q}(u - \dot{\alpha}_2) \tag{4.28}$$

By satisfying the asymptotically stable condition in the sense of Lyapunov in Theorem 2.2 for equation (4.28), a control law can be chosen as

$$\begin{aligned} &-c_3\tilde{q} = u - \dot{\alpha}_2 \\ &\Rightarrow u \equiv \alpha_3(c_1, c_2, c_3, \gamma, \theta, q, \gamma_{ref}) = -c_3(q - \alpha_2) + \dot{\alpha}_2 \end{aligned} \tag{4.29}$$

where c_3 is a positive gain and $\dot{\alpha}_2$ is determined by the equations (4.22)-(4.26). This selection leads to

$$\dot{V}_3(\tilde{\gamma}, \tilde{\theta}, \tilde{q}) = -c_1\tilde{\gamma}^2 - c_2\tilde{\theta}^2 - c_3\tilde{q}^2 < 0 \;\forall\; \tilde{\gamma}, \tilde{\theta}, \tilde{q} \neq 0 \tag{4.30}$$

Thus, there exist a CLF in equation (4.27), state feedbacks in equations (4.9), (4.15), and (4.29), and state transformations in equations (4.5), (4.11), and (4.20),

where the complete system can be transformed into a state decoupled system as

$$\begin{aligned} \dot{\tilde{\gamma}} &= -c_1\tilde{\gamma} \\ \dot{\tilde{\theta}} &= -c_2\tilde{\theta} \\ \dot{\tilde{q}} &= -c_3\tilde{q} \end{aligned} \tag{4.31}$$

Examining solutions of the system (4.31) indicates the time response of tracking error ($\tilde{\gamma}$) of the system is globally asymptotically stable at the origin with positive gains with no or small overshoot. This property implies that the time response of flight path angle (γ) has well-behaved command tracking. Further investigation of the system (4.31) also shows that desired settling time and rise time of the system are obtained by tuning the gains. From these considerations, one can conclude that the stability and performance specifications of the system (4.4) are achieved with the BSC law (4.29).

4.3 F-16 MODEL FLIGHT PATH SIMULATION STUDY

Figure 4.2 shows the block diagram of the proposed backstepping-based control algorithm for flight path angle of the longitudinal dynamic model with functions f_γ, f_θ, f_q defined in equation (4.4). Assume that the state feedbacks q, θ, and γ are able to be determined by the sensor systems. Depending on these signals, the BSC generates the control input to the aircraft. Note the control system architecture in Figure 4.2 is very similar to conventional inner-outer loop design strategy.

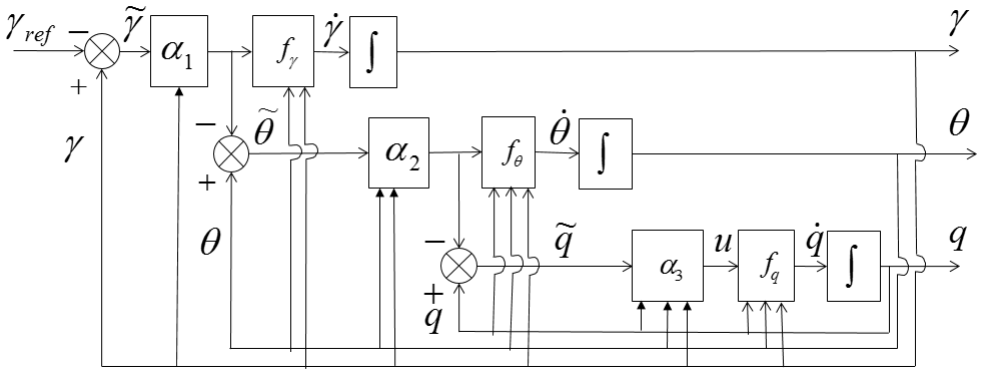

Figure 4.2: Block Diagram of Backstepping-Based Flight Path Angle Control

A wide array of numerical values for c_1, c_2, and c_3 provide stability. In this research, optimal gains are chosen using the modified genetic algorithm (MGA) in References [52]. Gains of the BSC are chosen to meet the desired performance specifications and optimize the objective function in terms of error between desired and operating flight path angles and control input δ_E activity shown in equation (4.32)

$$\begin{aligned} J &= w_e \int_0^T (\gamma_{ref} - \gamma)^2 dt + w_\delta \int_0^T \delta_E^2 dt \\ (c_1, c_2, c_3) &= \{(c_1, c_2, c_3) | J^* = \min_{c_1, c_2, c_3} J \leq J\} \end{aligned} \tag{4.32}$$

where w_e and w_δ are weights which are used to balance between performance specifications. In this study, the weights are determined by using a trial and error technique in order to achieve the control design goals.

Minimization of the J objective function occurs over the design variables c_1, c_2, c_3. This approach can also be used to update online gains in the presence of changing parameters, such as the reduction of weight of the aircraft due to fuel consumption or the offloading of cargo or ordnance. A similar approach is applied successfully for roll-to-roll web control systems by the authors in References [38], [40].

To explore feasibility of the proposed design method, a nonlinear simulation model of an F-16 aircraft is selected. The aerodynamic data of the F-16 aircraft model used for numerical simulation is provided in References [62], [66]. These data are derived from low-speed static and dynamic wind-tunnel tests at the NASA Langley Research Center. In this research, assume that the aircraft is in level fight at Mach 0.5 and at a height of 25000 ft. Also actuator and sensor dynamics and thrust point offset are not considered in this research. A software development based on Matlab/Simulink R2015a is employed using the RK45 integration routine for numerical simulation of the closed-loop system. A full nonlinear simulation model of the longitudinal dynamics of the F-16 is selected.

To evaluate the validity of the assumption that lift force is approximately a sinusoidal function with angle of attack for this model, an analysis of the aerodynamic data is considered here. By curve fitting the aerodynamic data at the indicated flight condition, lift is approximated as

$$L = \tilde{L}\sin(\alpha - \alpha_0) \tag{4.33}$$

where $\tilde{L}$ is a function of aircraft speed and altitude in general. In equation (4.33), α_0 is the angle of attack at zero lift. A value of $\alpha_0 = -2.05\ deg$ was determined from the data.

A graph of the actual data for the F-16 model and this approximation at a height of 25000 ft and at Mach 0.5 are shown in Figure 4.3 in which the solid line (or red line) shows the approximated lift force and the dashed line (or blue line) shows the correct lift force, confirming the approximate validity of the assumption. For other

flight conditions, the data can be fit to trim speed and altitude, or

$$L = \tilde{L}(V_T, h)\sin(\alpha - \alpha_0) \tag{4.34}$$

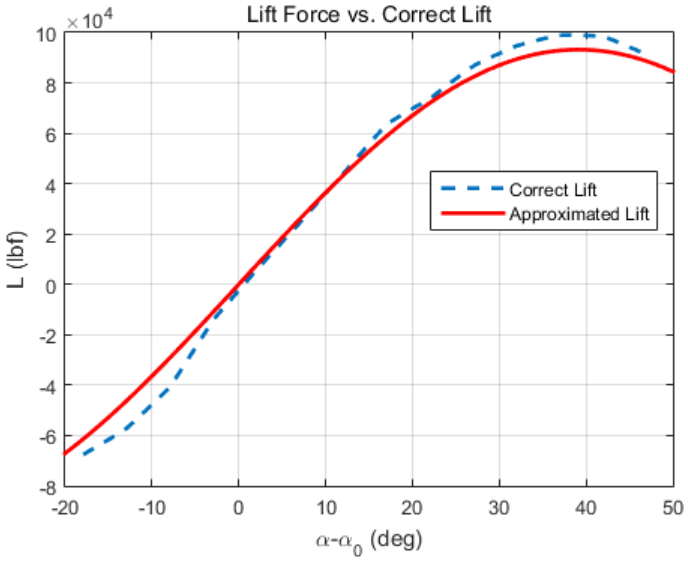

Figure 4.3: Approximated vs. Correct Lift Force

In order to evaluate the effectiveness of the proposed control algorithm, the closed-loop simulator is tested with three different cases involving two different flight path command profiles away from the trim condition, and an airframe parameter variation. In the first case, a small command of 10 degrees for flight path angle is applied, and in the second case, the reference flight path angle will be put at 5 degrees for the first five seconds, at 20 degrees for the next ten seconds, and then 15 degrees for the remaining times, as shown in Figure 4.4. Also, the stability robustness of the proposed algorithm is examined in the last case by implementing the simulation via different locations of mass center of the aircraft when using the first flight path command profile.

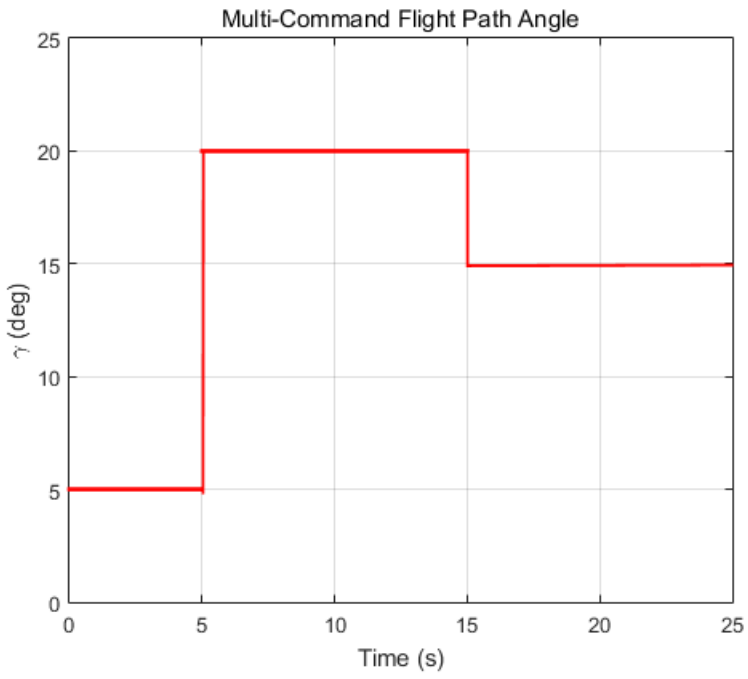

Figure 4.4: Reference Flight Path Multi-Command

Case 1: Simple Step Excitation

Figure 4.5 shows the time response of flight path angle for an applied command of 10 degrees. This result was generated with $c_1 = 1.72\ s^{-1}, c_2 = 1.73\ s^{-1}, c_3 = 1.72\ s^{-1}$. The result shows performance characteristics of the aircraft are obtained with no overshoot and a fast response. For other numerical simulations, settling time can be reduced by increasing the gains but limitations to this from the elevator actuation system will eventually be reached. Thus, a trade-off between settling time and actuation requirement exists for the closed-loop aircraft. Figure 4.6 and 4.7 show the travel and rate response of the elevator for the flight path angle command of 10 degrees, respectively. This result shows that the elevator travel response lies within the actuator capabilities.

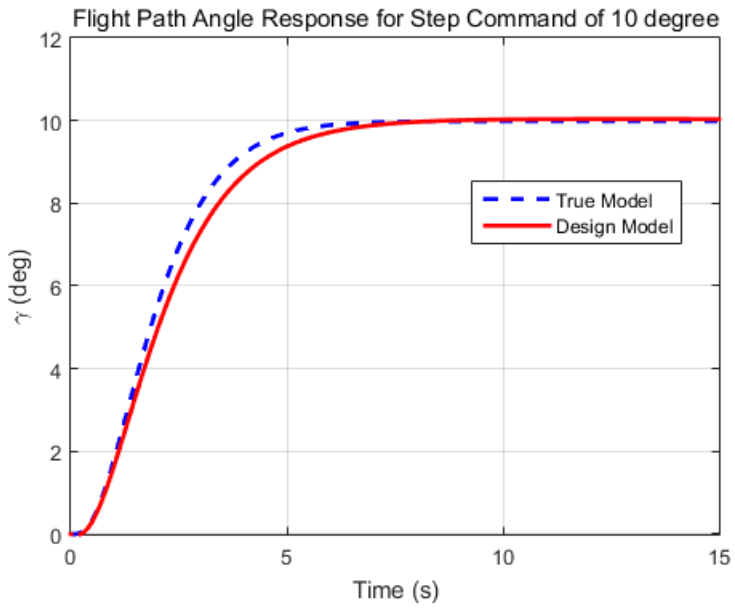

Figure 4.5: Flight Path Angle Response for Step Command of 10 degrees

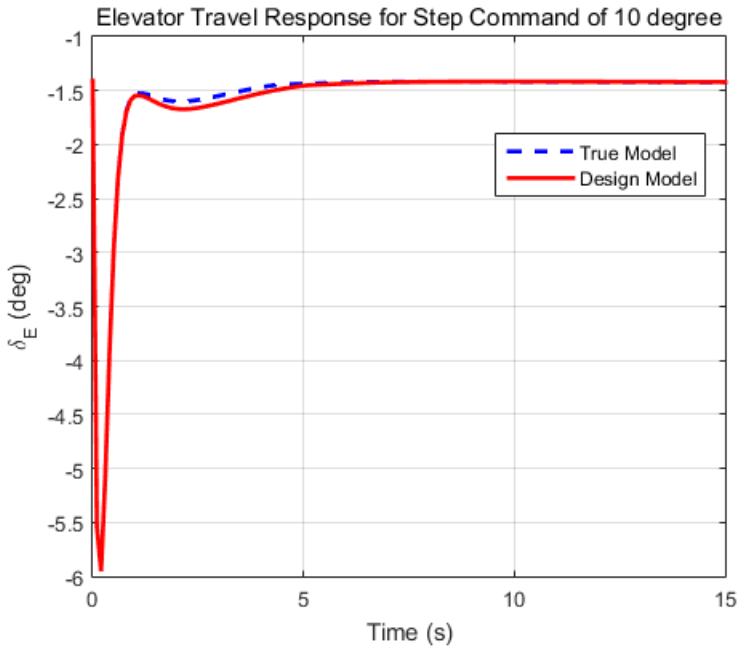

Figure 4.6: Elevator Travel Response for Step Command of 10 degrees

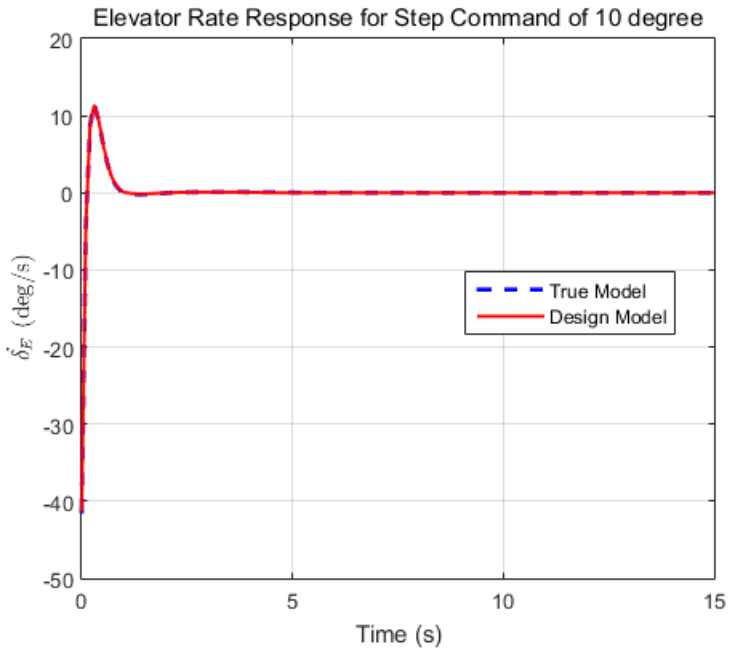

Figure 4.7: Elevator Rate Response for Step Command of 10 degrees

Case 2: Complex Step Excitation

Figure 4.8 shows the time response of flight path angle for a series of step commands of varying levels. Figures 4.9 and 4.10 show the corresponding elevator behavior. Figure 4.8 shows the settling time is approximately 5 seconds regardless of the step amplitude. The control system is able to follow the command across small and large inputs. Overall the flight path angle time response of the aircraft is well-behaved in tracking and the performance specifications are obtained with high reliability. Control gains for this case are the same as Case 1.

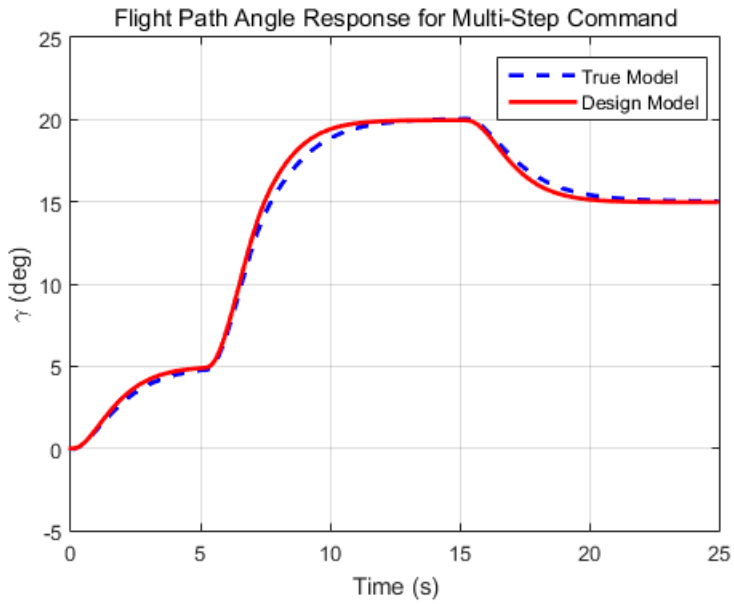

Figure 4.8: Flight Path Angle Response for Multi-Step Command

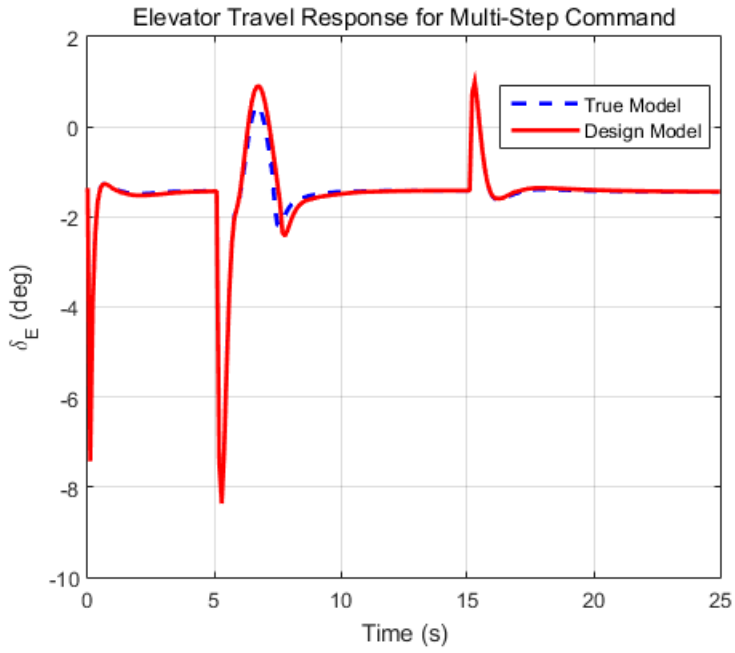

Figure 4.9: Elevator Travel Response for Multi-Step Command

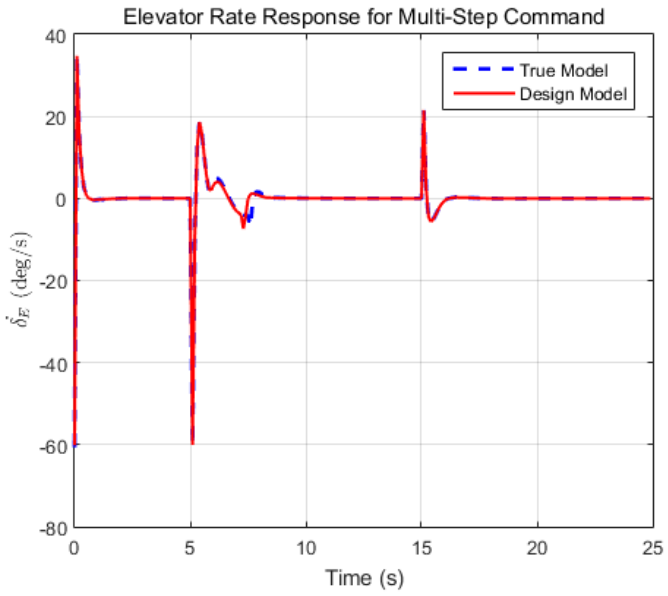

Figure 4.10: Elevator Rate Response for Multi-Step Command

Case 3: Simple Step Excitation with Aircraft Parameter Change

In Case 1 and Case 2, the non-dimensional mass center of the aircraft $\bar{x}_{cm} = 0.3$ is used for simulation. Figure 4.11 shows the flight path angle time response for a step command of 5 degrees with three different sets of mass centers. From Figure 4.11, it is clear that the flight path angle response in time is deteriorating as the mass center location increases. This deterioration can be reduced by gain-scheduling as shown in Figure 4.12. Figure 4.12 shows the flight path angle time response for a step command of 5 degrees at $\bar{x}_{cm} = 0.40$ with three different sets of gains shown in Table 4.1. The blue (dash) line corresponds to gain set 1 which was the set used for design at $\bar{x}_{cm} = 0.30$. The green (solid) line corresponds to gain set 3. From the results in Figure 4.12, it is clear that the performance of the aircraft in the presence of mass center location change is improved by reducing the gains.

Table 4.1: Feedback Gain Values

Case	$c_1(s^{-1})$	$c_2(s^{-1})$	$c_3(s^{-1})$
Gain set 1	1.72	1.73	1.72
Gain set 2	1.64	1.63	1.64
Gain set 3	1.53	1.54	1.57

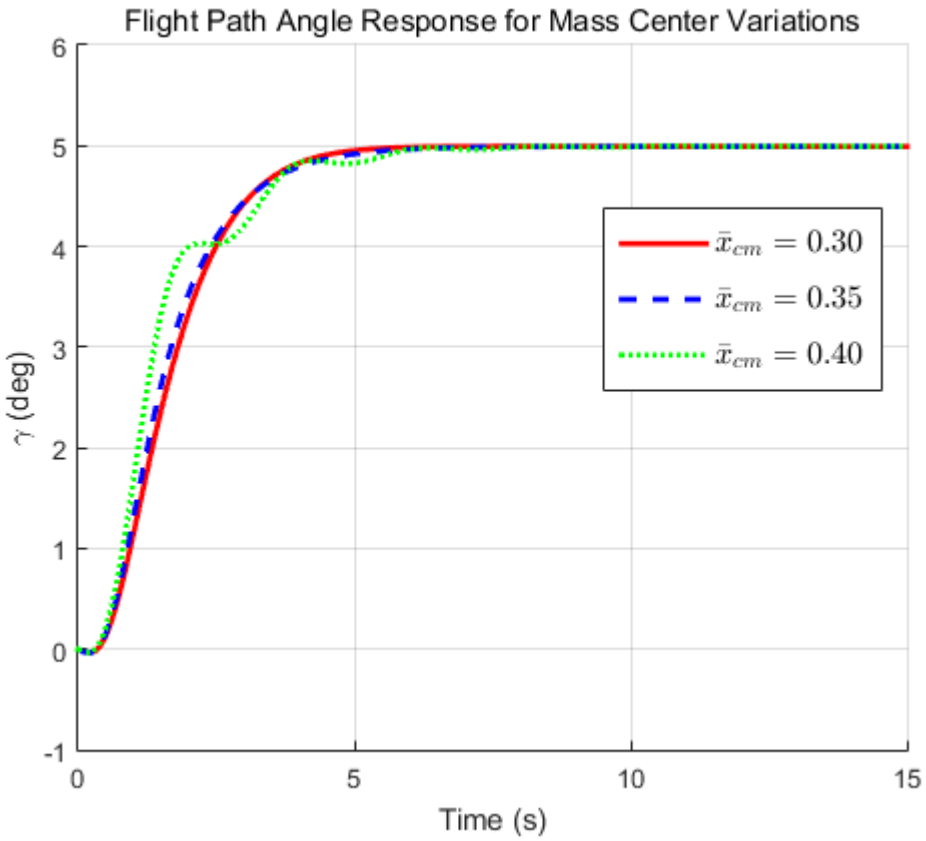

Figure 4.11: Flight Path Angle Response for Mass Center Variation

Thus, by applying the theory in Section 3.2 in Chapter 3, the input-output decoupling problem for the longitudinal dynamic model is obtained by coordinate transformations and a feedback control law with some simplifying assumptions. By applying

consecutively the coordinate transformation and choosing the feedback law for each subsystem from the lowest to highest order, and then re-writing the feedback law in the original coordinates, the resulting controller makes the original system a well-behaved command tracking and asymptotically globally stable system. Further, the response of the system has no overshoot. From the above simulation results, some comments are made.

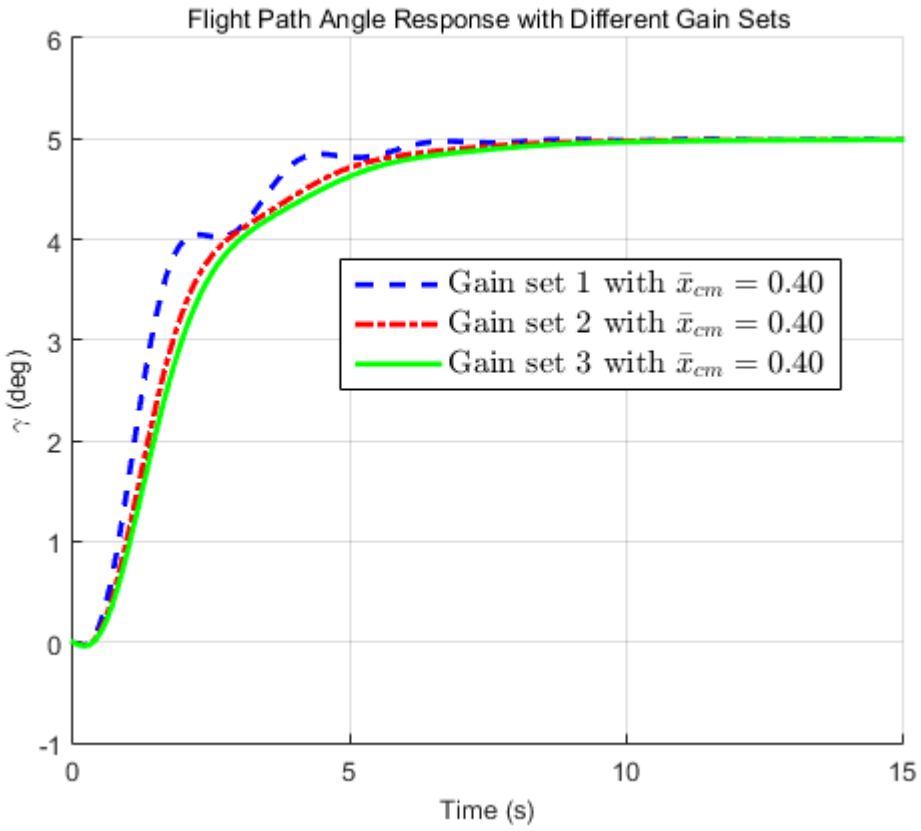

Figure 4.12: Flight Path Angle Response with Different Gain Sets

The flight path angle time response for a step command of 10 degrees shown in Figure 4.5 meets the performance specifications with no overshoot and with a settling

time of 6 seconds. The simulation result shown in Figure 4.8 demonstrates the proposed control algorithm works well in different operating conditions. Figure 4.12 shows the stability robustness of the proposed design is acceptable in the presence of aircraft mass center changes. Depending on the elevator time response shown in Figure 4.6 and 4.9, and maximum performance specifications regarding the control actuator in Reference [62], the control response lies within the allowable limit.

4.4 SUMMARY AND DISCUSSION

In this chapter, assumptions and analysis on the lift force of aircraft are considered to transform the nonlinear dynamic model into a standard strict-feedback form for control design, and then, a systematic procedure is addressed for formulating the backstepping controller for the achieved model. An achieved BSC-based flight path angle control method is then provided for the F-16 longitudinal dynamic model with optimal gains determined by the MGA. A block diagram is also given for system architecture insight and for developing the numerical integration within the nonlinear closed-loop simulation.

The assumptions on aerodynamic forces are improved significantly to achieve a more accurate model for the design in comparison with the existing works. A standard strict-feedback form of nonlinear longitudinal dynamics of aircraft is also obtained for control design under the proposed assumption. The numerical results show that the control method meets the performance specifications and robust stability of a high-performance aircraft in the presence of model uncertainty. Also, the

analytically predicted exponential time response behavior with no overshoot is validated by numerical results. With the rapid development of sensors and electronic devices, the proposed BSC-based algorithm results in a control system with high precision and is useful for applications with high digital computational capability.

Simulation studies show that limitations of the backstepping-based control design are encountered as predicted in Chapter 3. Assumptions on aerodynamic forces and constant speed aircraft made to achieve the strict-feedback form result in a divergence of flight path angle from command if the aircraft is maintained at that operating condition with a long enough time. The reason is that the speed of aircraft will decrease due to more drag or increased attack angle. This drift off can be improved by applying speed control and flight path angle control simultaneously to achieve better performance. Also, control input of the elevator deflection is not an explicit variable in the design model, and, thus, a control realization approach needs to be addressed to improve the feasibility of the proposed method.

CHAPTER 5

BACKSTEPPING VS. FEEDBACK LINEARIZATION

This chapter conducts a comparison of two nonlinear control design methodologies: backstepping and feedback linearization. In the first section, a focused literature review and problem statement are introduced. In the second section, a mathematical model of a triangular affine form is given for nonlinear dynamic systems. In the third section, theorems are considered and proven to show the equivalence of the feedback linearization-based design method and backstepping-based design approach for the triangular affine systems. In the fourth section, a detailed procedure for formulating the nonlinear feedback control laws for a triangular affine system is presented using the state space exact linearization and backstepping designs. A numerical study of flight path angle control for an F-16 aircraft model of nonlinear longitudinal dynamics is implemented in an analytical control law and a numerical nonlinear closed-loop simulation. The simulation results are provided and discussed. Finally, a summary and discussion of the proposed control methodologies are made at the end of the chapter.

5.1 INTRODUCTION

In recent years, many research activities have emphasized nonlinear control strategies using nonlinear dynamics as the design model. Advantages of this perspective are that nonlinearities are dealt with directly, plant systems are not approximated

to behave like a varying linear system, and differing levels of nonlinearity can be addressed through class relaxation concepts. Exact feedback linearization design for nonlinear dynamic systems is a common approach in References [12], [13], [15], [16], [18], [19]. Another popular approach is backstepping-based control design in References [8], [21], [22], [40], [43]. In both approaches, coordinate transformations and state feedbacks are applied in unique but similar ways to transform the triangular affine system into a state decoupled linear system. Figure 5.1 illustrates the similar but unique procedures. A fundamental question to be addressed here is whether these two design methods are truly unique or whether there exists some type of equivalence between the two methods.

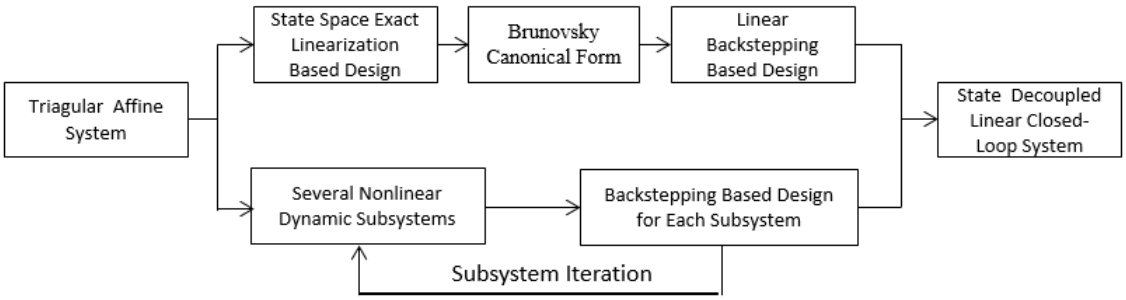

Figure 5.1: Backstepping-Based vs. Feedback Linearization-Based Designs

In the first approach, the sequence of coordinate transformations and state feedbacks is applied to transform the triangular affine system into normal form equations with a new input. This form is also called the Brunovsky canonical form for nonlinear dynamic systems of full relative degree. Then, the obtained linear dynamic system with new input is transformed into a state decoupled linear closed-loop system by

using the linear backstepping design, as shown in Figure 5.1. By returning to the triangular affine system state variables, the state feedback control law for the triangular affine system is achieved. In the second approach, the transformations and state feedbacks are implemented in a different way on triangular affine dynamic subsystems that achieve a final closed-loop system of the same structure in References [38], [40], [64]. In this approach, the triangular affine system is divided into several triangular affine subsystems such that the i^{th} subsystem consists of the $(i-1)^{th}$ subsystem plus an extra state, and the n^{th} subsystem is the original nonlinear n^{th} order dynamic system via coordinate transformations and feedbacks. By applying consecutively the coordinate transformation and choosing a feedback law via the control Lyapunov function for each subsystem from the lowest to highest order and re-writing the feedback law in the original coordinates, the resulting overall controller is achieved. Building an equivalence between these two methods is of interest.

In this chapter, the mathematical model for the triangular affine form of nonlinear dynamic systems is introduced first and then the chapter deals with the question of when both the state space exact linearization and backstepping approaches transform the triangular affine system into state decoupled linear systems that are convergent. A demonstration of flight path angle control of nonlinear flight dynamics is presented to illustrate the general equivalence in specific applications. The content of the chapter is the main outcomes of the author's work in References [67], [68].

5.2 TRIANGULAR AFFINE SYSTEM

In this section, a mathematical model of the single-input single-output triangular affine system is introduced. A theorem for full relative degree and a following proof are presented to confirm conditions in which a SISO triangular affine system is well-defined and has a full relative degree. For the well-defined and full relative degree system, a second theorem will provide an answer for the question on whether a SISO triangular affine system can be transformed into a state decoupled linear system via coordinate transformations and state feedback. The proof of the theorem is given for clarity.

Consider a SISO model of a nonlinear dynamic system as

$$\begin{aligned} \dot{x_1} &= f_1(x_1) + g_1(x_1)x_2 \\ \dot{x_2} &= f_2(x_1, x_2) + g_2(x_1, x_2)x_3 \\ \dot{x_3} &= f_3(x_1, x_2, x_3) + g_3(x_1, x_2, x_3)u \\ y &= h(x) = x_1 \end{aligned} \tag{5.1}$$

where x_i $(i = 1, 2, 3) \in R$ are state variables, $f_i(x), g_i(x)$ $(i = 1, 2, 3)$ are scalar-valued functions, $u \in R$ is the control input, $y \in R$ is the output. Assume that the functions $f_i(x), g_i(x)$ $(i = 1, 2, 3)$ are continuous and differentiable with respect to variables x_1, x_2, x_3. The functions $f_1(x_1), g_1(x_1)$ are only functions of variable x_1. The function $f_2(x_1, x_2), g_2(x_1, x_2)$ are only functions of variables x_1, x_2, and the functions $f_3(x_1, x_2, x_3), g_3(x_1, x_2, x_3)$ are only functions of variables x_1, x_2, x_3. Then the system with structure in equation (5.1) is called a third order SISO triangular affine system.

Theorem 5.1. *(Full Relative Degree)*

If the functions $g_1(x_1), g_2(x_1, x_2)$, and $g_3(x_1, x_2, x_3)$ in system (5.1) are nonzero at x^0, then system (5.1) has a well-defined and full relative degree $r = 3$ at x^0.

Proof.

For system (5.1), the functions f, g, h (see equation (3.3)) are $f(x) = [f_1 + g_1 x_2 \ f_2 + g_2 x_3 \ f_3]^T, g(x) = [0 \ 0 \ g_3]^T, h(x) = x_1$. Taking the Lie derivative of $h(x)$ with respect to $g(x)$ results in

$$L_g h(x) = \frac{\partial h(x)}{\partial x} g(x) = 0 \ \forall \ x \tag{5.2}$$

From equation (5.2), the system (5.1) has relative degree greater than 1 in terms of Definition 3.1. A higher relative degree will be certified by the term $L_g L_f h(x)$. First compute $L_f h(x)$.

$$L_f h(x) = \frac{\partial h(x)}{\partial x} f(x) = f_1(x_1) + g_1(x_1) x_2 \tag{5.3}$$

Taking the Lie derivative of $L_f h(x)$ with respect to $g(x)$ results in

$$L_g L_f h(x) = \frac{\partial \frac{\partial h(x)}{\partial x} f(x)}{\partial x} g(x) = 0 \ \forall \ x \tag{5.4}$$

From equation (5.4), one can conclude that system (5.1) has relative degree greater than 2 in terms of Definition 3.1. The term $L_g L_f^2 h(x)$ is used to determine the complete relative degree of system (5.1), i.e.,

$$L_f^2 h(x) = \frac{\partial \frac{\partial h(x)}{\partial x} f(x)}{\partial x} f(x)$$

$$L_f^2 h(x) = [\frac{\partial f_1(x_1)}{\partial x_1} + \frac{\partial g_1(x_1)}{\partial x_1} x_2][f_1(x_1) + g_1(x_1) x_2] + g_1(x_1)[f_2(x_1, x_2) + g_2(x_1, x_2) x_3] \tag{5.5}$$

Taking the Lie derivative of $L_f^2 h(x)$ with respect to $g(x)$ results in

$$L_g L_f^2 h(x) = g_1(x_1) g_2(x_1, x_2) g_3(x_1, x_2, x_3) \neq 0 \ at \ x = x^0 \tag{5.6}$$

From equation (5.6), the system (5.1) has a full relative degree $r = 3$ at x^0 in terms of Definition 3.1.

5.3 FEEDBACK LINEARIZATION FORMULATION

Theorem 5.2. *If the system* (5.1) *has full relative degree, then there exists a coordinate transformation and state feedback that transforms the nonlinear dynamic system* (5.1) *into a state decoupled linear system* (3.36) *by applying two steps:*
Step 1: State space exact linearization design in Reference [56] to achieve the Brunovsky form with a new input,
Step 2: Linear backstepping design in Reference [68] for the Brunovsky form with the new input.

Proof.

Step 1: State space exact linearization design to achieve the Brunovsky form with a new input.

Consider the coordinate transformations as

$$z_1 = x_1$$

$$z_2 = f_1(x_1) + g(x_1) x_2$$

$$z_3 = (\frac{\partial f_1(x_1)}{\partial x_1} + \frac{\partial g_1(x_1)}{\partial x_1} x_2)[f_1(x_1) + g_1(x_1) x_2] + g_1(x_1)[f_2(x_1, x_2) + g_2(x_1, x_2) x_3] \tag{5.7}$$

By taking the time derivative of the first relation of equation (5.7) and combining equation (5.1) result in

$$\dot{z}_1 = \dot{x}_1 = f_1(x_1) + g(x_1)x_2 \tag{5.8}$$

Using the second relation of equation (5.7) for equation (5.8), one gets

$$\dot{z}_1 = z_2 \tag{5.9}$$

Taking the time derivative of the second relation of equation (5.7) results in

$$\begin{aligned}\dot{z}_2 &= \frac{d}{dt}\{f_1(x_1) + g(x_1)x_2\} \\ &= (\frac{\partial f_1(x_1)}{\partial x_1} + \frac{\partial g_1(x_1)}{\partial x_1}x_2)[f_1(x_1) + g_1(x_1)x_2] + g_1(x_1)[f_2(x_1, x_2) + g_2(x_1, x_2)x_3]\end{aligned} \tag{5.10}$$

Using the third relation of equation (5.7) for equation (5.10) results in

$$\dot{z}_2 = z_3 \tag{5.11}$$

Taking the time derivative of the third relation of equation (5.7) results in

$$\begin{aligned}\dot{z}_3 &= \frac{d}{dt}\{f_{1x_1}F_1 + x_2 g_{1x_1}F_1 + g_1F_2\} \\ &= f_{1x_1x_1}F_1^2 + f_{1x_1}F_{1x_1}F_1 + f_{1x_1}g_1F_2 + x_2\{g_{1x_1x_1}F_1^2 + g_{1x_1}F_{1x_1}F_1 + g_1g_{1x_1}F_2\} \\ &+ 2g_{1x_1}F_1F_2 + g_1\{F_{2x_1}F_1 + F_{2x_2}F_2 + g_2F_3\} + g_1g_2g_3u \\ &= L_f^3h(x) + g_1g_2g_3u\end{aligned} \tag{5.12}$$

where $f_{1x_1} = \frac{\partial f_1}{\partial x_1}, f_{2x_2} = \frac{\partial f_2}{\partial x_2}, g_{1x_1} = \frac{\partial g_1}{\partial x_1}, g_{2x_2} = \frac{\partial g_2}{\partial x_2}, f_{1x_1x_1} = \frac{\partial^2 f_1}{\partial x_1^2}, g_{1x_1x_1} = \frac{\partial^2 g_1}{\partial x_1^2}, F_1 = f_1(x_1)+g_1(x_1)x_2, F_2 = f_2(x_1, x_2)+g_2(x_1, x_2)x_3, F_3 = f_3(x_1, x_2, x_3), F_{1x_1} = \frac{\partial F_1}{\partial x_1}, F_{1x_2} =$

$\frac{\partial F_1}{\partial x_2}, F_{2x_1} = \frac{\partial F_2}{\partial x_1}, F_{2x_2} = \frac{\partial F_2}{\partial x_2}$. By selecting the state feedback with new input v as

$$u = \frac{1}{g(x_1)g_2(x_1,x_2)g_3(x_1,x_2,x_3)}\{v - L_f^3 h(x)\} \tag{5.13}$$

where $L_f^3 h(x) = f_{1x_1x_1}F_1^2 + f_{1x_1}F_{1x_1}F_1 + f_{1x_1}g_1F_2 + x_2\{g_{1x_1x_1}F_1^2 + g_{1x_1}F_{1x_1}F_1 + g_1g_{1x_1}F_2\} + 2g_{1x_1}F_1F_2 + g_1\{F_{2x_1}F_1 + F_{2x_2}F_2 + g_2F_3\}$, the equation (5.12) is re-written as

$$\dot{z}_3 = v \tag{5.14}$$

Collecting from equations (5.9), (5.11), and (5.14), the new model in z_1, z_2, z_3 coordinates is re-written in Brunovsky form with a new input v.

$$\begin{aligned} \dot{z} &= \begin{pmatrix} 0 & 1 & 0 \\ 0 & 0 & 1 \\ 0 & 0 & 0 \end{pmatrix} z + \begin{pmatrix} 0 \\ 0 \\ 1 \end{pmatrix} v \\ y &= \begin{pmatrix} 1 & 0 & 0 \end{pmatrix} z \end{aligned} \tag{5.15}$$

Step 2: Linear backstepping design for the Brunovsky form with a new input.

The z_2 variable is regarded as a control input in the first relation in equation (5.15) which is considered as the first subsystem. Thus, z_2 is chosen to make the first subsystem globally asymptotically stable. The chosen z_2 function is called a virtual control law. First introduce $\hat{z}_1$ as

$$\hat{z}_1 = z_1 - z_{ref} \tag{5.16}$$

where z_{ref} is considered a command or desired value of the system. Differentiating equation (5.16) in time and combining with equation (5.15) results in

$$\dot{\hat{z}}_1 = \dot{z}_1 = z_2 \tag{5.17}$$

For the system (5.17), a CLF $V_1(\hat{z}_1)$ in terms of Definition 2.8 can be chosen such that when the virtual control law is applied, its time derivative becomes negatively definite. The positive definite function is chosen as

$$V_1(\hat{z}_1) = \frac{1}{2}\hat{z}_1^2 \tag{5.18}$$

By taking the derivative of equation (5.18) in time and combining with equation (5.17), one finds the result

$$\dot{V}_1(\hat{z}_1) = \hat{z}_1\dot{\hat{z}}_1 = \hat{z}_1 z_2 \tag{5.19}$$

By satisfying the asymptotically stable condition in Theorem 2.2 for equation (5.19), a virtual control law denoted as α_1 for z_2 can be chosen as

$$\begin{gathered} -c_1\hat{z}_1 = z_2 \\ \implies z_2 \equiv \alpha_1(c_1, z_1, z_{ref}) = -c_1(z_1 - z_{ref}) \end{gathered} \tag{5.20}$$

where c_1 is a positive gain. By doing so, the CLF derivative is negatively definite.

$$\dot{V}_1(\hat{z}_1) = -c_1\hat{z}_1^2 < 0 \;\forall\; \hat{z}_1 \neq 0 \tag{5.21}$$

By choosing the state feedback in equation (5.20) and a change of coordinate indicated below

$$\hat{z}_2 = z_2 - \alpha_1 \tag{5.22}$$

the second subsystem of equation (5.15) can be re-written as follows

$$\begin{aligned} \dot{\hat{z}}_1 &= -c_1 \hat{z}_1 \\ \dot{\hat{z}}_2 &= z_3 - \dot{\alpha}_1 \end{aligned} \tag{5.23}$$

A CLF $V_2(\hat{z}_1, \hat{z}_2)$ in terms of Definition 2.8 can be chosen such that it makes the subsystem in equation (5.23) asymptotically stable with the control law, i.e.,

$$V_2(\hat{z}_1, \hat{z}_2) = V_1(\hat{z}_1) + \frac{1}{2}\hat{z}_2^2 \tag{5.24}$$

By taking the derivative of equation (5.24) in time and combining with equation (5.23), one achieves

$$\dot{V}_2(\hat{z}_1, \hat{z}_2) = -c_1 \hat{z}_1^2 + \hat{z}_2(z_3 - \dot{\alpha}_1) \tag{5.25}$$

To meet the asymptotically stable condition in Theorem 2.2 for equation (5.25), a virtual control law can be chosen such that

$$\begin{aligned} -c_2 \hat{z}_2 &= z_3 - \dot{\alpha}_1 \\ \implies z_3 \equiv \alpha_2(c_1, c_2, z_1, z_2, z_{ref}) &= -c_2(z_2 - \alpha_1) + \dot{\alpha}_1 \end{aligned} \tag{5.26}$$

where c_2 is a positive gain. By doing so, the CLF derivative is negatively definite.

$$\dot{V}_2(\hat{z}_1, \hat{z}_2) = -c_1 \hat{z}_1^2 - c_2 \hat{z}_2^2 < 0 \ \forall \ \hat{z}_1, \hat{z}_2 \neq 0 \tag{5.27}$$

By choosing the state feedbacks in equation (5.20) and equation (5.26), and coordinate transformations in equation (5.16), equation (5.22), and the transformation indicated below

$$\hat{z}_3 = z_3 - \alpha_2 \tag{5.28}$$

the third subsystem of equation (5.15) (complete system) can be re-written as follows

$$\begin{aligned} \dot{\hat{z}}_1 &= -c_1 \hat{z}_1 \\ \dot{\hat{z}}_2 &= -c_2 \hat{z}_2 \\ \dot{\hat{z}}_3 &= v - \dot{\alpha}_2 \end{aligned} \tag{5.29}$$

A CLF $V_3(\hat{z}_1, \hat{z}_2, \hat{z}_3)$ in terms of Definition 2.8 can be chosen such that it makes the subsystem in equation (5.29) asymptotically stable with the control law, i.e.,

$$V_3(\hat{z}_1, \hat{z}_2, \hat{z}_3) = V_2(\hat{z}_1, \hat{z}_2) + \frac{1}{2}\hat{z}_3^2 \tag{5.30}$$

Taking the derivative in time of equation (5.30) and combining with equation (5.29) result in

$$\dot{V}_3(\hat{z}_1, \hat{z}_2, \hat{z}_3) = -c_1 \hat{z}_1^2 - c_2 \hat{z}_2^2 + \hat{z}_3(v - \dot{\alpha}_2) \tag{5.31}$$

To meet the asymptotically stable condition in Theorem 2.2 for equation (5.31), a real control law can be chosen such that

$$\begin{aligned} -c_3 \hat{z}_3 &= v - \dot{\alpha}_2 \\ \implies v &= -c_3(z_3 - \alpha_2) + \dot{\alpha}_2 \end{aligned} \tag{5.32}$$

where c_3 is a positive gain. By doing so, the CLF derivative is negatively definite.

$$\dot{V}_3(\hat{z}_1, \hat{z}_2.\hat{z}_3) = -c_1 \hat{z}_1^2 - c_2 \hat{z}_2^2 - c_3 \hat{z}_3^2 < 0 \ \forall \ \hat{z}_1, \hat{z}_2, \hat{z}_3 \neq 0 \tag{5.33}$$

Thus, there exists a CLF in terms of Definition 2.8 in equation (5.30), virtual state feedbacks in equations (5.20), (5.26) and feedback control law in equation (5.32), and state transformations in equations (5.16), (5.22), and (5.28), such that the system

(5.15) is transformed into the system

$$\begin{aligned} \dot{\hat{z}}_1 &= -c_1 \hat{z}_1 \\ \dot{\hat{z}}_2 &= -c_2 \hat{z}_2 \\ \dot{\hat{z}}_3 &= -c_3 \hat{z}_3 \end{aligned} \tag{5.34}$$

The system (5.34) is exactly the same as the state decoupled linear system (3.36) formulated from the BSC methodology.

By looking at the systems (3.17) and (5.1), it is an easy step to realize that the system (5.1) is one specific form of the system (3.17). Thus, a similar backstepping-based design approach in Section 3.2 in Chapter 3 can be applied to transform the system (5.1) into the a state decoupled linear system (3.36). By doing so, clearly both feedback linearization-based design and backstepping-based design approaches are able to transform the nonlinear dynamic system (5.1) into separate state decoupled linear systems (3.36) by different formulations. However, the resulting state feedback control laws and achieved state decoupled linear systems in both approaches are the same. From those analyses, one can say that there exists an equivalence in some meaning between the two methods, and therefore, the stability and performance of one system achieved from one method can also be used to predict the characteristics of the other. A demonstration of this equivalence will be presented in the next section for a flight dynamic system.

5.4 FLIGHT PATH ANGLE CONTROL APPLICATION

In this section, the nonlinear longitudinal dynamics model is introduced and

then some assumptions are given to obtain the standard triangular affine form for design suitability. For the purpose of comparison, two control design approaches are again presented in detail in Section 5.4.1 and Section 5.4.2. The main point of this demonstration is to show the applicability of these approaches to flight systems while simultaneously preserving the equivalence condition. Therefore, both analytical and numerical methods are implemented.

Consider the aircraft longitudinal dynamics depicted in Figure 4.1. Some assumptions are considered to assist in transforming the aircraft model in equation (2.26) to the triangular affine structure in equation (5.1).

- Airspeed is constant for short period dynamics, i.e., $\dot{V}_T = 0$.
- Lift force is a linear function of the angle of attack or $L = L_0 + L_\alpha \alpha$, where L_0, L_α are constants for a designated flight condition.
- Pitch moment is a linear function or $M = M_0 + M_\alpha \alpha + M_q q + M_{\delta_E} \delta_E$, where $M_0, M_\alpha, M_q, M_{\delta_E}$ are constants for a designated flight condition.
- Thrust term $F_T sin\alpha$ that is much smaller than lift L is neglected for the controller design purposes.
- Thrust point offset is neglected or $z_{TF} = 0$ is valid for F-16 model.
- Neglection of wind speed is also considered for simplicity.

With these assumptions and use of the relationship $\alpha = \theta - \gamma$, the mathematical

model of longitudinal motion of the aircraft is re-written as

$$\begin{aligned}\dot{\gamma} &= -\frac{g}{V_T}cos\gamma + \hat{L}_0 + \hat{L}_\alpha(\theta - \gamma) \\ \dot{\theta} &= q \\ \dot{q} &= \hat{M}_0 + \hat{M}_\alpha(\theta - \gamma) + \hat{M}_q q + \hat{M}_{\delta_E}\delta_E\end{aligned} \tag{5.35}$$

where $\hat{L}_0 = \frac{L_0}{mV_T}, \hat{L}_\alpha = \frac{L_\alpha}{mV_T}, \hat{M}_0 = \frac{M_0}{I_y}, \hat{M}_\alpha = \frac{M_\alpha}{I_y}, \hat{M}_q = \frac{M_q}{I_y}, \hat{M}_{\delta_E} = \frac{M_{\delta_E}}{I_y}$. Variables and parameters appearing in equation (5.35) include $\hat{L}_0$: effective lift contribution from sources other than α, $\hat{L}_\alpha$: effective lift curve slope for α, $\hat{M}_0$: effective moment contributions from sources other than $\alpha, q, \delta_E, \hat{M}_\alpha$ and $\hat{M}_q$: effective moment contributions from sources α, q, $\hat{M}_{\delta_E}$: effective pitch curve slope for δ_E.

The objective is to design a nonlinear feedback control law for the nonlinear flight dynamics (5.35) such that the flight path angle (γ) tracks the command (γ_{ref}) with asymptotic stability. The performance specifications of the system should achieve well-behaved command tracking with zero or small acceptable overshoot. The two following approaches are used to achieve the design goals and to show that the same feedback control laws are achieved by the two methods.

5.4.1 FEEDBACK LINEARIZATION-BASED DESIGN

The system (5.35) is of the form of system (5.1) with $f_1(x_1) = -\frac{g}{V_T}cos\gamma + \hat{L}_0 - \hat{L}_\alpha\gamma, g_1(x_1) = \hat{L}_\alpha, f_2(x_1, x_2) = 0, g_2(x_1, x_2) = 1, f_3(x_1, x_2, x_3) = \hat{M}_0 + \hat{M}_\alpha\alpha + \hat{M}_q q,\ g_3(x_1, x_2, x_3) = \hat{M}_{\delta_E}$, and $h(x) = \gamma$. System (5.35) has a full relative degree of

$r = 3$ in terms of Theorem 5.1. To show this, first compute $L_g h(x)$.

$$L_g h(x) = \begin{bmatrix} 1 & 0 & 0 \end{bmatrix} \begin{bmatrix} 0 \\ 0 \\ \hat{M}_{\delta_E} \end{bmatrix} = 0 \ \forall \ x \Rightarrow r > 1 \tag{5.36}$$

From equation (5.36), system (5.35) has a relative degree greater than 1 in terms of Definition 3.1. The higher relative degree will be certified by $L_g L_f h(x)$. Therefore, compute $L_f h(x)$ as an initial step.

$$\begin{aligned} L_f h(x) &= \begin{bmatrix} 1 & 0 & 0 \end{bmatrix} \begin{bmatrix} -\frac{g}{V_T} cos\gamma + \hat{L}_0 + \hat{L}_\alpha(\theta - \gamma) \\ q \\ \hat{M}_0 + \hat{M}_\alpha \alpha + \hat{M}_q q \end{bmatrix} \\ &= -\frac{g}{V_T} cos\gamma + \hat{L}_0 + \hat{L}_\alpha(\theta - \gamma) \end{aligned} \tag{5.37}$$

By taking the Lie derivative of $L_f h(x)$ with respect to $g(x)$, the desired term is achieved.

$$L_g L_f h(x) = \begin{bmatrix} \frac{g}{V_T} sin\gamma - \hat{L}_\alpha & \hat{L}_\alpha & 0 \end{bmatrix} \begin{bmatrix} 0 \\ 0 \\ \hat{M}_{\delta_E} \end{bmatrix} = 0 \ \forall \ x \Rightarrow r > 2 \tag{5.38}$$

From equation (5.38), one can conclude that system (5.35) has relative degree greater than 2 in terms of Definition 3.1. For confirmation of the final relative degree, the

term $L_g L_f^2 h(x)$ must be checked.

$$\begin{aligned} L_f^2 h(x) &= \begin{bmatrix} \frac{g}{V_T} sin\gamma - \hat{L}_\alpha & \hat{L}_\alpha & 0 \end{bmatrix} \begin{bmatrix} -\frac{g}{V_T} cos\gamma + \hat{L}_0 + \hat{L}_\alpha(\theta - \gamma) \\ q \\ \hat{M}_0 + \hat{M}_\alpha \alpha + \hat{M}_q q \end{bmatrix} \\ &= (\frac{g}{V_T} sin\gamma - \hat{L}_\alpha)(-\frac{g}{V_T} cos\gamma + \hat{L}_0 + \hat{L}_\alpha(\theta - \gamma)) + \hat{L}_\alpha q \end{aligned} \tag{5.39}$$

A term that will be needed soon for the control law is $L_f^3 h(x)$. By taking the Lie derivative of $L_f^2 h(x)$ with respect to $f(x)$, one gets

$$L_f^3 h(x) = \frac{g}{V_T} F_\gamma^2 cos\gamma + E_\gamma^2 F_\gamma + \hat{L}_\alpha E_\gamma q + \hat{L}_\alpha \hat{M}_0 + \hat{L}_\alpha \hat{M}_\alpha(\theta - \gamma) + \hat{L}_\alpha \hat{M}_q q \tag{5.40}$$

where $F_\gamma = -\frac{g}{V_T} cos\gamma + \hat{L}_0 + \hat{L}_\alpha(\theta - \gamma), E_\gamma = \frac{g}{V_T} sin\gamma - \hat{L}_\alpha$. Now by taking the Lie derivative of $L_f^2 h(x)$ with respect to $g(x)$, one gets

$$L_g L_f^2 h(x) = \begin{bmatrix} \frac{g}{V_T} F_\gamma cos\gamma + E_\gamma^2 & \hat{L}_\alpha E_\gamma & \hat{L}_\alpha \end{bmatrix} \begin{bmatrix} 0 \\ 0 \\ \hat{M}_{\delta_E} \end{bmatrix} = \hat{L}_\alpha \hat{M}_{\delta_E} \neq 0 \ \forall \ x \tag{5.41}$$

From equation (5.41), the term $L_g L_f^2 h(x) \neq 0 \ \forall \ x$. Thus system (5.35) has full relative degree of $r = 3$.

The feedback control law

$$\begin{aligned} \delta_E &= \frac{v - L_f^3 h(x)}{L_g L_f^2 h(x)} \\ &= \frac{v - (\frac{g}{V_T} F_\gamma^2 cos\gamma + E_\gamma^2 F_\gamma + \hat{L}_\alpha E_\gamma q + \hat{L}_\alpha \hat{M}_0 + \hat{L}_\alpha \hat{M}_\alpha(\theta - \gamma) + \hat{L}_\alpha \hat{M}_q q)}{\hat{L}_\alpha \hat{M}_{\delta_E}} \end{aligned} \tag{5.42}$$

transforms system (5.35) into Brunovsky canonical form in Reference [15] as

$$\begin{aligned} \dot{z}_1 &= z_2 \\ \dot{z}_2 &= z_3 \\ \dot{z}_3 &= v \end{aligned} \tag{5.43}$$

where the output equation is $y = h(x) = z_1$ and v is the new input signal. The linear backstepping-based design in Reference [68] is used to drive the new input v of system (5.43) as

$$v = -c_1c_2c_3(\gamma - \gamma_{ref}) - (c_1c_2 + c_1c_3 + c_2c_3)L_fh(x) - (c_1 + c_2 + c_3)L_f^2h(x) \tag{5.44}$$

where c_1, c_2, c_3 are positive gains. By combining equation (5.42) and equation (5.44), the state feedback control law for the nonlinear flight dynamics is achieved as shown by

$$\begin{aligned} \delta_E = \frac{1}{\hat{L}_\alpha \hat{M}_{\delta_E}} \{ &-c_1c_2c_3(\gamma - \gamma_{ref}) - (c_1c_2 + c_1c_3 + c_2c_3)L_fh(x) - (c_1 + c_2 + c_3)L_f^2h(x) \\ &- (\frac{g}{V_T}F_\gamma^2 cos\gamma + E_\gamma^2 F_\gamma + \hat{L}_\alpha E_\gamma q + \hat{L}_\alpha \hat{M}_0 + \hat{L}_\alpha \hat{M}_\alpha(\theta - \gamma) + \hat{L}_\alpha \hat{M}_q q)\} \end{aligned} \tag{5.45}$$

After a coordinate transformation

$$\begin{aligned} \tilde{z}_1 &= z_1 - \gamma_{ref} \\ \tilde{z}_2 &= z_2 + c_1(z_1 - \gamma_{ref}) \\ \tilde{z}_3 &= z_3 + c_1c_2(z_1 - \gamma_{ref}) + (c_1 + c_2)z_2 \end{aligned} \tag{5.46}$$

and utilizing the feedback control law (5.44), the nonlinear flight dynamic system

(5.43) is transformed into a state decoupled linear system (3.36), or

$$\begin{aligned} \dot{\tilde{z}}_1 &= -c_1 \tilde{z}_1 \\ \dot{\tilde{z}}_2 &= -c_2 \tilde{z}_2 \\ \dot{\tilde{z}}_3 &= -c_3 \tilde{z}_3 \end{aligned} \tag{5.47}$$

where c_1, c_2, c_3 are positive gains.

Thus, feedback linearization-based design is able to transform the nonlinear dynamic system (5.35) into separate state decoupled linear systems (5.47). To show that the resulting state feedback control law (5.45) and achieved state decoupled linear system (5.47) in this approach is able to be achieved by another approach, a backstepping-based design is considered next. In Section 5.4.2, the backstepping-based design approach is presented for clarity and an equivalence in some meaning between the two methods is discussed.

5.4.2 BACKSTEPPING-BASED CONTROL DESIGN

Step 1.

The θ variable is regarded as a control input in the first relation of equation (5.35) which is considered the first subsystem. Thus, θ is chosen to make the first subsystem globally asymptotically stable. The chosen α_1 function is called a virtual control law. By introducing z_1 as

$$z_1 = \gamma - \gamma_{ref} \tag{5.48}$$

and by differentiating both sides in time and combining with equation (5.48),

$$\dot{z}_1 = \dot{\gamma} = -\frac{g}{V_T} cos(z_1 + \gamma_{ref}) + \hat{L}_0 - \hat{L}_\alpha (z_1 + \gamma_{ref}) + \hat{L}_\alpha \theta \tag{5.49}$$

For the equation (5.49) system, a CLF $V_1(z_1)$ can be chosen such that when the virtual control law is applied, its time derivative becomes negatively definite. The positive definite function is chosen as

$$V_1(z_1) = \frac{1}{2} z_1^2 \tag{5.50}$$

By taking the derivative in time of equation (5.50) and combining with equation (5.49), one finds the result

$$\dot{V}_1(z_1) = z_1 \dot{z}_1 = z_1 (-\frac{g}{V_T} cos(z_1 + \gamma_{ref}) + \hat{L}_0 - \hat{L}_\alpha (z_1 + \gamma_{ref}) + \hat{L}_\alpha \theta) \tag{5.51}$$

By satisfying the asymptotically stable condition in the sense of Lyapunov for equation (5.51), a virtual control law denoted as α_1 for θ can be chosen as

$$\begin{aligned} -c_1 z_1 &= -\frac{g}{V_T} cos(z_1 + \gamma_{ref}) + \hat{L}_0 - \hat{L}_\alpha (z_1 + \gamma_{ref}) + \hat{L}_\alpha \theta \\ \Rightarrow \theta_{ref} \equiv \alpha_1(c_1, \gamma, \gamma_{ref}) &= \frac{1}{\hat{L}_\alpha} [-c_1(\gamma - \gamma_{ref}) + \frac{g}{V_T} cos\gamma - \hat{L}_0 + \hat{L}_\alpha \gamma] \end{aligned} \tag{5.52}$$

where c_1 is a positive gain. By doing so, the CLF derivative is negatively definite.

$$\dot{V}_1(z_1) = z_1 \dot{z}_1 = -c_1 z_1^2 \ \forall \ z_1 \neq 0 \tag{5.53}$$

Step 2.

By choosing the state feedback in equation (5.52) and a change of coordinate indicated below

$$z_2 = \theta - \alpha_1(c_1, \gamma, \gamma_{ref}) \tag{5.54}$$

the second subsystem can be re-written as follows

$$\begin{aligned} \dot{z}_1 &= -c_1 z_1 \\ \dot{z}_2 &= q - \frac{1}{\hat{L}_\alpha}(-c_1 F_\gamma - E_\gamma F_\gamma) \end{aligned} \tag{5.55}$$

where $F_\gamma = -\frac{g}{V_T} cos\gamma + \hat{L}_0 + \hat{L}_\alpha(\theta - \gamma), E_\gamma = \frac{g}{V_T} sin\gamma - \hat{L}_\alpha$

A CLF $V_2(z_1, z_2)$ can be chosen such that it makes the subsystem in equation (5.55) asymptotically stable with the virtual control law α_2 for q, i.e.,

$$V_2(z_1, z_2) = V_1(z_1) + \frac{1}{2} z_2^2 \tag{5.56}$$

Taking the derivative of equation (5.56) in time and combining with equation (5.55) results in

$$\dot{V}_2(z_1, z_2) = -c_1 z_1^2 + z_2(q - \frac{1}{\hat{L}_\alpha}(-c_1 F_\gamma - E_\gamma F_\gamma)) \tag{5.57}$$

To meet the asymptotically stable condition in the sense of Lyapunov for equation (5.57), a virtual control law α_2 can be chosen such that

$$\begin{aligned} &-c_2 z_2 = q - \frac{1}{\hat{L}_\alpha}(-c_1 F_\gamma - E_\gamma F_\gamma) \\ &\Rightarrow q_{ref} \equiv \alpha_2(c_1, c_2, \gamma, \theta, \gamma_{ref}) = \frac{1}{\hat{L}_\alpha}[-c_1 c_2(\gamma - \gamma_{ref}) - (c_1 + c_2) F_\gamma - E_\gamma F_\gamma] \end{aligned} \tag{5.58}$$

where c_2 is a positive gain. By doing so, the CLF derivative is negatively definite.

$$\dot{V}_1(z_1) = -c_1 z_1^2 - c_2 z_2^2 \; \forall \; z_1, z_2 \neq 0 \tag{5.59}$$

Step 3.

By choosing the state feedbacks in equations (5.52) and (5.58), and a change of coordinate in equations (5.48), (5.54), and (5.60) indicated below

$$z_3 = q - \alpha_2(c_1, c_2, \gamma, \theta, \gamma_{ref}) \tag{5.60}$$

the third subsystem can be re-written as follows

$$\begin{aligned} \dot{z}_1 &= -c_1 z_1 \\ \dot{z}_2 &= -c_2 z_2 \\ \dot{z}_3 &= \hat{M}_0 + \hat{M}_\alpha(z_2 + \alpha_1) - \hat{M}_\alpha(z_1 + \gamma_{ref}) + \hat{M}_q q + \hat{M}_{\delta_E}\delta_E - \dot{\alpha}_2 \end{aligned} \tag{5.61}$$

where $\alpha_2(c_1, c_2, \gamma, \theta, \gamma_{ref})$ is determined in equation (5.58), leading to

$$\dot{\alpha}_2 = \frac{1}{\hat{L}_\alpha}\{-c_1 c_2 F_\gamma - (c_1 + c_2)(E_\gamma F_\gamma + \hat{L}_\alpha q) - \frac{g}{V_T} F_\gamma^2 cos\gamma - E_\gamma^2 F_\gamma - \hat{L}_\alpha E_\gamma q\} \tag{5.62}$$

A CLF $V_3(z_1, z_2, z_3)$ can be chosen such that it makes the final subsystem (5.61) globally asymptotically stable with the control law δ_E, i.e.,

$$V_3(z_1, z_2, z_3) = V_2(z_1, z_2) + \frac{1}{2} z_3^2 \tag{5.63}$$

Taking the derivative of equation (5.63) in time and combining with equation (5.61) results in

$$\begin{aligned} \dot{V}_3(z_1, z_2, z_3) = -c_1 z_1^2 - c_2 z_2^2 + z_3\{&\hat{M}_0 + \hat{M}_\alpha(z_2 + \alpha_1) - \hat{M}_\alpha(z_1 + \gamma_{ref}) + \hat{M}_q q \\ &+ \hat{M}_{\delta_E}\delta_E - \dot{\alpha}_2\} \end{aligned} \tag{5.64}$$

To meet the asymptotically stable condition in the sense of Lyapunov for equation (5.64), a control law δ_E can be chosen such that

$$\begin{aligned} -c_3 z_3 &= \hat{M}_0 + \hat{M}_\alpha(z_2+\alpha_1) - \hat{M}_\alpha(z_1+\gamma_{ref}) + \hat{M}_q q + \hat{M}_{\delta_E}\delta_E - \dot{\alpha}_2 \\ \Rightarrow \delta_E &= \frac{1}{\hat{M}_{\delta_E}}[-c_3(q-\alpha_2) - \hat{M}_0 - \hat{M}_\alpha\theta + \hat{M}_\alpha\gamma - \hat{M}_q q + \dot{\alpha}_2] \end{aligned} \tag{5.65}$$

where c_3 is a positive gain.

By substituting for α_2 and $\dot{\alpha}_2$ from equations (5.58), (5.62), respectively, into equation (5.65), the control δ_E is achieved as

$$\begin{aligned} \delta_E = \frac{1}{\hat{L}_\alpha \hat{M}_{\delta_E}}\{&-c_1c_2c_3(\gamma-\gamma_{ref}) - (c_1c_2+c_1c_3+c_2c_3)F_\gamma - (c_1+c_2+c_3)(E_\gamma F_\gamma + \hat{L}_\alpha q) \\ &- (\frac{g}{V_T}F_\gamma^2 cos\gamma + E_\gamma^2 F_\gamma + \hat{L}_\alpha E_\gamma q + \hat{L}_\alpha\hat{M}_0 + \hat{L}_\alpha\hat{M}_\alpha(\theta-\gamma) + \hat{L}_\alpha\hat{M}_q q)\} \end{aligned} \tag{5.66}$$

where c_1, c_2, c_3 are positive gains. Introduce the Lie derivative notation in Definition 2.4, or

$$\begin{aligned} L_f h(x) &= F_\gamma \\ L_f^2 h(x) &= E_\gamma F_\gamma + \hat{L}_\alpha q \end{aligned} \tag{5.67}$$

By combining the equation (5.66) and equation (5.67), one gets

$$\begin{aligned} \delta_E = \frac{1}{\hat{L}_\alpha \hat{M}_{\delta_E}}\{&-c_1c_2c_3(\gamma-\gamma_{ref}) - (c_1c_2+c_1c_3+c_2c_3)L_f h(x) - (c_1+c_2+c_3)L_f^2 h(x) \\ &- (\frac{g}{V_T}F_\gamma^2 cos\gamma + E_\gamma^2 F_\gamma + \hat{L}_\alpha E_\gamma q + \hat{L}_\alpha\hat{M}_0 + \hat{L}_\alpha\hat{M}_\alpha(\theta-\gamma) + \hat{L}_\alpha\hat{M}_q q)\} \end{aligned} \tag{5.68}$$

By doing so, the CLF derivative is again negatively definite.

$$\dot{V}_3(z_1,z_2,z_3) = -c_1z_1^2 - c_2z_2^2 - c_3z_3^2 \;\forall\; z_1,z_2,z_3 \neq 0 \tag{5.69}$$

Thus, there exists a CLF in equation (5.63), state feedback laws in equations (5.52), (5.58), and (5.65), and a change of state transformations in equations (5.48), (5.54), and (5.60), such that the system (5.35) is transformed into a state decoupled linear system (5.70), which is the same as system (5.47) with positive gains c_1, c_2, c_3.

$$\begin{aligned} \dot{z}_1 &= -c_1 z_1 \\ \dot{z}_2 &= -c_2 z_2 \\ \dot{z}_3 &= -c_3 z_3 \end{aligned} \tag{5.70}$$

Comparing equation (5.45) with equation (5.68), and equation (5.47) with equation (5.70), respectively, leads to the conclusion that both feedback linearization-based and backstepping-based design approaches are equivalent. Also, the designed dynamic system is asymptotically stable and the output tends to zero without overshoot with positive gains. In other words, the tracking performance of the two systems occur with no overshoot. The desired settling time and rise time of the systems are obtained by tuning the gains. Thus, the stability and performance specifications are achieved by either of the two proposed control designs.

5.4.3 EQUIVALENCE CONTROL STUDY OF F-16 MODEL

The aerodynamic data of the F-16 aircraft model used for numerical simulation here is the same as in Section 4.3 in Chapter 4. The closed-loop simulator based on the control law in equation (5.66) or (5.42) and a similar block diagram in Figure 3.1 in Chapter 3 is tested with two different flight path command profiles away from the trim condition. In the first profile, a small command of 5 degrees for flight path angle

is applied and in the second profile, the reference flight path angle will be put at 5 degrees for the first five seconds, at 20 degrees for the next ten seconds, and then 15 degrees for the remaining time. Also, the numerical results are validated with both true model and design model for comparison.

Case 1: Simple Step Excitation

Figure 5.2 shows the time response of flight path angle for an applied command of 5 degrees. This result was generated with $c_1 = 1.32\ s^{-1}, c_2 = 1.23\ s^{-1}, c_3 = 1.42\ s^{-1}$. These specific gain values were computed from an optimization process described further in Reference [52]. The result shows tracking performance characteristics of the aircraft are obtained with no overshoot and a fast response. Figures 5.3 and 5.4 show the elevator travel and elevator rate responses required to achieve the flight path angle response in Figure 5.2. Peak travel and rate values are within actuation technology for typical high-performance airframes. For other numerical simulations, settling time can be reduced by increasing the gains but limitations from the elevator actuation system will eventually be reached. Thus, a trade-off between settling time and actuation requirement exists for the closed-loop aircraft. The responses shown here are obtainable from either the feedback linearization design technique or the backstepping design technique, as the two methods give identical control laws and closed-loop systems in this application. One concern of either design technique is the significance of modeling assumptions required to bring the original nonlinear aircraft dynamics model in equation (4.1) to the nonlinear triangular affine form in equation (5.1).

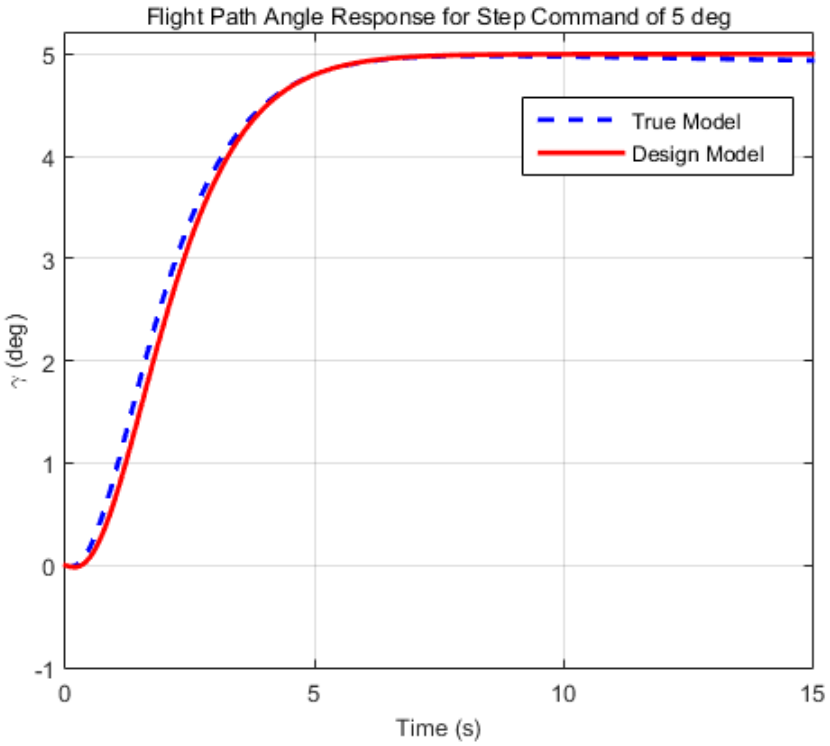

Figure 5.2: Flight Path Angle Response for Step Command of 5 degrees

Figure 5.2 shows the two closed-loop flight path angle responses when the control law is applied to the original or true model and the simplified or design model. For the 5 degree command case, very little difference between the two models is noted. The response using the original model experiences a slightly different but non-significant change to the rise and steady state behavior. Accurate and quick tracking performance is maintained with the original aircraft model.

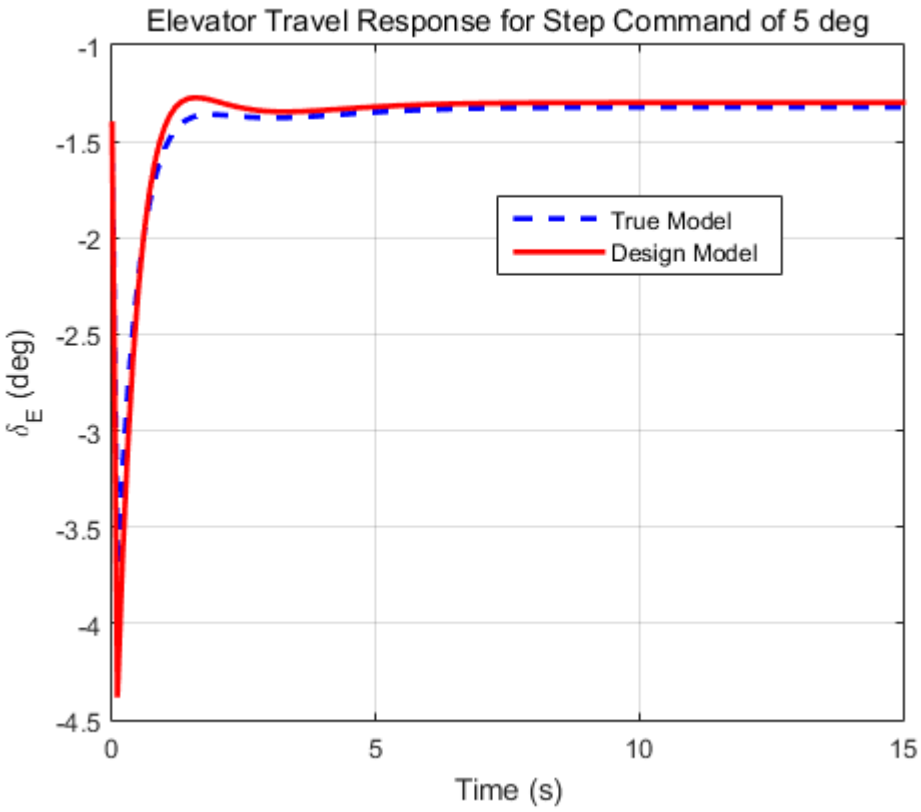

Figure 5.3: Elevator Travel Response for Step Command of 5 degrees

Case 2: Complex Step Excitation

Figure 5.5 shows the time response of flight path angle for a series of step commands of varying levels. The data shows the settling time is approximately 6 seconds regardless of the step amplitude. The control system is able to follow the command across small and large inputs. Figure 5.5 again shows a comparison when the control law is applied to the original and simplified models. Note when applied to the true (or original) model, the response experiences an overshoot transient for the 15 degree command change out to $\gamma = 20$ degrees but rises faster than the design model (or

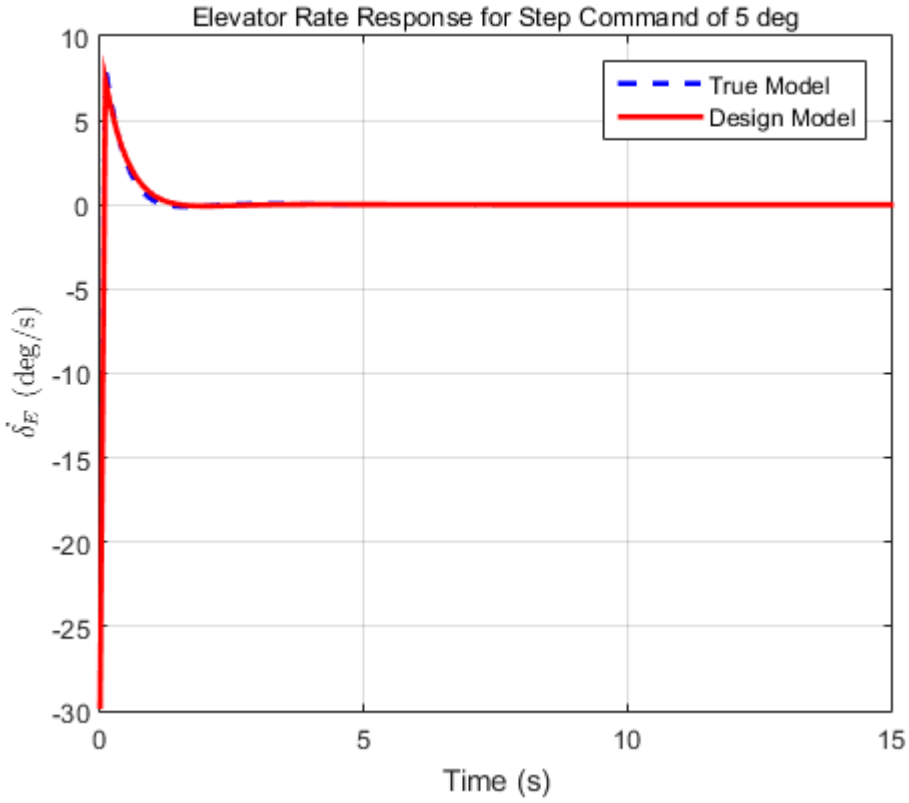

Figure 5.4: Elevator Rate Response for Step Command of 5 degrees

simplified model) response. Overall, the flight path angle time response of the aircraft is well-behaved in tracking and the performance specifications are obtained with high reliability. Figures 5.6 and 5.7 show the required elevator activity to achieve this performance. Note the larger flight path commands incur increased elevator rate. Due to the established equivalence between the feedback linearizing controller and the backstepping controller, either technique leads to the augmented response in Figure 5.5.

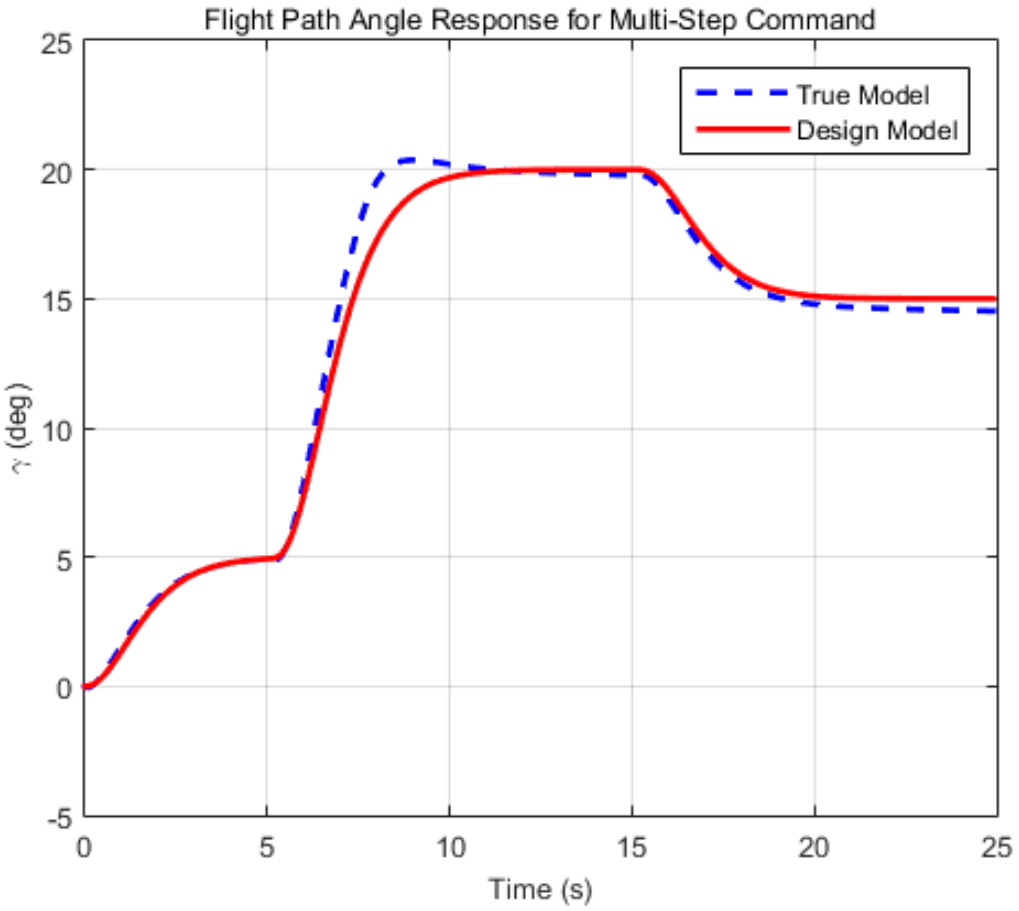

Figure 5.5: Flight Path Angle Response for Multi-Step Command

Thus, by applying the proposed theory, the state decoupling problem for the longitudinal dynamic model is obtained by coordinate transformations and a feedback control law with some simplifying assumptions. The resulting controller makes the original system a well-behaved command tracking and asymptotically globally stable system. Further, the response of the system has no overshoot. From the above simulation results, some comments are made.

- The flight path angle time response for a step command of 5 degrees shown in Figure 5.2 meets the performance specifications with no overshoot and with a

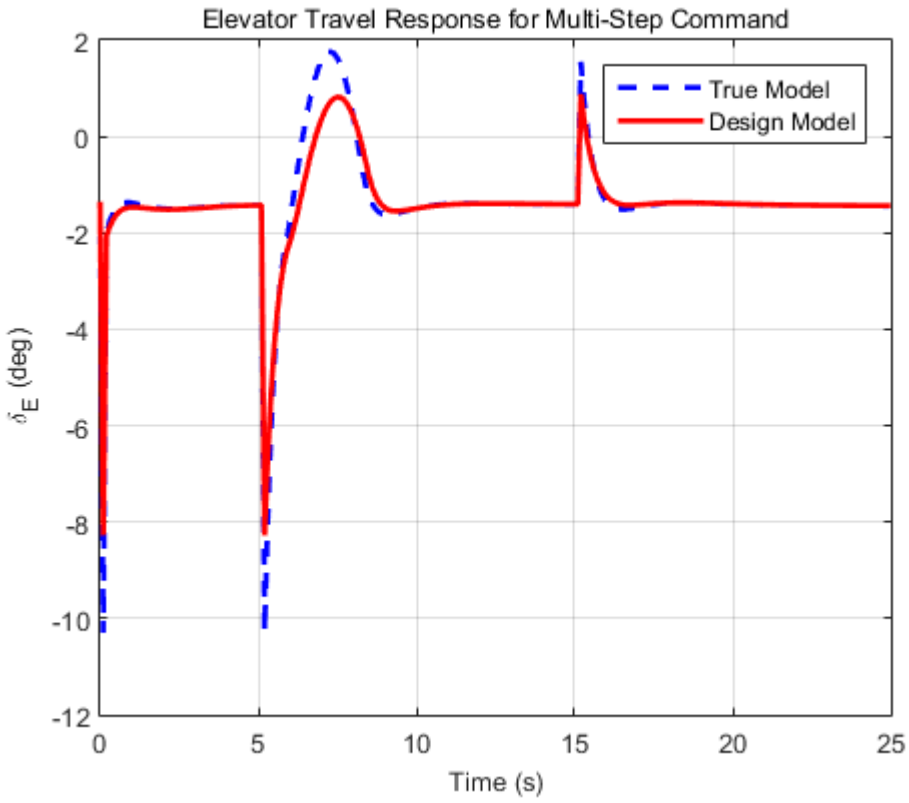

Figure 5.6: Elevator Travel Response for Multi-Step Command

settling time of 6 seconds.

- The simulation result shown in Figure 5.5 demonstrates the proposed control algorithm works well in different operating conditions.

- The comparison result shown in Figure 5.2 and Figure 5.5 suggests the simplifying assumptions are valid for this specific numerical model and input amplitude range.

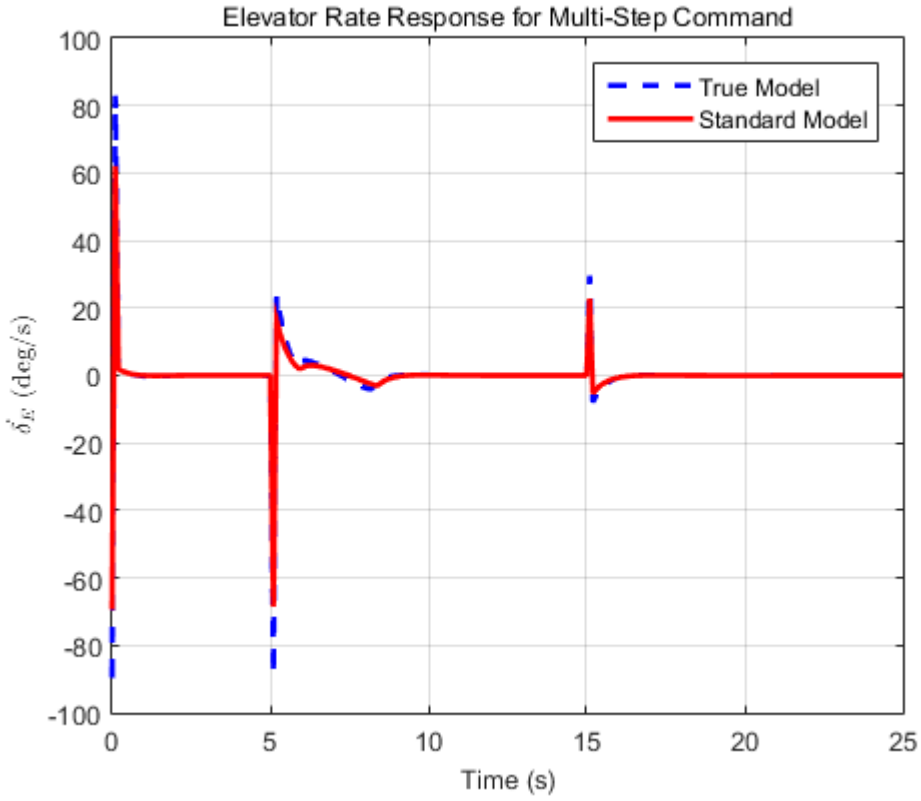

Figure 5.7: Elevator Rate Response for Multi-Step Command

5.5 SUMMARY AND DISCUSSION

This chapter investigates an equivalence of the feedback linearization-based design method and the backstepping-based design approach for a specific class of nonlinear dynamic systems under some assumptions. The specific class is denoted a triangular affine system. Implications from the equivalence are that the stability and performance properties of one method are the same for the other method. Thus, a property known to exist only for one method could be used to prove the property also holds for the other. Also, suspected advantage of one method over the other is proven to be a false conjecture. Both approaches are able to transform the nonlinear dynamic

system into a canonical state decoupled linear dynamic system form by the coordinate transformations and nonlinear state feedbacks. Further, the resulting nonlinear feedback control law obtained by the feedback linearization method matches exactly with the nonlinear controller achieved by the backstepping-based design approach. The open question arises on whether there exists a broader mergence between feedback linearization-based and backstepping-based design approaches for more general model structure.

Demonstrations are considered and validated via flight path angle control corresponding to the longitudinal dynamics of a high-performance aircraft simulation model. Algorithms are tested and evaluated with analytical models and nonlinear closed-loop simulation. The analytical control law and numerical simulation results show that the proposed control design algorithms are applicable, reliable, and highly accurate. With the rapid development of the digital computer, the nonlinear feedback controllers prove helpful for providing enhanced stability and performance.

CHAPTER 6

INTEGRATOR-BACKSTEPPING CONTROL FOR FLIGHT DYNAMICS

In this chapter, the integrator-backstepping-based control in Section 3.3 of Chapter 3 is applied for nonlinear flight dynamics of an aircraft. Particularly, the flight path angle control corresponding to the nonlinear longitudinal dynamics of an F-16 aircraft model is considered. Firstly, some assumptions of nonlinear longitudinal dynamics of an aircraft are introduced to transform the original nonlinear model into the standard strict-feedback form in the presence of parameter errors and disturbances for design suitability. Secondly, control designs are implemented for the standard model in order to achieve the design goals. The integrator-backstepping control design steps are provided to formulate the IBSC law for the nominal standard model of nonlinear longitudinal dynamics of the aircraft. Finally, numerical simulation is implemented for the proposed approach to validate and evaluate the proposed algorithm via the nonlinear closed-loop augmentation of a high-performance aircraft model.

6.1 PROBLEM STATEMENT

Consider the aircraft longitudinal dynamics depicted in Figure 4.1. Some assumptions are considered to assist in transforming the aircraft model in equation (2.26)

to the standard strict-feedback form in the presence of parameter errors in equation (3.37).

- Airspeed is constant for short period dynamics, i.e., $\dot{V}_T = 0$.
- Lift force is a sinusoidal function of the angle of attack, or $L = (\tilde{L} + \delta_L)sin\alpha$, where $\tilde{L}$ is constant and δ_L is a parameter error term from the actual L.
- Thrust point offset is neglected or $z_{TF} = 0$ is valid for F-16 model.
- Influence of wind speed on attack angle is also considered as $(\alpha - \alpha_w)$, where α_w is a bounded random variable with $|\alpha_w| \leq 5^o$.
- Assume that wind velocity is small or $\sin\alpha_w \simeq \alpha_w$, and $\cos\alpha_w \simeq 1$.

With these assumptions and use of the relationship $\alpha = \theta - \gamma$, the mathematical model of longitudinal motion of the aircraft is re-written as

$$\begin{aligned}
\dot{\gamma} &= \frac{1}{mV_T}([\hat{L} + F_T]sin(\theta - \gamma) - mgcos\gamma) + \Phi(\alpha)\alpha_w \\
\dot{\theta} &= q \\
\dot{q} &= u
\end{aligned} \tag{6.1}$$

where

$$u = \frac{1}{I_y}(M + F_T z_{TF})$$

and where L is approximated by $\tilde{L} + \delta_L = \hat{L}$. Also the term $\Phi(\alpha)\alpha_w$ represents an approximation of the wind effect, where $\Phi(\alpha) = \frac{1}{mV_T}(\hat{L} + F_T)cos\alpha$.

The objective is to design a control law for the parameterized strict-feedback system (6.1) such that the flight path angle (γ) output signal tends to the command

(γ_{ref}) asymptotically where γ_{ref} is a constant, and global asymptotic stability is achieved with zero or acceptably small overshoot in the system in the presence of the model parameter errors and wind disturbance. The proposed control approach in Section 3.3 in Chapter 3 is used for achieving the design goals. In the next section, a IBSC formulation is provided for the nominal form of system (6.1).

6.2 CONTROL LAW FORMULATION

The main point of this demonstration is to show the formulation for the IBSC law applied to the nominal standard strict-feedback model of nonlinear longitudinal flight systems. Then a closed-loop system for a flight path angle control is provided to validate the proposed method. Consider a nominal strict-feedback form of longitudinal motion of the aircraft as

$$\begin{aligned}
\dot{\gamma} &= \frac{1}{mV_T}([\hat{L} + F_T]sin(\theta - \gamma) - mgcos\gamma) \\
\dot{\theta} &= q \\
\dot{q} &= u
\end{aligned} \tag{6.2}$$

where

$$u = \frac{1}{I_y}(M + F_T z_{TF})$$

Note that the system in equation (6.2) possesses the standard strict-feedback form similar to equation (3.2). The next step is to design the integrator-backstepping control law for nonlinear longitudinal dynamics of the aircraft by using the control design in Section 3.3. The complete system in equation (6.2) is divided into three

subsystems. The first consists of the first relation of equation (6.2), the second consists of the first two relations of equation (6.2), and the last consists of the whole system in equation (6.2). After applying the backstepping method with each subsystem, as noted above, the resulting IBSC logic is proven to possess globally asymptotic stability using the CLF. The following development is the procedure to formulate the IBSC law with a desired flight path angle (γ_{ref}).

Step 1.

The state variable θ is regarded a control input of the first relation of equation (6.2) which is considered as the first subsystem. Thus, θ is chosen to make the first subsystem globally asymptotically stable. The chosen α_1 for the θ function is called a virtual control law. By introducing a modified tracking error $\tilde{\gamma}$ as

$$\tilde{\gamma} = (\gamma - \gamma_{ref}) + \sigma \tag{6.3}$$

where $\sigma = c_0 \int_0^t e(\tau)d\tau, e(t) = \gamma - \gamma_{ref}$, and $e(t)$ is defined as the normal tracking error and c_0 is a positive gain. Differentiating both sides of equation (6.3) in time and combining with the first relation of equation (6.2) result in

$$\begin{aligned} \dot{\tilde{\gamma}} &= \dot{\gamma} + \dot{\sigma} \\ &= \frac{1}{mV_T}\{[\hat{L} + F_T]sin(\theta - \gamma) - mgcos\gamma\} + \dot{\sigma} \end{aligned} \tag{6.4}$$

where $\dot{\sigma} = c_0 e$ or $\dot{\sigma} = c_0(\gamma - \gamma_{ref})$.

For the system (6.4), a CLF $V_1(\tilde{\gamma})$ in terms of Definition 2.8 can be chosen such that when the virtual control law is applied, its time derivative becomes negatively

definite. The positive definite function is chosen as

$$V_1(\tilde{\gamma}) = \frac{1}{2}\tilde{\gamma}^2 \tag{6.5}$$

Taking the time derivative of equation (6.5) and combining with equation (6.4), one achieves

$$\begin{aligned} \dot{V}_1(\tilde{\gamma}) &= \tilde{\gamma}\dot{\tilde{\gamma}} \\ &= \tilde{\gamma}\{\frac{1}{mV_T}([\hat{L} + F_T]sin(\theta - \gamma) - mgcos\gamma) + \dot{\sigma}\} \end{aligned} \tag{6.6}$$

By satisfying the asymptotically stable condition in the sense of Lyapunov in Theorem 2.2 for equation (6.6), a virtual control law denoted as α_1 for θ can be chosen as

$$\begin{aligned} -c_1\tilde{\gamma} &= \frac{1}{mV_T}([\hat{L} + F_T]sin(\theta - \gamma) - mgcos\gamma) + \dot{\sigma} \\ \Rightarrow \theta_{ref} \equiv \alpha_1 &= \gamma + arcsin\{\frac{1}{\hat{L} + F_T}[-mV_T c_1\sigma - mV_T(c_0 + c_1)e + mgcos\gamma]\} \end{aligned} \tag{6.7}$$

where c_1 is the positive gain. By doing so, the CLF derivative is negatively definite

$$\dot{V}_1(\tilde{\gamma}) = \tilde{\gamma}\dot{\tilde{\gamma}} = -c_1\tilde{\gamma}^2 < 0 \;\forall\; \tilde{\gamma} \neq 0 \tag{6.8}$$

Step 2.

By choosing the state feedback in equation (6.7) and a change of coordinate in equation (6.3), the second subsystem can be re-written as follows

$$\begin{aligned} \dot{\tilde{\gamma}} &= -c_1\tilde{\gamma} \\ \dot{\theta} &= q \end{aligned} \tag{6.9}$$

The signal θ_{ref} is considered as a command for the system (6.9) and the modified tracking error for pitch angle is introduced as

$$\tilde{\theta} = \theta - \alpha_1 \tag{6.10}$$

With this, the second subsystem can be re-written as follows

$$\begin{aligned} \dot{\tilde{\gamma}} &= -c_1\tilde{\gamma} \\ \dot{\tilde{\theta}} &= q - \dot{\alpha}_1 \end{aligned} \tag{6.11}$$

where $\dot{\alpha}_1$ is determined as functions of the c_0, c_1 gains, the γ state, γ_{ref} command, the σ integrator, and known parameter $\hat{L}$. The state variable q is regarded as a control input in equation (6.11) and a CLF $V_2(\tilde{\gamma}, \tilde{\theta})$ can be chosen such that it makes the subsystem in equation (6.11) asymptotically stable with the virtual control law, i.e.,

$$V_2(\tilde{\gamma}, \tilde{\theta}) = V_1(\tilde{\gamma}) + \frac{1}{2}\tilde{\theta}^2 \tag{6.12}$$

By taking the time derivative of equation (6.12) and combining with equation (6.11), one finds the result

$$\dot{V}_2(\tilde{\gamma}, \tilde{\theta}) = -c_1\tilde{\gamma}^2 + \tilde{\theta}\dot{\tilde{\theta}} = -c_1\tilde{\gamma}^2 + \tilde{\theta}(q - \dot{\alpha}_1) \tag{6.13}$$

To meet the asymptotically stable condition in the sense of Lyapunov in Theorem 2.2 for equation (6.13), a virtual control law denoted as α_2 for q can be chosen such that

$$\begin{aligned} -c_2\tilde{\theta} &= q - \dot{\alpha}_1 \\ \Rightarrow q_{ref} \equiv \alpha_2 &= -c_2(\theta - \alpha_1) + \dot{\alpha}_1 \end{aligned} \tag{6.14}$$

where c_2 is a positive gain and $\dot{\alpha}_1$ is determined from equations (6.15), (6.16), (6.17).

$$\dot{\alpha}_1 = F_\gamma - \frac{mgF_\gamma sin\gamma + mV_T(c_0 + c_1)F_\gamma + mV_T c_0 c_1 e}{(\hat{L} + F_T)\sqrt{1 - X^2}} \tag{6.15}$$

$$X = \frac{1}{\hat{L} + F_T}\{-mV_T c_1 \sigma - mV_T(c_0 + c_1)e + mgcos\gamma\} \tag{6.16}$$

$$F_\gamma = \frac{1}{mV_T}([\hat{L} + F_T]sin(\theta - \gamma) - mgcos\gamma) \tag{6.17}$$

By doing so, the CLF derivative is negatively definite, or

$$\dot{V}_2(\tilde{\gamma}, \tilde{\theta}) = -c_1\tilde{\gamma}^2 - c_2\tilde{\theta}^2 < 0 \ \forall \ \tilde{\gamma}, \tilde{\theta} \neq 0 \tag{6.18}$$

Step 3.

By choosing the state feedbacks in equations (6.7), (6.14), and a change of state transformations in equations (6.3), (6.10), the complete system can be re-written as

$$\begin{aligned} \dot{\tilde{\gamma}} &= -c_1\tilde{\gamma} \\ \dot{\tilde{\theta}} &= -c_2\tilde{\theta} \\ \dot{q} &= u \end{aligned} \tag{6.19}$$

The signal q_{ref} is considered as a command for the system (6.19) and the modified tracking error for pitch rate is introduced in equation (6.20), i.e.,

$$\tilde{q} = q - \alpha_2 \tag{6.20}$$

With this, the third subsystem (or complete system) is re-written as follows

$$\begin{aligned} \dot{\tilde{\gamma}} &= -c_1\tilde{\gamma} \\ \dot{\tilde{\theta}} &= -c_2\tilde{\theta} \\ \dot{\tilde{q}} &= u - \dot{\alpha}_2 \end{aligned} \tag{6.21}$$

where $\dot{\alpha}_2$ is determined by equations (6.22), (6.23), (6.24), (6.25), and (6.26).

$$\dot{\alpha}_2 = -c_2(q - \dot{\alpha}_1) + \ddot{\alpha}_1 \tag{6.22}$$

$$\ddot{\alpha}_1 = \dot{F}_\gamma + \frac{\ddot{X}(1 - X^2) + X\dot{X}^2}{(1 - X^2)^{3/2}} \tag{6.23}$$

$$\dot{F}_\gamma = \frac{1}{mV_T}\{(\hat{L} + F_T)(q - F_\gamma)cos(\theta - \gamma) + mgF_\gamma sin\gamma\} \tag{6.24}$$

$$\dot{X} = \frac{1}{\hat{L} + F_T}\{-mV_T c_0 c_1 e - mV_T(c_0 + c_1)F_\gamma - mgF_\gamma sin\gamma\} \tag{6.25}$$

$$\ddot{X} = \frac{1}{\hat{L} + F_T}\{-mV_T c_0 c_1 F_\gamma - mV_T(c_0 + c_1)\dot{F}_\gamma - mg\dot{F}_\gamma sin\gamma - mgF_\gamma^2 cos\gamma\} \tag{6.26}$$

Thus, the real control u can be chosen to make the system (6.21) globally asymptotically stable.

A CLF $V_3(\tilde{\gamma}, \tilde{\theta}, \tilde{q})$ in terms of Definition 2.8 can be chosen such that it makes the system (6.21) asymptotically stable with the associated control law. The CLF function in terms of Definition 2.8 is

$$V_3(\tilde{\gamma}, \tilde{\theta}, \tilde{q}) = V_2(\tilde{\gamma}, \tilde{\theta}) + \frac{1}{2}\tilde{q}^2 \tag{6.27}$$

Taking the derivative of equation (6.27) in time and combining with equation (6.21) results in

$$\begin{aligned} \dot{V}_3(\tilde{\gamma},\tilde{\theta},\tilde{q}) &= -c_1\tilde{\gamma}^2 - c_2\tilde{\theta}^2 + \tilde{q}\dot{\tilde{q}} \\ &= -c_1\tilde{\gamma}^2 - c_2\tilde{\theta}^2 + \tilde{q}(u - \dot{\alpha}_2) \end{aligned} \tag{6.28}$$

To meet the asymptotically stable condition in the sense of Lyapunov in Theorem 2.2 for equation (6.28), an integrator-backstepping control law for the system (6.2) u is chosen such that

$$\begin{aligned} -c_3\tilde{q} &= u - \alpha_2 \\ \Rightarrow u \equiv \alpha_3 &= -c_3(q - \alpha_2) + \dot{\alpha}_2 \end{aligned} \tag{6.29}$$

where c_3 is a positive gain. By doing so, the required sign condition on $\dot{V}_3(\tilde{\gamma},\tilde{\theta},\tilde{q})$ is achieved.

$$\dot{V}_3(\tilde{\gamma},\tilde{\theta},\tilde{q}) = -c_1\tilde{\gamma}^2 - c_2\tilde{\theta}^2 - c_3\tilde{q}^2 < 0 \;\forall\; \tilde{\gamma},\tilde{\theta},\tilde{q} \neq 0 \tag{6.30}$$

Thus, there exists a CLF in terms of Definition 2.8 in equation (6.27), state feedback laws in equations (6.7), (6.14) and (6.29), and change of state transformations in equations (6.3), (6.10) and (6.20), so that the system is transformed into a state decoupled linear system as

$$\begin{aligned} \dot{\tilde{\gamma}} &= -c_1\tilde{\gamma} \\ \dot{\tilde{\theta}} &= -c_2\tilde{\theta} \\ \dot{\tilde{q}} &= -c_3\tilde{q} \end{aligned} \tag{6.31}$$

By examining system (6.31), one can conclude that the system time response is globally asymptotically stable and converges to the origin. This behavior implies that

the flight path angle of the aircraft will have a well-tracking response that follows the command. Also, the desired settling time and rise time of the system are achieved by optimally tuning the gains in Reference [52]. Thus, the stability and performance specifications of the system (6.2) are obtained with the IBSC law (6.29). A block diagram of the integrator-backstepping-based control design is provided in Figure 6.1.

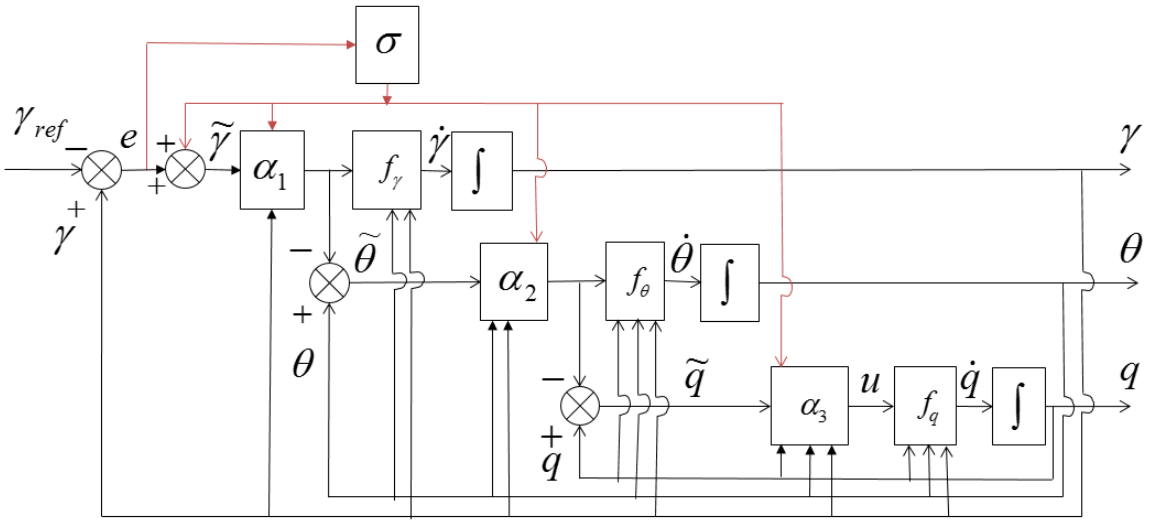

Figure 6.1: Block Diagram of Integrator-Backstepping-Based Flight Path Angle Control

6.3 F-16 MODEL FLIGHT PATH SIMULATION STUDY

The aerodynamic data of the F-16 aircraft model used for numerical simulation is the same as in Section 4.3 in Chapter 4. The closed-loop simulator based on the control law in equation (6.29) and block diagram in Figure 6.1 is tested with two different flight path command profiles away from the trim condition. In the first profile, a small command of 5 degrees for flight path angle is applied to the

design model and true model without the presence of disturbances. In the second profile, the reference flight path angle will be put at 5 degrees in the presence of wind disturbance (α_w) which has a random behavior but magnitude between -5 and 5 degrees in Figure 6.2. Also, the stability robustness of the proposed algorithm is examined in the last case by implementing the wind disturbance in Figure 6.3, in which the wind angle of attack is constant. The validation of assumptions for achieving the standard model is verified by comparing the simulation results with both the design model and true model. Also, these results were generated with gains $c_1 = 1.32\ s^{-1}, c_2 = 1.23\ s^{-1}, c_3 = 1.42\ s^{-1}$, similar to the gain set in Reference [52]. These specific gain values were computed from an optimization process described further in Reference [52].

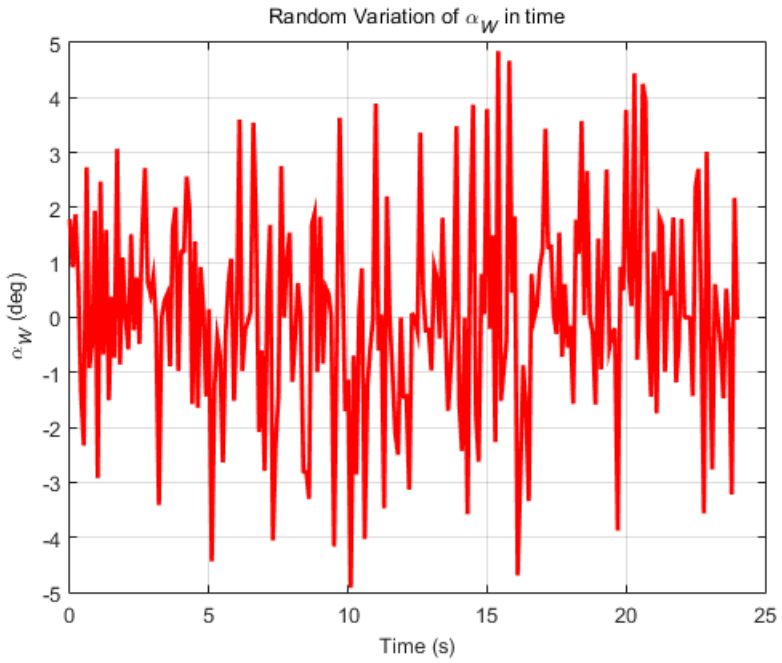

Figure 6.2: Attack Angle Wind Disturbance with Random but Bounded Magnitude

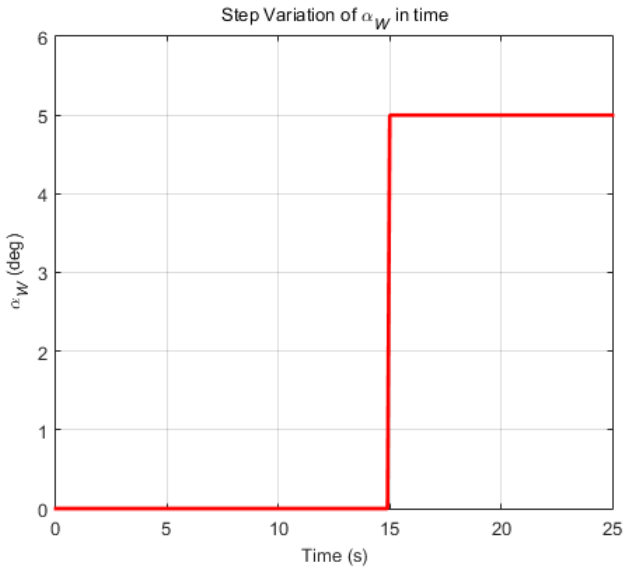

Figure 6.3: Attack Angle Wind Disturbance with Constant Magnitude

Case 1: Step Excitation without Wind Disturbance

Figure 6.4 shows the time responses of flight path angle for an applied command of 5 degrees without the presence of wind on the flight condition. The red (or solid) line shows time response of flight path angle of the aircraft for the design model. The blue (or dash) line represents the response for the true model. Time responses in the two models are with no overshoot and with a 6 second settling time. The small difference in simulation results for the two models validates the given assumptions. The outcomes are verified again in the prediction by the proposed theoretical development in Section 3.3 in Chapter 3. Overall, the flight path angle time response of the aircraft is well-behaved in tracking and the performance specifications are achieved with high reliability. Figure 6.5 shows the elevator time responses in which the red (or solid) line shows the elevator time response for the aircraft design model,

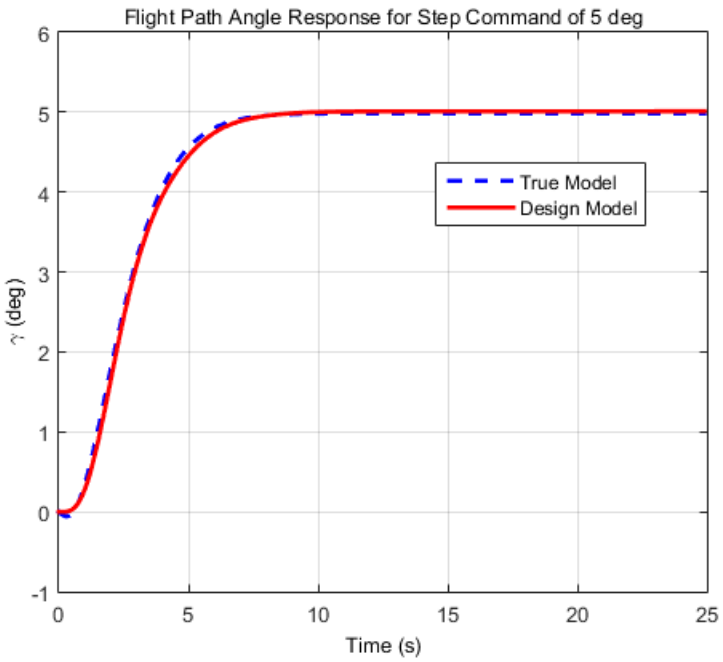

Figure 6.4: Flight Path Angle Response for Step Command of 5 degrees

while the blue (or dash) line represents the aircraft true model. The response of the elevator simulated with the design model has a larger magnitude than the response simulated with the true model. This difference is due to the approximated lift of the aircraft.

Case 2: Step Excitation with Random Wind Disturbance

Figure 6.6 shows the time responses of flight path angle for an applied command of 5 degrees for the true model under two different disturbances. The solid line shows the time response of flight path angle of the aircraft with the presence of random magnitude wind disturbance, as shown in Figure 6.2. The dash line represents the response without any disturbance. The results show that the response of flight path

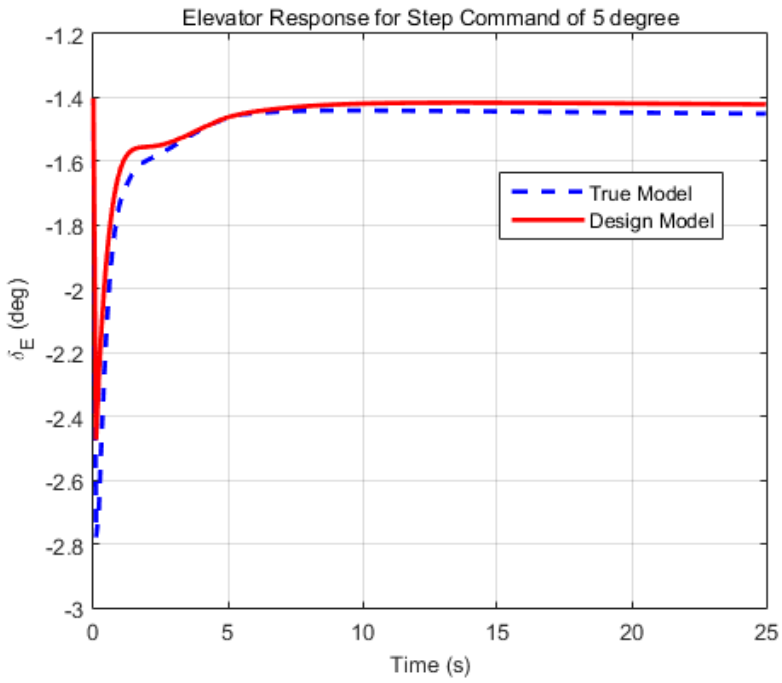

Figure 6.5: Elevator Response for Step Command of 5 degrees

angle of the aircraft has small variation around the command but the closed-loop tracking behavior is still acceptable. Figure 6.7 shows the corresponding elevator response.

Case 3: Step Excitation with Constant Wind Disturbance

Figure 6.8 and Figure 6.9 show the time responses of flight path angle and the elevator of the aircraft with a single excitation of 5 degrees for the true model. In this simulation, the disturbance on the attack angle is applied at a constant magnitude of 5 degrees, as shown in Figure 6.3. The solid line in Figure 6.8 shows the time response of flight path angle of the aircraft with the wind disturbance and the dash line represents the response without any disturbance. The result shows the time

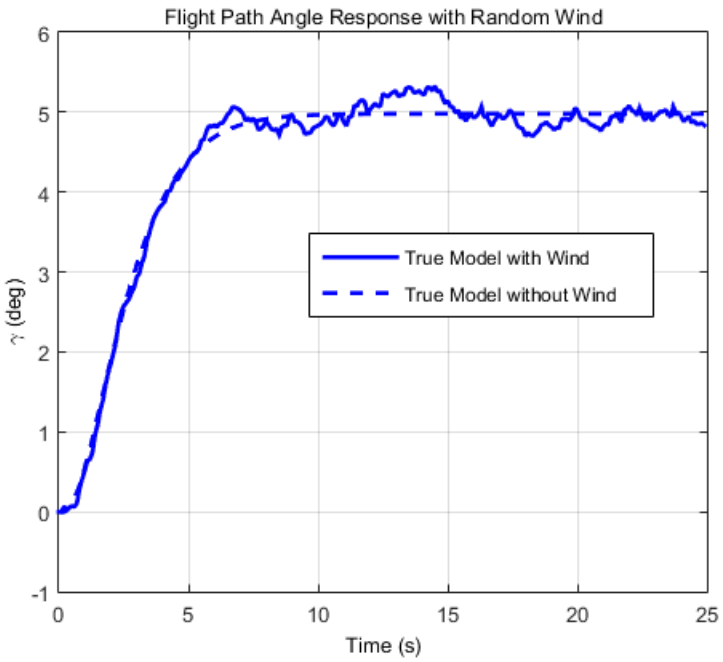

Figure 6.6: Flight Path Angle Response for Step Command of 5 degrees with Random Disturbance

response of flight path angle is recovered in the presence of the disturbance on attack angle after 5 seconds. Figure 6.9 shows that the elevator of the aircraft needs to be adjusted in order to track the command. Also, the results in Figure 6.7 and Figure 6.9 show the elevator response lies within the actuator capabilities in Reference [62]. From the primary results, some conclusions are made below.

- The proposed control algorithm is employed in a numerical nonlinear closed-loop simulation. The IBSC law provides stability and well-behaved tracking of a command for a class of nonlinear strict-feedback systems.

- The simulation results represent robust stability of the proposed control strategy in the presence of the model parameter error and disturbance.

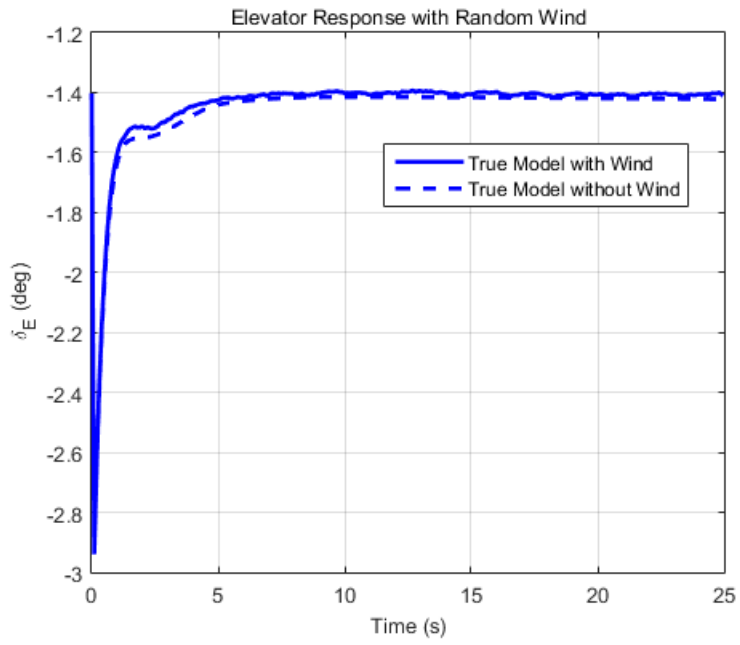

Figure 6.7: Elevator Response for Step Command of 5 degrees with Random Disturbance

6.4 SUMMARY AND DISCUSSION

The research investigates an integrator-backstepping control methodology for a strict-feedback form of a nonlinear dynamic system in the presence of model parameter errors and disturbances. A systematic procedure is addressed firstly for formulating the IBSC law for the nominal strict-feedback model of a nonlinear flight dynamic system. The formulation starts with a definition of a modified tracking error by adding an integral term to the normal tracking error, and then, a recursive sequence of coordinate transformations and control Lyapunov function feedback selections results in an IBSC law to make the system well-behaved in tracking and asymptotically stable. To show the applicability, the flight path angle control corresponding to the

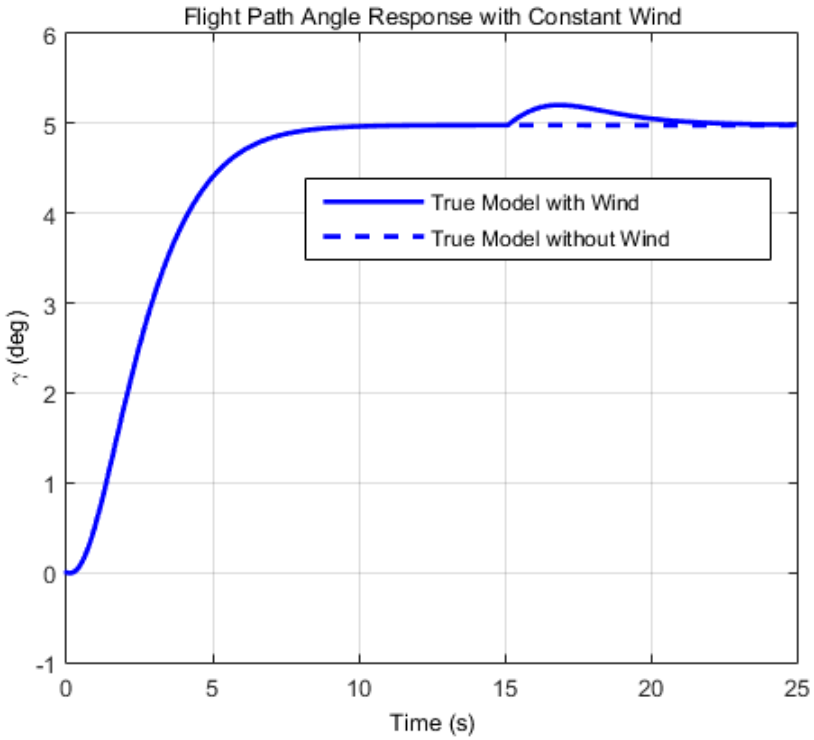

Figure 6.8: Flight Path Angle Response for Step Command of 5 degrees with Constant Disturbance

nonlinear longitudinal dynamics of the F-16 aircraft model is addressed. An assumption on the lift force of the aircraft as a sinusoidal function of attack angle and wind disturbance supports the simplifying of the longitudinal dynamics of an aircraft to the standard strict-feedback form of nonlinear flight dynamics in the presence of the disturbance. The control design is applied for the standard nominal model to achieve the IBSC law for nonlinear longitudinal dynamics of an aircraft. A numerical simulation is implemented to validate and evaluate the proposed algorithm via nonlinear closed-loop augmentation of a high-performance aircraft model.

Numerical results indicate that the control design goals, such as well-behaved

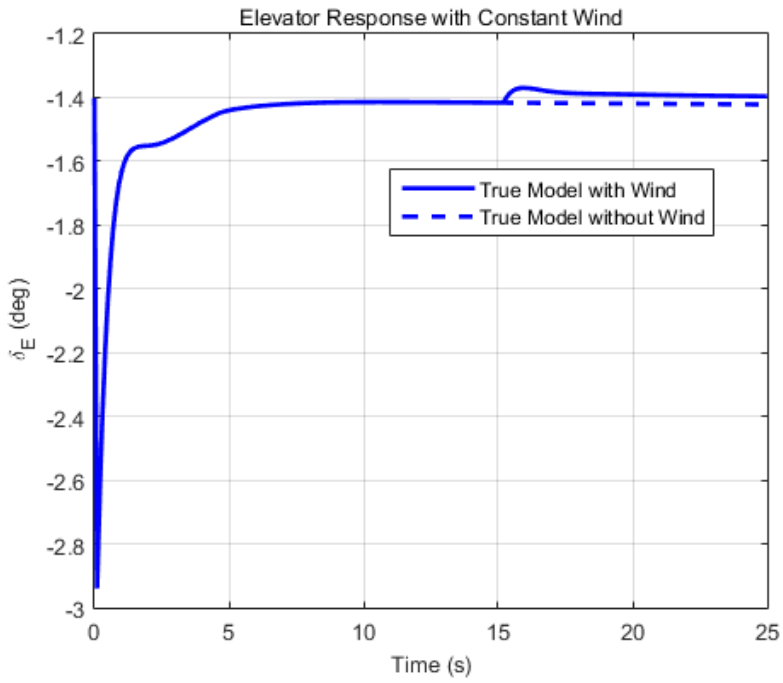

Figure 6.9: Elevator Response for Step Command of 5 degrees with Constant Disturbance

command following with no overshoot and asymptotic stability, are achieved by using the integrator-backstepping-based control method. Besides the IBSC-based control method providing improvements on performance and stability as compared to the BSC-based control, the modified logic is able to eliminate the effects of disturbances. However, the IBSC-based control design needs an extra gain and variable as compared to the BSC-based control in order to implement the control action. In reality, the use of either a BSC-based or an IBSC-based control depends on system properties and requirements of the design goals. The IBSC-based control method is a good candidate for control analysis and design of the nonlinear dynamic systems in which the design model is not known precisely and the performance of the system is required with high accuracy.

CHAPTER 7

BACKSTEPPING-BASED ROLL ANGLE CONTROL

In this chapter, the research is presented on the proposed BSC/IBSC-based rolling angle control of an L-59 aircraft model under varying pitch and yaw angles. In the first section, an introduction of an L-59 aircraft model and range of operational conditions are presented, and then a backstepping control law formulation is provided in the second section. In the third section, the control allocation and concepts of semi-variable and variable gains are introduced. Finally, experimental results are presented in the fourth section and a summary and remarks will end the chapter.

7.1 INTRODUCTION

Consider the L-59 model airplane in the 2014-2015 free-to-roll (FTR) experiment in Figure 7.1 The mathematical model of the FTR L-59 aircraft model is written in a

Figure 7.1: L-59 Aircraft Model at NASA Langley Research Center

multi-input single-output (MISO) strict-feedback form of nonlinear dynamic systems in References [69], [70].

$$\begin{aligned} \dot{\phi} &= p \\ \dot{p} &= \frac{1}{I_{xx}}(mgz_{cg}sin\phi + \bar{q}SbC_l(E)) \end{aligned} \tag{7.1}$$

where E is a vector of explanatory variables, the parameters and variables are defined in Table 7.1 and Table 7.2, respectively. The vector E includes the variables α-attack angle, β-sideslip angle, p-roll rate, δ_{a_l}-left aileron, and δ_{a_r}-right aileron. By

Table 7.1: Definition of Experimental Variables

Variables	Description	Value	Unit
I_{xx}	Moment of Inertia	0.08	$slug - ft^2$
S	Wing reference area	3.14	ft^2
b	Wing reference span	3.937	ft
z_{cg}	Center of gravity position with respect to the roll axis	-0.0108	ft
mg	Test model weight	27.45	lbf

Table 7.2: Definition of Measured Variables

Variables	Description	Range	Unit
ϕ	Roll or Bank angle	-90 to 90	deg
p	Roll rate	-200 to 200	deg/s
$\dot{p}$	Roll acceleration	-200 to 200	$\frac{deg}{s^2}$
δ_{a_l}	Left aileron deflection command	-25 to 25	deg
δ_{a_r}	Right aileron deflection command	-25 to 25	deg
α	Angle of attack	0 to 40	deg
β	Sideslip angle	-40 to 40	deg
$\bar{q}$	Dynamic pressure	2	lbf/ft^2
$C_l(E)$	Body axis aerodynamic rolling moment function	[-]	[−]
θ	Sting pitch angle	0 to 25	deg
ψ	Sting yaw angle	-20 to 20	deg

introducing the new control input $u = C_l(E)$, the system (7.1) can be re-written as

a SISO strict-feedback system (7.2).

$$\begin{aligned} \dot{\phi} &= p \\ \dot{p} &= \frac{1}{I_{xx}}(mgz_{cg}sin\phi + \bar{q}Sbu) \end{aligned} \tag{7.2}$$

Problem Statement

The objective is to design a control law u for the SISO strict-feedback system (7.2) such that $\phi(t) \longrightarrow \phi_{ref}$ asymptotically where ϕ_{ref} is a constant. Further, global asymptotic stability is to be achieved with zero or acceptably small overshoots approximated to be 2 % and a 1.2 second settling time in the presence of model parameter errors and varying sting pitch and yaw angles. With the achieved new control input, a follow on problem is to allocate the new input u to the real inputs δ_{a_l}-left aileron and δ_{a_r}-right aileron to achieve the performance specifications.

7.2 F2R CONTROL DESIGN OF L-59 AIRCRAFT MODEL

The system (7.2) is a second order SISO strict-feedback system. Therefore, the BSC/IBSC-based strategy in Chapter 3 is applied to the system (7.2) in order to achieve the control laws which satisfy the requirements. Note that the IBSC-based method is exactly the same as the BSC-based method with the exception of a zero gain for the integrator term. Thus, the IBSC formulation is only presented in this chapter. The following development provides steps for formulating the IBSC law.

Step 1.

The state variable p is regarded as a control input of the first relation in equation (7.2), which is considered as the first subsystem. Thus, the variable p is chosen to make the first subsystem globally asymptotically stable. The chosen α_1 for the p function is called a virtual control law. By introducing a modified tracking error ξ_1 as

$$\xi_1 = (\phi - \phi_{ref}) + \sigma \tag{7.3}$$

where $\sigma = c_0 \int_0^t e(\tau)d\tau$, $e(t) = \phi - \phi_{ref}$, and $e(t)$ is defined as the normal tracking error and c_0 is a positive gain. Differentiating both sides of equation (7.3) in time and combining with the first relation of equation (7.2), one achieves

$$\dot{\xi}_1 = p + \dot{\sigma} \tag{7.4}$$

where $\dot{\sigma} = c_0 e$.

For the system (7.4), a CLF $V_1(\xi_1)$, in terms of Definition 2.8, can be chosen such that when the virtual control law is applied, its time derivative becomes negatively definite. The positive definite function is chosen as

$$V_1(\xi_1) = \frac{1}{2}{\xi_1}^2 \tag{7.5}$$

Taking the derivative of equation (7.5) in time and combining with equation (7.4) achieves

$$\dot{V}_1(\xi_1) = \xi_1 \dot{\xi}_1 = \xi_1(p + \dot{\sigma}) \tag{7.6}$$

By satisfying the asymptotically stable condition in the sense of Lyapunov in Theorem 2.2 for equation (7.6), a virtual control law denoted as α_1 for p can be chosen as

$$\begin{aligned} -c_1\xi_1 &= p + \dot{\sigma} \\ \Rightarrow p \equiv \alpha_1 &= -(c_0 + c_1)(\phi - \phi_{ref}) - c_1\sigma \end{aligned} \tag{7.7}$$

where c_1 is a positive gain. By doing so, the CLF derivative is negatively definite.

$$\dot{V_1}(\xi_1) = \xi_1\dot{\xi_1} = -c_1\xi_1^2 < 0 \;\forall\; \xi_1 \neq 0 \tag{7.8}$$

Step 2.

By choosing the state feedback in equation (7.7) and a change of coordinate in equations (7.3), (7.9), as shown below

$$\xi_2 = p - \alpha_1 \tag{7.9}$$

the second subsystem or full system can be re-written as follows

$$\begin{aligned} \dot{\xi_1} &= -c_1\xi_1 \\ \dot{\xi_2} &= \frac{1}{I_{xx}}(mgz_{cg}sin\phi + \bar{q}Sbu) - \dot{\alpha}_1 \end{aligned} \tag{7.10}$$

where $\dot{\alpha}_1$ is determined below

$$\dot{\alpha}_1 = -(c_0 + c_1)p - c_0c_1(\phi - \phi_{ref}) \tag{7.11}$$

A CLF $V_2(\xi_1, \xi_2)$ can be chosen such that it makes the subsystem in equation (7.10) asymptotically stable with the control law, i.e.,

$$V_2(\xi_1, \xi_2) = V_1(\xi_1) + \frac{1}{2}\xi_2^2 \tag{7.12}$$

By taking the derivative of equation (7.12) in time and combining with equation (7.10), one finds the result

$$\dot{V}_2(\xi_1, \xi_2) = -c_1\xi_1^2 + \xi_2\{\frac{1}{I_{xx}}(mgz_{cg}sin\phi + \bar{q}Sbu) - \dot{\alpha}_1\} \tag{7.13}$$

To meet the asymptotically stable condition in the sense of Lyapunov in Theorem 2.2 for equation (7.13), a nonlinear control law can be chosen such that

$$\begin{aligned} -c_2\xi_2 &= \frac{1}{I_{xx}}(mgz_{cg}sin\phi + \bar{q}Sbu) - \dot{\alpha}_1 \\ \Rightarrow u &= \frac{I_{xx}}{\bar{q}Sb}\{-c_2(p - \alpha_1) + \dot{\alpha}_1 - \frac{1}{I_{xx}}mgz_{cg}sin(\phi)\} \end{aligned} \tag{7.14}$$

where c_2 is a positive gain, and α_1 and $\dot{\alpha}_1$ are determined by equations (7.7) and (7.11), respectively. By doing so, the CLF derivative is negatively definite, or

$$\dot{V}_2(\xi_1, \xi_2) = -c_1\xi_1^2 - c_2\xi_2^2 < 0 \ \forall \ \xi_1, \xi_2 \neq 0 \tag{7.15}$$

By choosing the state feedback in equation (7.7), the control law in equation (7.14), and changes of coordinate in equations (7.3) and (7.9), the system (7.2) is transformed into the state decoupled linear system as

$$\begin{aligned} \dot{\xi}_1 &= -c_1\xi_1 \\ \dot{\xi}_2 &= -c_2\xi_2 \end{aligned} \tag{7.16}$$

Analysis and discussion of the system (7.16) concerning how the proposed control augmentation works was made in Section 3.3 of the Chapter 3.

7.3 CONTROL ALLOCATION AND GAIN DESIGN

By introducing the new control input $u = C_l(E)$, the MISO system (7.1) can be re-written in equation (7.2) or in a SISO form that is convenient for the backstepping

approach. The next step is to allocate the u control input on the right and left aileron deflections. With the achieved u in equation (7.14) and $C_l(E)$ in terms of other state variables, one problem is to find the solutions for $\delta_{a_l}, \delta_{a_r}$ from the equation $u = C_l(E)$ with a given current set of state variables in order to make the output track the command. Two approaches are proposed:

- Find the solution of an algebraic equation by iteration methods.
- Find the solution of an algebraic equation by optimization methods.

A second problem is to find acceptable values for the gains c_0, c_1, c_2 appearing in the control law. Two approaches are proposed:

- Find the solution of an optimization problem for optimal constant gains.
- Analytical transformation for semi-variable gains.

7.3.1 CONTROL ALLOCATION

Iteration Methods

This approach leads to finding the solutions of one algebraic equation of two variables. In general, the method is not robust. If the values of the initial guess are very close to the real solutions, only then may the method provide global solutions. For the simulation and experimental studies, the values of the initial guess for the iteration are selected as previous values of the iteration or the equilibrium values. The advantage of the method is a simple structure which may speed up the iteration process for the solution but may not provide robust behavior in general.

Optimization Methods

In general, if the number of variables in an algebraic equation set is more than number of equations, then optimization subject to the constraints is a good candidate for finding the solutions. Instead of finding the solutions $\delta_{a_l}, \delta_{a_r}$ of the equation $u = C_l(E)$, the optimization formulation leads to finding the solution to minimize the tracking error sum, or

$$\underset{\delta_{a_l},\delta_{a_r}}{\text{minimize}} \quad J = \int_0^t (\phi - \phi_{ref})^2 dt \tag{7.17}$$

subject to the constraints

$$\begin{aligned} \delta_{a_l}\delta_{a_r} &\leq 0 \\ u - C_l(E) &= 0 \end{aligned} \tag{7.18}$$

Another similar formulated problem is

$$\underset{\delta_{a_l},\delta_{a_r}}{\text{minimize}} \quad J = \int_0^t (u - C_l(E))^2 dt \tag{7.19}$$

subject to the constraints

$$\delta_{a_l}\delta_{a_r} \leq 0 \tag{7.20}$$

7.3.2 GAIN SCHEDULES

Constant Gains

The approach leads to finding the optimal solutions for c_0, c_1, c_2 to minimize the

tracking error sum and aileron deflections

$$\underset{c_0,c_1,c_2}{\text{minimize}} \quad J = \int_0^t [w_e(\phi - \phi_{ref})^2 + w_u(\delta_{a_r}^2 + \delta_{a_l}^2)]dt \tag{7.21}$$

subject to the constraints

$$\begin{aligned} \delta_{a_l}\delta_{a_r} &\leq 0 \\ u - C_l(E) &= 0 \end{aligned} \tag{7.22}$$

where w_e, w_u are the weights, which are determined via the requirements of the performance specifications. Those values are selected by a trial and error technique. The new input u is determined by equation (7.14). By using the command "fmincon" in Matlab/Simulink 2013, the optimal gains for the BSC law are achieved as $c_1 = 4.13\ s^{-1}, c_2 = 4.28\ s^{-1}$ for BSC and $c_0 = 4.12\ s^{-1}, c_1 = 4.13\ s^{-1}, c_2 = 4.28\ s^{-1}$ for the IBSC.

Semi-Variable Gains

The control formulation provides a feedback design in which the output will track the command without overshoot. The question arises on how to handle the settling time. From equation (7.16), it is clear that the settling time will increase if the gains are decreased and vice versa. The following development provides a method in which the settling time is assigned by the requirement of performance specifications, and then, the gains are calculated as a function of the settling time.

Taking the integral of both sides of the first relation of equation (7.16) with zero

gain for the integrator and returning with the original variables, one gets

$$\phi - \phi_{ref} = (\phi_0 - \phi_{ref})e^{-c_1 t} \tag{7.23}$$

The settling time t_s is defined such that the output reaches 99 percent of the command value or $\phi(t_s) = 0.99\phi_{ref}$. By doing so, the gain c_1 can be calculated from equation (7.23) as

$$c_1 = -\frac{1}{t_s} ln \frac{-0.01\phi_{ref}}{\phi_0 - \phi_{ref}} \tag{7.24}$$

Taking the integral of both sides of the second relation of equation (7.16) and returning to the original variables, one gets

$$p - \alpha_{1ref} = (p_0 - \alpha_{1ref})e^{-c_2 t} \tag{7.25}$$

where $\alpha_{1ref} = 0.01 c_1 \phi_{ref}$ is used as command for the second gain. Defining the settling time t_s to be when the output p reaches 99 percent of the command value α_{1ref} in equation (7.25) or $p(t_s) = 0.99\alpha_{1ref}$. Thus, a value for c_2 can be estimated from

$$c_2 = -\frac{1}{t_s} ln \frac{-0.01\alpha_{1ref}}{p_0 - \alpha_{1ref}} \tag{7.26}$$

Substituting the values $\phi_0 = 0\ deg,\ p_0 = 0\ deg/s,\ t_s = 1.1$ second in equation (7.24) and equation (7.26) results in the gain values $c_1 = 4.1865\ s^{-1}, c_2 = 4.1865\ s^{-1}$. It is clear that if the initial conditions are $\phi_0 = p_0 = 0$ and a settling time of 1.1 s is assigned, then the semi-variable gains are close to the optimal constant gains. One advantage of semi-variable gains is that the settling time can be assigned specifically for the output response from Reference [70]. The values of c_1, c_2 in equations (7.24)

and equation (7.26), respectively, require positive values. Thus, the values of c_1, c_2 must satisfy the following expressions.

$$\frac{-0.01\alpha_{1ref}}{p_0 - \alpha_{1ref}} < 1, \frac{-0.01\phi_{ref}}{\phi_0 - \phi_{ref}} < 1 \tag{7.27}$$

Note that the condition in equation (7.27) limits the operational range of the method. Thus, a combined use of constant gains or a modified version will provide for a better control strategy.

The above mentioned gains are used for the simulation and experimental studies of rolling angle control for an L-59 aircraft model. The BSC/IBSC-based control with the proposed gains shows the limitations and advantages in different operational conditions. Simulation results are not presented here, but conclusions are similar and consistent with results presented in Chapters 4, 5, and 6. To show the applicability during real implementation, an analysis of experimental results when applied to the actual physical model is emphasized in this study.

7.4 EXPERIMENTAL STUDY

In this section, experimental studies are implemented for rolling angle control for the L-59 aircraft model. Both BSC and IBSC-based control methods with optimal gains are used for experiments.

7.4.1 EXPERIMENTAL CONDITIONS

The data of the L-59 aircraft model, as shown in Figure 7.1, is provided in Table 7.1 and Table 7.2. The aerodynamic data of the L-59 aircraft model for experiments is

derived from wind-tunnel tests with constant dynamic pressure at the NASA Langley Research Center. The experiments are tested with two different roll angle and pitch angle profiles. The roll angle profile consists of ∓ 20 *deg* doublets shown in Figure 7.2. For pitch angle, several cases are considered with a constant small angle of 5 degrees. Also, one case is considered using a varying pitch angle profile indicated in Figure 7.3. In this second profile, multiple changes in pitch angle are applied for the study in order to verify the robustness of the proposed method for different flight conditions. Also, the experimental results were generated with different types of gains that are constant gains, semi-variable gains, and variable gains. The values of constant gains were computed from an optimization process described in Section 7.3 and expressions for the semi-variable gains are represented in equation (7.24) and equation (7.26).

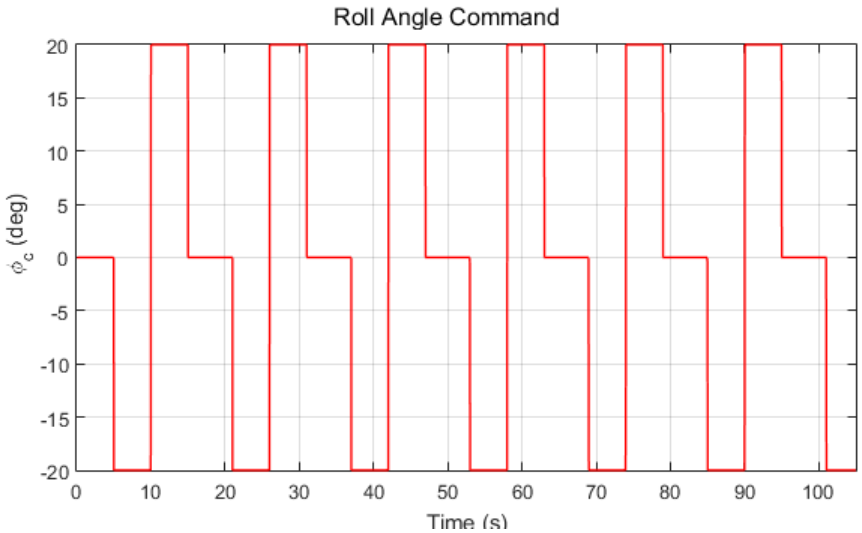

Figure 7.2: Roll Angle Command in Time

The experimental study is implemented with different conditions. To show the improvement of the BSC-based control strategy, a PD or proportional-derivative-based control using available aerodynamic coefficients was implemented for the first half of the experiment. In this time window, system identification was turned on for estimating new aerodynamic coefficients. With the achieved aerodynamic coefficients, the BSC-based control was applied for the remaining period in the experiments.

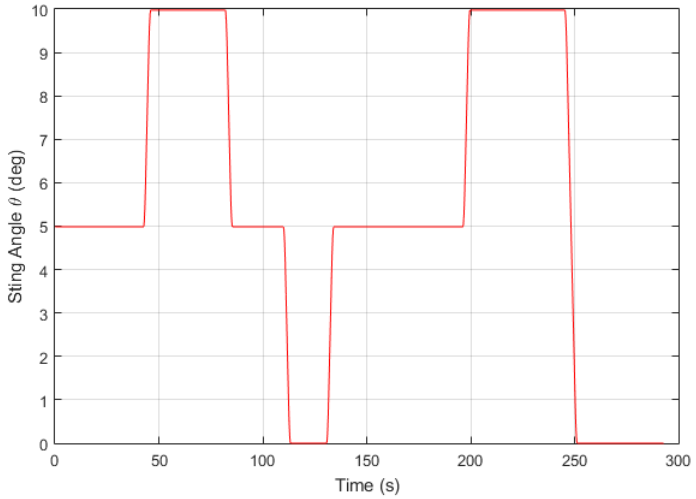

Figure 7.3: Varying Pitching Angles in Time

7.4.2 EXPERIMENTAL RESULTS

Note that the IBSC-based method is exactly the same as the BSC-based method with the exception of a zero gain for integrator term or $c_0 = 0$. For simplicity, the terminology "BSC-based control" is used for implying both IBSC or BSC for the rest of the chapter.

Case 1: Constant Gains without Integrator

Figure 7.4 shows time responses of the roll angle with constant gains and without an integrator. The red or dash line presents a desired command for roll angle and the blue line or solid line shows the experimental result of the controlled roll angle of the L-59 model mounted in the wind-tunnel with freedom to rotate about the roll axis.

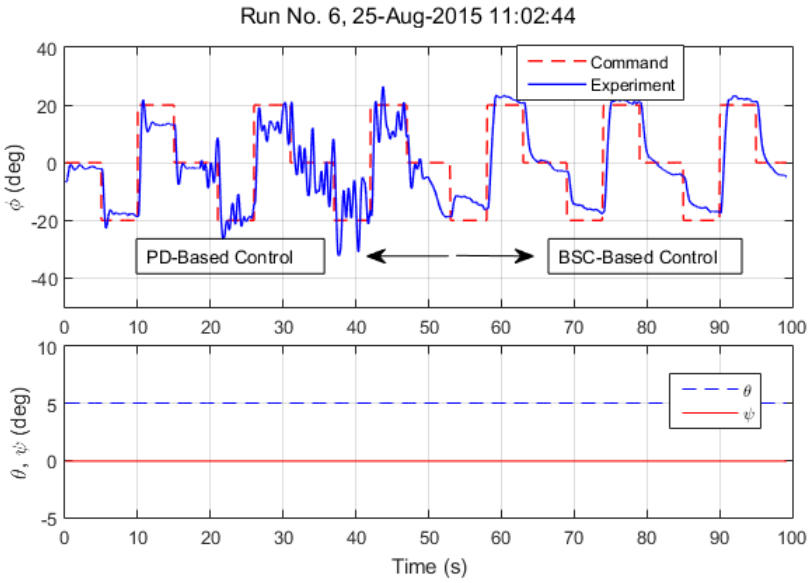

Figure 7.4: Roll Angle Response with Constant Gains and without Integrator

Figure 7.5 shows time responses of the states and control variables with constant gains and without an integrator. The experimental response of roll angle in Figure 7.4 using the BSC control has a well-behaved command tracking behavior without overshoot. The result also shows that the performance is improved significantly compared to the results using a proportional-derivative (PD) based control. However, the roll angle time response appears to have a small steady state error, which had

been predicted theoretically in other simulations with system parameter error in Chapter 3. Also, the experimental responses of aileron deflections in Figure 7.5 show the decrease in the BSC-based magnitude as compared to the PD-based control.

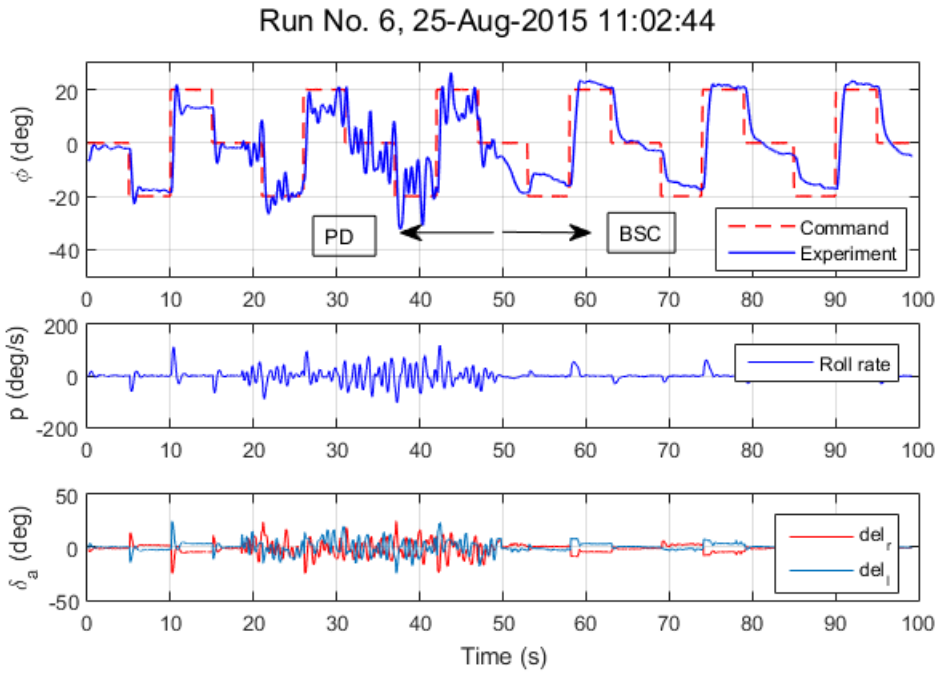

Figure 7.5: Time Response of State and Control Variables with Constant Gains and without Integrator

Case 2: Constant Gains with Integrator

Figure 7.6 shows time responses of the roll angle with constant gains and with an integrator. The red line or dash line presents the desired command for roll angle and the blue line or solid line shows the experimental result of controlled roll angle. Figure 7.7 shows time responses of the states and control variables with constant gains and with an integrator. From the results in Figure 7.6 and Figure 7.7, some discussions are made similarly to Case 1. However, the BSC-based control with an

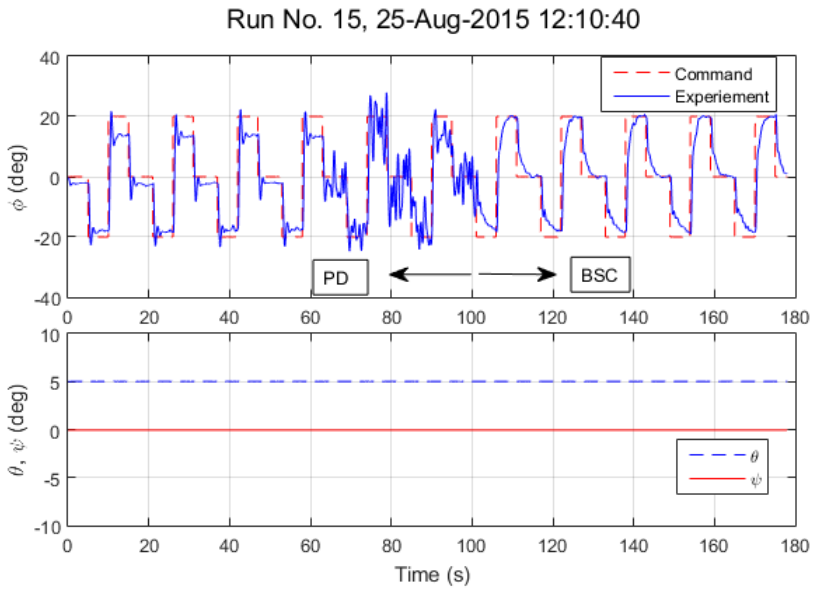

Figure 7.6: Roll Angle Response with Constant Gains and with Integrator

integrator provides a time response of roll angle with no steady state error and the outcome also shows that the settling time in this case is higher than in Case 1.

Case 3: Semi-Variable Gains with Integrator

Figure 7.8 shows time responses of the roll angle with semi-variable gains and with an integrator. The red line or dash line presents a desired command for the roll angle and the blue line or solid line shows the experimental result. Figure 7.9 shows time responses of the states and control variables with semi-variable gains and with an integrator. From the results in Figure 7.8 and Figure 7.9, conclusions are made similarly to Case 2. However, the BSC-based control with semi-variable gains provides a shorter settling time or faster response compared to Case 2.

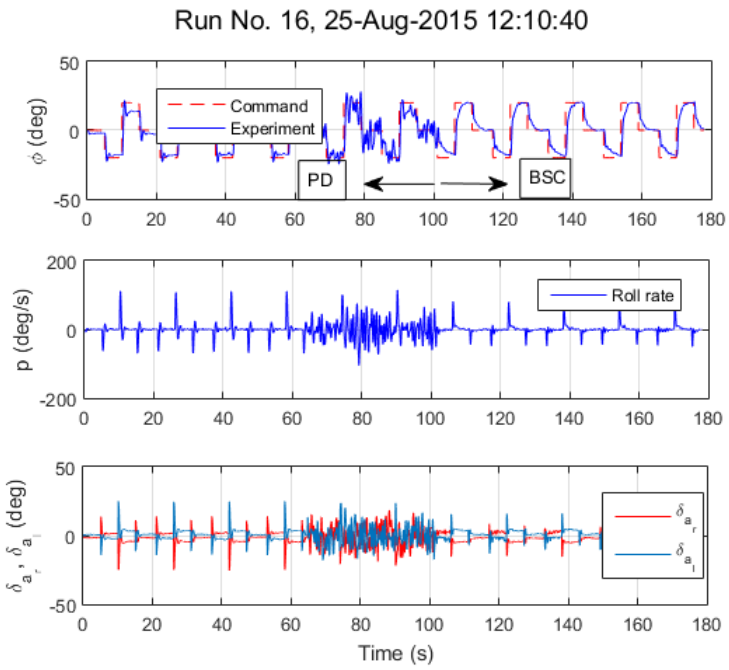

Figure 7.7: Time Response of State and Control Variables with Constant Gains and with Integrator

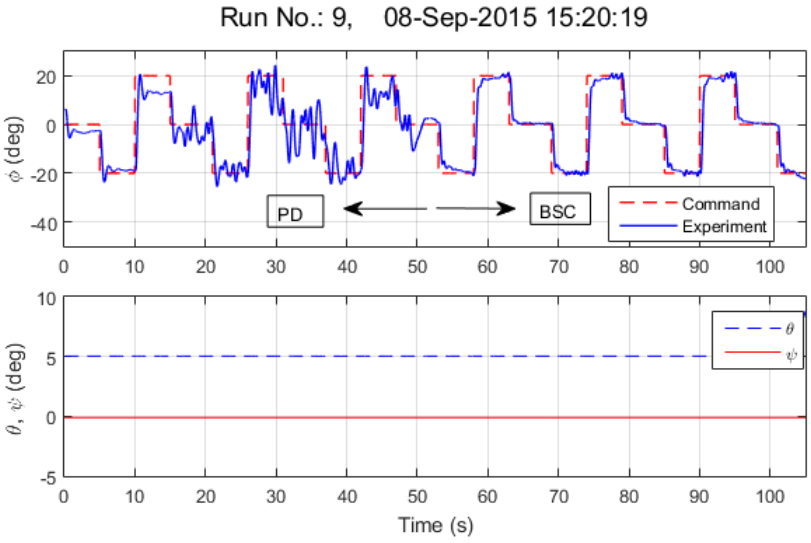

Figure 7.8: Roll Angle Response with Semi-Variable Gains and with Integrator

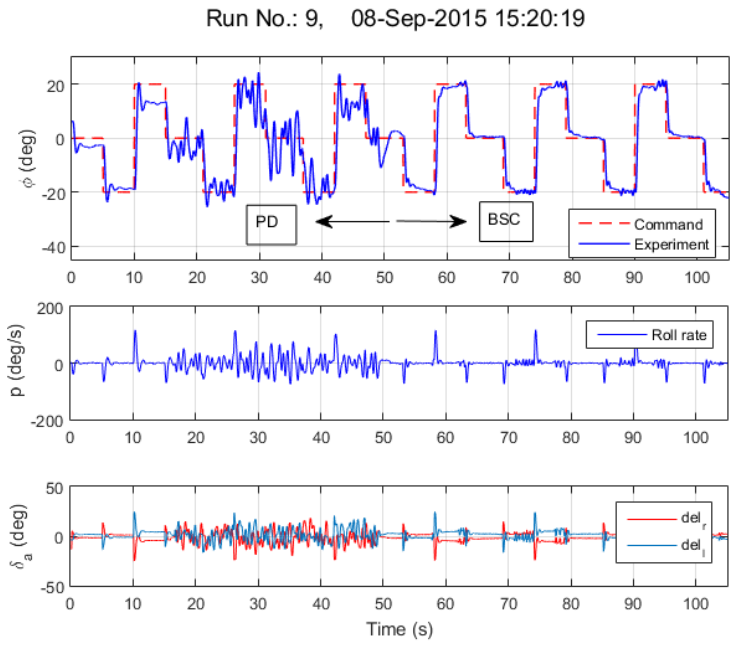

Figure 7.9: Time Response of State and Control Variables with Semi-Variable Gains and with Integrator

Case 4: Semi-Variable Gains with Integrator and Multiple Pitch Angles

Figure 7.10 shows time responses of roll angle with semi-variable gains with integrator, and with varying pitching angle profile from Figure 7.3. The red line or dash line presents a desired command for roll angle and the blue line or solid line shows the experimental result of controlled roll angle. Figure 7.11 shows time responses of the states and control variables with semi-variable gains and an integrator, and varying pitch angle. Results in Figure 7.10 show that the roll angle time response has a well-behaved command tracking behavior in the presence of varying pitch angles. Results in Figure 7.11 indicate the proposed control method provides precision and reliability in controlling roll angle.

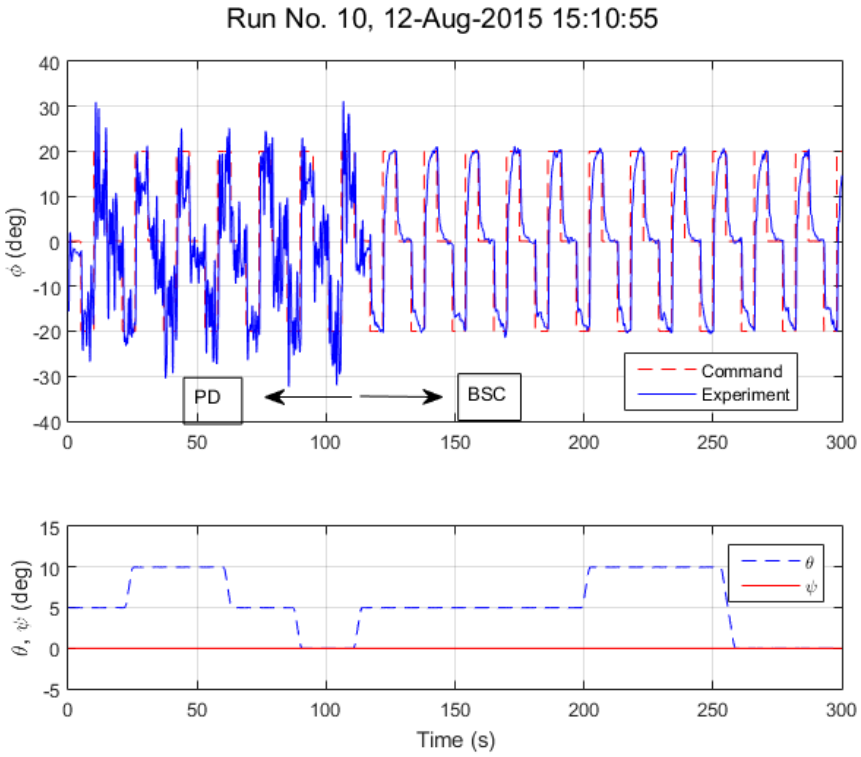

Figure 7.10: Roll Angle Response with Semi-Variable Gains and Integrator, and with Multiple Pitch Angles

7.5 SUMMARY AND DISCUSSION

This chapter provides a brief discussion about the L-59 aircraft model used for experimental study. The governing equations for pure roll dynamics of the aircraft are derived for control design purposes. Then, IBSC/BSC formulations and control strategy for the roll dynamics are presented. Also, gain selection for experimental investigations is considered. With the achieved control strategy, experiments on roll angle control with different pitch profiles for the L-59 aircraft model are implemented for verification of theoretical development.

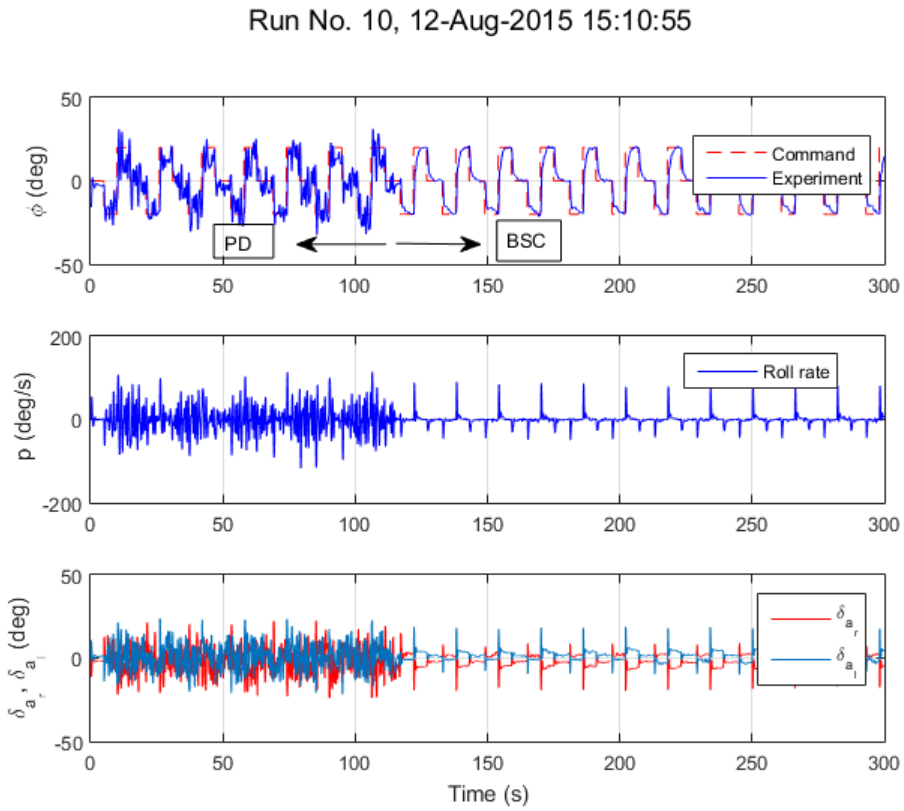

Figure 7.11: Time Response of State and Control Variables with Semi-Variable Gains and Integrator, and with Multiple Pitch Angles

Experimental results show the benefits and limitations of the IBSC/BSC-based control method. Experimental results indicate steady state error occurs as the BSC-based control is applied in the presence of parameter errors. The results also indicate that the IBSC-based control is able to eliminate the steady state error in the presence of those modeling errors or from disturbances in the pitch angle. From those experimental results, a verification of theoretical prediction from the proposed control method is made.

CHAPTER 8

CONCLUSION AND FUTURE WORK

In this chapter, a summary, discussion, and conclusion of the overall dissertation are made. Advances and limitations of the proposed nonlinear backstepping control methodology are drawn out for applications to aircraft flight dynamic systems. Then, future works with open topics related to the dissertation research are presented at the end of the chapter.

8.1 CONCLUSION

With the rapid developments of high-performance computers, sensor technology, and PC integrated control hardware such as PCI, PXI, and Labview FPGA, many advanced control design methods for nonlinear dynamic systems have been addressed to improve performance and stability. Nonlinear flight control design for aircraft dynamic systems have also been considered by many researchers in recent years. A backstepping-based control design for aircraft flight dynamics is one of the most advanced methods in which nonlinear dynamic equations of the aircraft are used for control analysis and design. Through investigation, there are some limitations in recent analyses and design methods for nonlinear flight dynamics of the aircraft. Thus, the dissertation research is proposed to achieve a better and more robust control method of aircraft flight dynamics.

For theoretical developments, a general strict-feedback system, a standard model

for the backstepping-based approach, is introduced and analyzed. Then, the research shows that a general nonlinear dynamic system with affine form and full relative degree can be transformed directly into the strict-feedback form of nonlinear dynamic systems. If the above conditions are not available, then the necessary assumptions have to be stated such that a nonlinear dynamic system can be transformed indirectly into the strict-feedback form of nonlinear dynamic systems. For the achieved strict-feedback form of nonlinear dynamic systems, the research provides a systematic procedure for formulating the backstepping control law. With the achieved BSC law, a BSC-based control algorithm is then provided for numerical strategy. Analytical and numerical results indicate that approximated parameters in the design model with large enough variation may lead to degraded performance or even instability. Thus, the integrator-backstepping-based control design for strict-feedback systems are addressed to improve the performance and stability in the presence of parameter error or external disturbances. In this approach, a definition of the modified tracking error is introduced by adding an integral term to the normal tracking error and then, a systematic procedure is addressed for formulating an integrator-backstepping control law for a general strict-feedback system. An IBSC-based control strategy is provided for closed-loop simulation testing. An example is implemented by applying the proposed control methods for assessing validity. Both analytical and numerical results indicate that the proposed control strategy provides a robust control system with high precision.

To show the applicability of the proposed control methodology for nonlinear flight

dynamic systems, the flight path angle control study of longitudinal dynamics for the F-16 aircraft model is implemented. The research started with assumptions in which the aircraft speed is constant and the aircraft lift force is a sinusoidal function of attack angle and altitude. The assumptions are analyzed, validated, and compared to show the advantages and disadvantages of the design model. By doing so, the full nonlinear flight dynamics of aircraft is transformed into the standard strict-feedback form. For the achieved standard model, a systematic procedure is given for formulating the backstepping control law for the standard strict-feedback form of nonlinear longitudinal dynamics of aircraft. An achieved BSC-based control algorithm for flight path angle of an F-16 aircraft model is then provided for numerical simulation study. Simulation results for the full nonlinear model of different flight conditions show that the proposed control strategy meets the demands of the required performance specifications with no or small acceptable overshoot and robust stability. Also, the numerical results validate the analytical prediction in which the output will track asymptotically the command with no or small acceptable overshoot. For the testing of the robust control design, the numerical outcomes which are implemented for different variations of the aircraft mass centers confirm the robustness of the proposed control design.

Through investigation, there is proven an equivalence between the feedback linearization-based design and the backstepping-based design for a triangular affine form of nonlinear dynamic systems. The dissertation research provides a theorem

in which both feedback linearizion-based and the backstepping-based designs for triangular affine systems result in the same feedback control laws. Similarly, some assumptions on aerodynamic forces and moments are made to transform aircraft nonlinear flight dynamics into a triangular affine model. Then, both approaches are applied for formulating the feedback control laws for the triangular affine system. A flight path angle control study of the F-16 aircraft model is then provided for proving equivalence and applicability. Analytical and numerical results indicate validation of the theoretical prediction and applicability of the proposed control method.

In practice, the effectiveness of model assumptions and disturbances such as wind velocities and turbulence on aircraft plays an essential role in performance and stability. A considerable range of model errors may lead to degraded performance like steady state error or even instability by using the BSC-based control design. Thus, an improvement of the backstepping strategy is made by introducing a modified tracking error in which the integral term of normal error is added to the normal tracking error. Then a similar systematic procedure, such as the BSC-based design, is provided to formulate the integrator-backstepping control law for strict-feedback form of the longitudinal aircraft dynamics. An IBSC-based control algorithm for flight path angle of longitudinal dynamics of the aircraft is provided for numerical simulation. Results show the improvements of the IBSC-based control design over the BSC-based control strategy in which the steady state errors due to the approximated design model or wind disturbance is eliminated. The performance and stability of the aircraft are also recovered and track asymptotically to a command in the presence of wind velocities

acting on the aircraft.

In conclusion, the backstepping technique shows an important potential on control analysis and design of nonlinear dynamic systems, and has been a motivating basis for exploring new directions in control design for engineering systems in general, and particularly for nonlinear aircraft flight dynamic systems. The applications of this technique for engineering systems combined with powerful digital computers and highly accurate sensor technology result in a control strategy with robust and high precision control behavior.

8.2 FUTURE WORK

Although the research shows that a nonlinear dynamic system with affine form and full relative degree can be transformed directly into a nonlinear strict-feedback form of nonlinear dynamic systems, the dissertation only shows a specific type of state transformation. With this type of transformation and feedbacks, a nonlinear dynamic system can be transformed directly into a linear form of strict-feedback system. A more generalized version of advanced state transformations may provide a better design model in which benefits of nonlinear properties may be maintained via coordinate transformations and feedbacks. Thus, the achieved design model that is closer to the physical system may result in a control system with more robustness and high quality.

The numerical outcomes show that the backstepping technique results in a considerable improvement on flight path angle control for nonlinear flight dynamic systems of an aircraft. However, the overall process of control analysis and design for

longitudinal dynamics of aircraft assumes that the aircraft velocity is constant and aerodynamic forces and moments are linear or sinusoidal functions of state variables and inputs. Through these assumptions, responses of real systems may be different from a numerical simulation model. Deeper work considering the contributions of every single parameter on aerodynamic forces and moments may provide a control system with closer physical behavior. This enhanced parameter description may require the control signal to be computed numerically from solving a set of nonlinear algebraic equations, as opposed to closed-form expression seen in this dissertation. Thus, a suitable control realization in these situations should be addressed for the applicability of the proposed control method.

Although simulation results indicate that the IBSC-based control design provides a robust control method in the presence of wind turbulence, the research is not able to show the boundaries of the disturbances in which the proposed methods are still able to achieve the performance and stability. A traditional robust design concept should be addressed to provide clarity of the proposed method.

In the dissertation, assumptions of the decoupling of the longitudinal and lateral-directional dynamics are made to achieve the single-input single-output standard model for the longitudinal dynamic system for control analysis and design. A backstepping-based control strategy for the full nonlinear aircraft model where both longitudinal and lateral-directional dynamics are present simultaneously needs to be addressed and may provide a better and more robust flight control system.

BIBLIOGRAPHY

[1] R. C. Dorf and R. H. Bishop. *Modern Control Systems*. Prentice-Hall, Inc., 2000.

[2] G. F. Franklin, J. D. Powell, and A. Emami-Naeini. *Feedback Control of Dynamics Systems*. Pretince Hall Inc, 2006.

[3] F. L. Lewis. *Applied Optimal Control and Estimation*. Prentice Hall PTR, 1992.

[4] G. Tao. *Apdaptive Control Design and Analysis*. Wiley, 2003.

[5] A. Datta, M. T. Ho, and S. P. Bhattacharyya. *Structure and Synthesis of PID Controllers*. Springer Science & Business Media, 2000.

[6] P. J. Antsaklis and A. N. Michel. *Linear Systems*. Springer Science & Business Media, 2006.

[7] W. J. Rugh. *Linear System Theory*. Prentice hall Upper Saddle River, 1996.

[8] H. K. Khalil and J. W. Grizzle. *Nonlinear Systems*. Prentice hall New Jersey, 1996.

[9] J. M. Maciejowski. *Multivariable Feedback Design*. Addison-Wesley Wokingham, 1989.

[10] W.J. Rugh. Analytical framework for gain scheduling. *Control Systems*, 11(1):79–84, 1991.

[11] W.J. Rugh and S. S. Jeff. Research on gain scheduling. *Automatica*, 36(10):14011425, 2000.

[12] A. Isidori. Exact linearization and zero dynamics. In *Proceedings of the 31st IEEE Conference on Decision and Control*, Honolulu, Hawaii, 1990.

[13] A. Isidori and A. J. Krener. Feedback linearization of nonlinear systems. *Control System, Robotics and Automation*, 7(2):118–121, 1991.

[14] A. Isidori. Dissipation inequalities in nonlinear h-infinity control. In *Proceedings of the 31st IEEE Conference on Decision and Control*, Tucson, Arizona, 1992.

[15] A. Isidori. *Nonlinear Control Systems*. Springer, 1995.

[16] A. Isidori. *Nonlinear Control Systems II*. Springer, 1999.

[17] A. Isidori and C.I. Byrnes. Output regulation of nonlinear systems. *IEEE Transactions on Automatic Control*, 35(2):131–140, 1990.

[18] A. J. Krener. On the equivalence of control systems and the linearization of nonlinear systems. *SIAM Journal on Control*, 11(4):670–676, 1973.

[19] A. J. Krener and W. Respondek. Nonlinear observers with linearizable error dynamics. *SIAM Journal on Control and Optimization*, 23(2):197–216, 1985.

[20] K. J. Astrom and B. Wittenmark. *Adaptive Control*. Courier Corporation, 2013.

[21] P. V. Kokotovic. The joy of feedback: Nonlinear and adaptive. *IEEE Control Systems Magazine*, 12(3):7–17, 1992.

[22] R. A. Freeman and P. V. Kokotovic. *Robust Nonlinear Control Design: State-Space and Lyapunov Techniques*. Springer Science & Business Media, 2008.

[23] D. Enns, D. Bugajski and R. Hendrick. Dynamic inversion: An evolving methodology for flight control design. *International Journal of Control*, 59(1):71–91, 1994.

[24] J. Farrell, M. Sharma, and M. Polycarpou. Backstepping-based flight control with adaptive function approximation. *Journal of Guidance, Control, and Dynamics*, 28(6):1089–1102, 2005.

[25] N. Halyo, D. D. Moerder, J. R. Broussard, and D. B. Taylor. A variable-gain output feedback control design methodology. Technical Report NAS1-17493, NASA, 1989.

[26] O. Harkegard. *Backstepping and Control Allocation with Applications to Flight Control*. Linkping studies in science and technology. thesis no 820, Department of Electrical Engineering, Linkping University, SE–581 83 Linkping, Sweden, 2003.

[27] O. Harkegard and S. T. Glad. A backstepping design for flight path angle control. In *Proceedings of the 39th IEEE Conference on Decision and Control, 2000*, Sydney, NSW, 2000.

[28] H. S. Ju and C. C. Tsai. Longitudinal axis flight control law design by adaptive backstepping. *IEEE Transactions on Aerospace and Electronic Systems*, 43(1):311–329, 2007.

[29] B. S. Kim and A. J. Calise. Nonlinear flight control using neural networks. *Journal of Guidance, Control, and Dynamics*, 20(1):26–33, 1997.

[30] S. H. Lane and R. F. Stengel. Flight control design using nonlinear inverse dynamics. *Automatica*, 24(4):471–483, 1988.

[31] T. Lee and Y. Kim. Nonlinear adaptive flight control using backstepping and neural networks controller. *Journal of Guidance, Control, and Dynamics*, 24(4):675–682, 2001.

[32] A. J. Ostroff. High-alpha application of variable-gain output feedback control. *Journal of Guidance, Control, and Dynamics*, 15(2):491–511, 1992.

[33] J. Reiner, G. J. Balas, and W. L. Garrard. Robust dynamic inversion for control of highly maneuverable aircraft. *Journal of Guidance, Control, and Dynamics*, 18(1):18–24, 1995.

[34] J. Reiner, G. J. Balas, and W. L. Garrard. Flight control design using robust dynamic inversion and time-scale separation. *Automatica*, 32(11):1493–1504, 1996.

[35] M. Sharma and D. G. Ward. Flight-path angle control via neuro-adaptive backstepping. In *Proceedings of the AIAA Guidance, Navigation, and Control Conference*, AIAA-2002-4451, Monterey, California, 2002.

[36] S. A. Snell, D. F. Enns, and W. L. Grrard. Nonlinear inversion flight control for a supermaneuverable aircraft. *Journal of Guidance, Control, and Dynamics*, 15(4):976–984, 1992.

[37] S. A. Snell and P. W. Stout. Flight control law using nonlinear dynamic inversion combined with quantitative feedback theory. *Journal of Dynamic Systems, Measurement, and Control*, 120(2):208–215, 1998.

[38] T. T. Tran, K. H. Choi, D. E. Chang, and D. S. Kim. Web tension and velocity control of two-span roll-to-roll system for printed electronics. *Journal of Advanced Mechanical Design, Systems, and Manufacturing*, 5(4):329–346, 2011.

[39] K. H. Choi, T. T. Tran, and D. S. Kim. Back-stepping controller based web tension control for roll-to-roll web printed electronics system. *Journal of Advanced Mechanical Design, Systems, and Manufacturing*, 5(1):7–21, 2011.

[40] T. T. Tran and K. H. Choi. A backstepping-based control algorithm for multi-span roll-to-roll web system. *The International Journal of Advanced Manufacturing Technology*, 70(1-4):45–61, 2014.

[41] M. Krstic, I. Kanellakopoulos, and P. V. Kokotovic. *Nonlinear and Adaptive Control Design*. Wiley, 1995.

[42] A. J. Calise and R. T. Rysdyk. Nonlinear adaptive flight control using neural networks. *Control Systems*, 18(6):14–25, 1998.

[43] L. Sonneveldt, Q. P. Chu, and J. A. Mulder. Nonlinear flight control design using constrained adaptive backstepping. *Journal of Guidance, Control, and Dynamics*, 30(2):322–336, 2007.

[44] M. L. Steinberg. Comparison of intelligent, adaptive, and nonlinear flight control laws. *Journal of Guidance, Control, and Dynamics*, 24(4):693–699, 2001.

[45] A. Ataei-Esfahani and Q. Wang. Nonlinear control design of a hypersonic aircraft using sum-of-squares method. In *American Control Conference, 2007. ACC'07*, New York, New york, 2007.

[46] C. I. Marrison and R. F. Stengel. Design of robust control systems for a hypersonic aircraft. *Journal of Guidance, Control, and Dynamics*, 21(1):58–63, 1998.

[47] S. Seshagiri and H. K. Khalil. Robust output feedback regulation of minimum-phase nonlinear systems using conditional integrators. *Automatica*, 41(1):43–54, 2005.

[48] Q. Wang and R. F. Stengel. Robust control of nonlinear systems with parametric uncertainty. *Automatica*, 38(9):1591–1599, 2002.

[49] Q. Wang and R. F. Stengel. Robust nonlinear flight control of a high-performance aircraft. *Control Systems Technology, IEEE Transactions on*, 13(1):15–26, 2005.

[50] K. H. Choi, T. T. Tran, P. Ganesh, N. M. Nguyen, K. H. Lee, and D. S. Kim. Web register control algorithm for roll-to-roll system based printed electronics. In *IEEE Conference on Automation Science and Engineering (CASE)*, Toronto, Ontario, 2010.

[51] K. H. Choi, T. T. Tran, and D. S. Kim. A precise control algorithm for single-span roll-to-roll web system using the backstepping controller. In *2009. ISIE 2009. IEEE International Symposium on Industrial Electronics*, Seoul, South Korea, 2009.

[52] K. H. Choi, T. T. Tran, and D. S. Kim. A wew approach for intelligent control system design using the modified genetic algorithm. *International Journal of Intelligent Systems Technologies and Applications*, 9(3):300–315, 2010.

[53] K. H. Choi, T. T. Tran, B. S. Yang, and D. S. Kim. On a new approach for gravure/offset printing pressure control algorithm development using the full state feedback controller. In *IEEE International Symposium on Assembly and Manufacturing, 2009*, Suwon, South Korea, 2009.

[54] M. Vidyasagar. *Nonlinear Systems Analysis*. SIAM, 2002.

[55] S. Sastry. *Nonlinear systems: Analysis, Stability, and Control*. Springer New York, 2013.

[56] A. Isidori. On feedback equivalence of nonlinear systems. *Systems and Control Letters*, 2(2):118 – 121, 1982.

[57] M. R. Napolotano. *Aicraft Dynamics: From Modeling to Simulation.* John Wiley & Sons, 2012.

[58] T. R. Yechout, S. L. Morris, D. E. Bossert, and W. F. Hallgren. *Introduction to Aircraft Flight Mechanics.* AIAA, 2003.

[59] X. V. Nguyen. *Flight Mechanics of High-Performance Aircraft.* Cambridge University Press, 1995.

[60] X. V. Nguyen. *Optimal Trajectories in Atmospheric Flight.* Elsevier, 2012.

[61] B. L. Stevens and F. L. Lewis. *Aircraft Control and Simulation.* John Wiley & Sons, 2003.

[62] L. T. Nguyen, M. E. Ogburn, W. P. Gilbert, K. S. Kibler, P. W. Brown, and P. L. Deal. Simulator study of stall/post-stall characteristics of a fighter airplane with relaxed longitudinal static stability. Technical Report NASA-TP-1538, L-12854, NASA, 1979.

[63] J. K. Hedrick and A. Girard. Control of nonlinear dynamic systems: Theory and applications. *Controllability and Observability of Nonlinear Systems*, (40), 2005.

[64] T. T. Tran and B. Newman. Back-stepping based flight path angle control algorithm for longitudinal dynamics. In *Proceedings of the AIAA Guidance, Navigation, and Control Conference*, AIAA-2012-4612, Minneapolis, Minesota, 2012.

[65] T. T. Tran and B. Newman. Integrator-backstepping control design for nonlinear flight system dynamics. In *Proceedings of the AIAA Guidance, Navigation, and Control Conference*, AIAA-2015-1321, Kissimmee, Florida, 2015.

[66] L. T. Nguyen, M. E. Ogburn, W. P. Gilbert, K. S. Kibler, P. W. Brown, and P. L. Deal. Control-system techniques for improved departure/spin resistance for fighter aircraft. Technical Report NASA-1689, NASA, 1980.

[67] T. T. Tran and B. Newman. Equivalence between state space exact linearization based and back-stepping based design approaches. In *Proceedings of the AIAA Guidance, Navigation, and Control Conference*, AIAA-2013-5102, Boston, Massachusetts, 2013.

[68] T. T. Tran and B. Newman. Nonlinear flight control design for longitudinal dynamics. In *Proceedings of the AIAA Guidance, Navigation, and Control Conference*, AIAA-2015-1321, Kissimmee, Florida, 2015.

[69] O. R. Gonzalez and A. Streit. 2014 free-to-roll experiment. Technical report, NASA, 2014.

[70] T. T. Tran, O. R. Gonzalez, and A. Streit. 2015 free-to-roll experiment. Technical report, NASA, 2015.

VITA

Thanh Trung Tran
Department of Aerospace Engineering
Old Dominion University
Norfolk, VA 23529

Education

- 02/2008 to 06/2012: Ph.D. (2012), Mechanical Engineering, Department of Mechanical Engineering, Jeju National University, Jeju, South Korea.
- 10/2002 to 12/2005: M.S.(2005), Applied Mechanics, Department of Mechanical and Automation Engineering, Vietnam National University, Hanoi, Vietnam.
- 08/1998 to 07/2002: B.S. (2002), Applied Mechanics, Department of Mathematics, Mechanics and Informatics, Vietnam National University, Hanoi, Vietnam.

Research Interests

- Primary Research Theme: Dynamics and Control
- Secondary Research Theme: Manufacturing System Design
- Third Research Theme: Computational Intelligence and Intelligent Systems

Typeset using LaTeX.